FIELD-SCALE ROOT-ZONE SOIL MOISTURE:

SPATIO-TEMPORAL VARIABILITY AND MEAN ESTIMATION

A Thesis Submitted to the College of Graduate Studies and Research

In Partial Fulfillment of the Requirements

For the Degree of Master of Science

In the Department of Civil and Geological Engineering

University of Saskatchewan

Saskatoon

By

Amber Marie Peterson

PERMISSION TO USE

In presenting this thesis in partial fulfilment of the requirements for a Postgraduate degree from the University of Saskatchewan, I agree that the Libraries of this University may make it freely available for inspection. I further agree that permission for copying of this thesis in any manner, in whole or in part, for scholarly purposes may be granted by the professor or professors who supervised my thesis work or, in their absence, by the Head of the Department or the Dean of the College in which my thesis work was done. It is understood that any copying or publication or use of this thesis or parts thereof for financial gain shall not be allowed without my written permission. It is also understood that due recognition shall be given to me and to the University of Saskatchewan in any scholarly use which may be made of any material in my thesis.

DISCLAIMER

Reference in this thesis to any specific commercial products, process, or service by trade name, trademark, manufacturer, or otherwise, does not constitute or imply its endorsement, recommendation, or favoring by the University of Saskatchewan. The views and opinions of the author expressed herein do not state or reflect those of the University of Saskatchewan, and shall not be used for advertising or product endorsement purposes.

Requests for permission to copy or to make other use of material in this thesis in whole or part should be addressed to:

Head of Department of Civil and Geological Engineering
University of Saskatchewan
Engineering Building
57 Campus Drive
Saskatoon, SK S7N 5A9

ABSTRACT

This thesis is focused around improving soil moisture estimates of spatial variability and mean at the field scale, which are useful for many different applications. The objectives were: (1) examine soil moisture spatial patterns and variability within field scale, and (2) compare field-scale soil moisture determination methods. An observational study was conducted, in which soil moisture was monitored over a 500^2 m^2 area during two and a half growing seasons at a prairie pasture in central Saskatchewan. Analysis of the spatial patterns of root-zone soil moisture revealed two distinct spatial patterns representing wet (spring) and dry (fall) periods. The relationship between spatial variability and mean soil moisture was found to follow an unusual concave trend, where variability was smallest at mid-range moisture contents. These spatial variability characteristics are a result of differences in participation level. Some locations were non-participating having only small moisture changes over the growing season, while others were dynamic having large changes. At the pasture site, these participation differences are a result of high soil heterogeneity, which may be characteristic of Solonetzic soils. In the second part of this thesis, methods to determine mean field-scale root-zone soil moisture were evaluated. The cosmic-ray neutron probe has the most potential for providing field-scale measurements. However, these measurements are only representative of moisture in the top 20 cm of soil, and need to be scaled up in order to represent the entire root-zone (0–110 cm). The three scaling methods applied to obtain lower root-zone soil moisture were: (1) a single time stable location, (2) representative landscape unit, where a single monitoring profile for each vegetation type was used, and (3) modeling by exponential filter. The representative landscape unit approach estimated soil moisture changes well, but not volumetric water content. The time stability method performed the best, followed by the exponential filter. However, the exponential filter has more potential, as the time stability method is difficult to apply to other field sites; particularly those without existing soil moisture instrumentation, due to its calibration requirements. The findings of this thesis make a contribution to the large body of existing literature on soil moisture variability and scaling. Suggestions for future research are provided.

ACKNOWLEDGEMENTS

I would first and foremost like to thank my supervisors Dr. Warren Helgason and Dr. Andrew Ireson. Their strong mentorship, advice, and encouragement throughout all stages of my research was invaluable. I would also like to thank my advisory committee members: Dr. Bing Si; Dr. Grant Ferguson; and my external examiner Dr. Jane Elliott for taking the time to critically evaluate my work.

Fieldwork was a major component of this project. I would personally like to thank Bruce Johnson, Dell Bayne, and Dr. Xicai Pan for their technical expertise and assistance with data collection. I appreciate the support of Dr. Brenda Toth and Erica Tetlock at Environment Canada for sharing their knowledge and lending equipment.

Funding for this research was provided by the Natural Sciences and Engineering Research Council of Canada (NSERC) through a discovery grant awarded to Dr. Andrew Ireson titled “Groundwater – surface water interactions in the prairies”, as well as the program of the Canada Excellent Research Chair at the Global Institute for Water Security, University of Saskatchewan.

The support of my fellow graduate students, lab group, and many other faculty and staff at the University of Saskatchewan is very much appreciated. I am particularly grateful for the educational discussions that we have shared.

Finally, I am blessed by the generous love and support of my family and close friends.

TABLE OF CONTENTS

LIST OF TABLES

LIST OF FIGURES

CHAPTER 1: INTRODUCTION

Although soil moisture accounts for an extremely small portion, about 0.15%, of the Earth's liquid freshwater (Shiklomanov and Sokolov 1983) it is of major importance in the partitioning of fluxes in both the water and energy cycle. In the hydrological cycle, the soil moisture status determines the partitioning of rainfall into runoff and infiltration. In semi-arid or arid environments, where water is limited, soil moisture is the primary control on evapotranspiration. In these types of environments, important interactions and feedbacks exist between soil moisture, climate (Seneviratne et al. 2010), and vegetation (Rodriguez-Iturbe et al. 1999). The variability of moisture available to plants influences plant growth, and therefore the spatial and seasonal vegetation patterns (Rodriguez-Iturbe et al. 1999). Estimates of soil moisture are therefore important for many types of hydrological, meteorological, and agricultural applications.

An early review of soil moisture estimation methods (Schmugge et al. 1980) identified that soil moisture estimations, to be most beneficial, need to be frequent, cover the entire root-zone (top 1–2 m), and be descriptive of moisture variability over large study areas. Even today, this need cannot currently be met by instrumentation alone and modeling is often used. Modeling in this case can refer to the upscaling of point measurements, the downscaling of coarse remotely sensed measurements, or the use of water balance models driven by meteorological data. To evaluate and improve these models, soil moisture data at a high monitoring frequency, and representing an intermediate scale such as field scale, will be needed. In addition to the enhancement of hydrological models, field scale monitoring of soil moisture can be important for improving our knowledge of hydrological fluxes (Vereecken et al. 2008), and in closing the water balance at small scales (Robinson et al. 2008).

In this thesis, field scale is defined as the size of the smallest watershed management unit. This management unit is specified by the Center for Watershed Protections to having an approximate area between 0.1 and 1 km^2 (Zielinski 2002). A gap in soil moisture monitoring techniques exist at this scale, which is thought by Robinson et al. (2008) to be partly due to the development of two main branches; point measurements and remote sensing. A need for intermediate scale soil moisture instrumentation has been created by increasing interest in hydrological and ecological processes at small watershed scales (Robinson et al. 2008), and in the quality control of remote sensing data; with intermediate scale soil moisture instruments being able to improve the spatial support of measurements within soil moisture networks (Crow et al. 2012).

The purpose of this research is to create knowledge that will improve estimates of root-zone soil moisture at the field scale. As a result, the following objectives were chosen:

1) Examine soil moisture spatial patterns and variability within the field scale, and;

2) Compare field scale soil moisture determination methods.

Data for this project was collected at a prairie pasture site in Central Saskatchewan during a two and a half year soil moisture monitoring program.

This thesis follows the manuscript style. Chapter 2 contains background information on soil moisture variability and current soil moisture instrumentation that will set the stage for the subsequent chapters. Chapters 3 and 4 are standalone manuscripts addressing objectives 1 and 2 as individual projects. Additional background information and a brief description of the methods are included at the beginning of these manuscripts. Chapter 5 is a synthesis and conclusion chapter tying the two manuscripts together. A single reference list will follow chapter 5. Appendix A contains an in depth summary of the soil moisture data, instrumentation, and calibration. Appendix B contains tables and figures supplemental to Chapters 3 and 4.

CHAPTER 2: BACKGROUND

2.1 Factors Controlling Soil Moisture Variability

Soil moisture is known to be highly variable in both space and time. Knowledge of soil moisture variability can be important in determining areas of similar hydrologic response for distributed models (Hawley et al. 1983), and in the interpretation of remote sensing data (e.g. Mohanty and Skaggs 2001; Jacobs et al. 2004). It is also important in the design of monitoring strategies; with the occurrence of high spatial variability implying that a larger amount of point measurements or samples are needed to determine field average (e.g. Hills and Reynolds 1969; Brocca et al. 2010a).

Many studies (e.g. Reynolds 1970; Gómez-Plaza et al. 2001; Mohanty and Skaggs 2001; Zhao et al. 2010; Biswas et al. 2012) have examined the association between potential controlling factors and the spatial variability. Such studies have been important steps in determining if knowledge of the spatial variability of these controlling factors can be used to predict soil moisture patterns. The factors to consider when examining soil moisture variability are dependent on the scale of interest. At the centimeter scale the local variations in particle and pore sizes become important (Hawley et al. 1983), while at very large scales it is the spatial variability of meteorological conditions, such as precipitation and solar radiation, which have the most control. At the intermediate or field scale, topography, vegetation and soil heterogeneity are the main factors controlling soil moisture (Reynolds 1970; Hawley et al. 1983; Mohanty and Skaggs 2001).

Topography is one of the most studied controls in the literature, likely due the large availability of topography data (Western et al. 2004). It was found to be the dominant controlling factor in studies by Henninger et al. (1976), Hawley et al. (1983) and three of the five sites in the study by Western et al. (2004). Its importance can be expected in hill slopes and valleys where the redistribution of water is topographically driven (Mohanty et al. 2000).

However, it was found by Western et al. (1999) that non-topographical controls usually account for over half of soil moisture variability, thus limiting the usefulness of predicting moisture content based on topographical indices.

Vegetation is important in determining the amount of transpiration that will occur. Plants can have deep roots, and therefore deplete soil moisture well below the surface. Generally, studies such as those completed by Hawley et al. (1983) and Gómez-Plaza et al. (2001) found that the presence of vegetation reduced the amount of spatial variability explained by topography and soil texture. Gómez-Plaza et al. (2001) did a comparison study between vegetated and non-vegetated land cover in a semi-arid region. The authors found that the dominant controls on soil moisture for the vegetated cover were upslope contributing area, aspect, and soil depth, while for the non-vegetated cover soil texture and slope were the most important factors. It was also found that seasonal changes in vegetation may cause changes to spatial variability (Reynolds 1970).

Soil heterogeneity is important in controlling the infiltration and water holding capacity of soil. Soil texture is the soil property commonly used in correlation studies, and it was found by Hawley et al. (1983) that within the same texture class, soil type variations are insignificant. In some environments, soil texture was found to be the factor with the highest correlation to soil moisture (e.g. Western et al. 2004; Biswas et al. 2012).

Other important factors controlling soil moisture variability are the initial (antecedent) soil moisture pattern, and the spatial variability of precipitation. Albertson and Montaldo (2003) demonstrated that spatial variability of soil moisture can be increased or decreased by considering the spatial variability of hydrological fluxes (i.e. infiltration or evapotranspiration) and the initial soil moisture state. Rainfall is often assumed to be homogeneous at the field scale. In cold regions, the largest contribution to recharge and runoff is from major snowmelt events. The influence of the spatial distribution of snow accumulation on soil moisture was found to be significant in the study by Williams et al. (2009), with the influence being highest in the spring and decreasing towards fall.

In summary, there have been many conflicting reports of which controlling factor is most important, and results are likely site specific. Quite often the use of multiple controlling factors is necessary to explain soil moisture variability (e.g. Western et al. 1999; Mohanty and Skaggs 2001; Biswas et al. 2012). Studies have also shown that although watersheds appear similar,

there may still be differences in the factors influencing the soil moisture spatial patterns (Mohanty and Skaggs 2001; Western et al. 2004). To complicate matters, these spatial patterns may also change with time. Controlling factors can be classified as either static or dynamic (Reynolds 1970), which alludes to the fact that some of these correlations may be temporally variable. The influence of the dominant soil moisture control can change seasonally, with seasonal changes being marked by vegetation changes (Reynolds 1970) or a switch between dry and wet conditions (Grayson et al. 1997). In Chapter 3, the temporal stability of spatial patterns of soil moisture at a prairie pasture site are examined. The results are described in the context of the controlling factors discussed here.

2.2 Soil Moisture Determination Methods

Soil moisture determination methods fall into one of two main categories; observations and models. Soil moisture measurements, if they exist at the appropriate resolution and scale, are ideal for many types of hydrological, meteorological, and agricultural applications. When there are no measurements available, or the measurements are not to the desired depth or resolution, models must be used.

Ground-based and remote sensing are the two main groups of soil moisture instrumentation. Ground-based, point-scale soil moisture instrumentation are the most commonly used type of instrumentation, due to its low cost. The main limitation of point measurement instrumentation is that, while it can be used to obtain high resolution profile measurements, it does not represent soil moisture spatially. Satellite remote sensing instruments, on the other hand, measure soil moisture at a large spatial scale, usually with a resolution greater than 100 km^2 (Crow et al. 2012). Limitations of satellite remote sensing also include a shallow measurement depth, typically the top 5 cm, and validation using the scaling of ground-based measurements (Crow et al. 2012). Because of the limitations associated with both satellite remote sensing and typical ground-based instrumentation (point-scale), there is a real need for soil moisture instrumentation that can provide measurements on an intermediate scale (Western et al. 2002; Robinson et. al. 2008). Existing methods for measuring intermediate scale soil moisture were recently reviewed by Robinson et al. (2008), Ochsner et al. (2013), and Vereecken

et al. (2014). While intermediate can refer to a large range of scales, this section will focus on ways to obtain soil moisture observations only at the intermediate scale relating to field scale. Several different measurement techniques are discussed.

a. Geophysical Methods

Geophysical methods are discussed in detail in the reviews of Robinson et al. (2008) and Vereecken et al. (2014). The main geophysical techniques that can be used to estimate soil moisture are ground penetrating radar (GPR), electromagnetic induction, and electrical resistance. These methods use the transmission and reflection times of electromagnetic waves in soil to determine soil water content. An advantage is that unlike remote sensing methods, geophysical methods can provide measurements up to several meters depth (Robinson et al. 2008). With mobile applications of GPR, detailed soil moisture maps of an entire field can be produced. A major disadvantage is that results of GPR are sensitive to all of the soil properties that influence electrical conductivity, such as differences in the mineral composition of the soil and the presence of dissolved salts (Doolittle and Collins 1995). This limits the range of soils for which GPR is suitable (Doolittle and Collins 1995).

b. Active and passive remote sensing

Remote sensing instruments are non-invasive techniques for measuring soil moisture, making them suitable for mobile applications. These types of remote sensing instruments measure the reflectance (active) or emission (passive) of radiation by the soil; which is largely controlled by the dielectric properties of the soil, and can therefore be used to give an estimate of soil moisture. The use of microwave radiometers (passive) and radars (active) attached to aircraft (e.g. Schmugge et al. 1974; Jackson et al. 1999; Ryu and Famiglietti 2005) can be used to obtain field scale soil moisture estimates and have been proven to be useful in mapping soil moisture over regional scales. Disadvantages of remote sensing are: the shallow measurement depth, and difficulties interpreting the signal due to the effect of vegetation and surface roughness (Robinson et al. 2008).

c. Cosmic-ray neutrons

Cosmic-ray neutrons are naturally produced through the collision of primary and secondary cosmic-rays with atmospheric and terrestrial nuclei (Simpson 1951; Desilets and

Zreda 2001). Cosmic-ray neutrons are considered to be fast neutrons. Fast neutrons are most effectively slowed by hydrogen, and as a result their levels can be related to moisture content. Early applications of cosmic-ray neutrons in hydrology were the measurement of water equivalent in snow packs (Kodama et al. 1979), and soil moisture (Kodama et al. 1985). However, in these studies by Kodama et al. (1979, 1985) the neutron detectors were placed inside the snow and soil which made the measurements applicable only at the point-scale.

Above ground, a cosmic-ray neutron probe can provides an areal average of soil moisture for a radius of ~330 m (Zreda et al. 2008), with an effective measurement depth of up to 30 cm for most soils (Franz et al. 2012a). Advantages of the cosmic-ray neutron probe is that it is insensitive to properties such as surface roughness, the physical state of the water, and soil properties (Desilets et al. 2010), such as texture, salinity and bulk density. A disadvantage of the cosmic-ray neutron probe is that it senses all water within the footprint (e.g. Desilets et al. 2010), such as surface water, water stored in biomass, precipitation, and water vapor. With calibration soil moisture can be separated from these other hydrogen sources. However, fast growing vegetation has been shown to affect measurement results (Rivera Villareyes et al. 2011; Hornbuckle et al. 2012).

d. Soil moisture campaigns

Soil moisture campaigns (i.e. spatial repetition of point measurements) have been widely used as a way to obtain high resolution soil moisture measurements at the field scale. During these campaigns large numbers of point soil moisture measurements are obtained by soil sampling, or the mobile use of point-scale instruments, such as time domain reflectometry (TDR) probes or theta probes. These soil moisture campaigns are generally used to obtain measurements of surface soil moisture only, and have been used in the validation of remote sensing instruments (e.g. Jackson et al. 1999; Mohanty and Skaggs 2001). Other studies have used soil moisture campaigns to investigate the spatial variability of soil moisture (e.g. Hawley et al. 1983; Western et al. 1999), and in exploring upscaling methods to reduce the number of point measurements required to obtain representative field average soil moisture (e.g. Hills and Reynolds 1969; Grayson and Western 1998; Brocca et al. 2010a).

e. Other

There are two other methods for measuring soil moisture at the field scale that have not been mentioned yet. These are global positioning system (GPS) multipath (Larson et al. 2010), and distributed temperature sensing (Striegl and Loheide 2012). These methods are discussed in detail in Ochsner et al. (2013). GPS multipath is capable of providing field scale measurements, but has a shallow measurement depth similar to that of active and passive remote sensing instruments (~5 cm). Distributed temperature sensing can estimate soil moisture at high spatial and temporal resolutions along a buried fiber optic cable.

In summary, there are several different techniques that can be used to provide measurements of soil moisture at the field scale. Each method has advantages and disadvantages associated with them. Soil moisture campaigns and geophysical methods are most suitable for examining soil moisture variability within field scale, however they would be time consuming and costly to continuously apply. The method with the most potential for monitoring average field scale soil moisture is the cosmic-ray neutron probe. The cosmic-ray neutron probe has a deeper measurement depth than active and passive remote sensing instruments. However, its measurement depth only represents up to 30% of the entire root-zone, which is considered to be the top meter of soil. To represent root-zone soil moisture, the cosmic-ray neutron probe needs to be coupled with upscaling methods. This is the focus of the manuscript in Chapter 4.

CHAPTER 3: SPATIAL PATTERNS AND CONTROLS

3.1 Preamble

This manuscript addresses the first objective, which was to examine soil moisture spatial patterns and variability within the field scale. Section 2.1 contained background information on the factors controlling soil moisture variability. This manuscript examines the spatial patterns of soil moisture at a prairie pasture site. It provides an explanation for these patterns and their stability with time.

3.2 Abstract

Temporal changes in the spatial patterns of root-zone soil moisture (0–110 cm) were analyzed for a semi-arid cold-region prairie pasture site using data collected over two and a half growing seasons. Distinct spatial patterns of root-zone soil moisture were found for early in the growing season (wet conditions) and late in the growing season (dry conditions). Spatial variability of root-zone soil moisture was lowest under intermediate wetness conditions. For comparison, surveys of surface soil moisture (0–6 cm) were also examined. Contrary to root-zone soil moisture, the spatial variability of surface soil moisture was highest for intermediate moisture conditions and lowest for extreme wet and dry conditions. Hence, the shape of the relationship between the mean soil moisture and the spatial variability changed as soil moisture was integrated over different depths. The unique spatio-temporal variability characteristics of root-zone soil moisture found in this study was attributed to the presence of several soil profiles for which the moisture content below the top 30 cm remained almost constant throughout the year. The physical attributes of these static or non-participating profiles are discussed.

3.3 Introduction

The fact that soil moisture varies greatly over a wide range of scales provides one of the most formidable challenges in hydrology. Quantification of the spatio-temporal variability of root-zone soil moisture is necessary for the accurate prediction of important hydrological fluxes (Vereecken et al. 2008). As such, representations of soil moisture variability in space are a necessary input for land–surface and hydrology models. Understanding spatial variability, and the associated controlling factors, is critical for correctly interpreting soil moisture information, particularly in the context of validating and downscaling large-scale remotely-sensed soil moisture products (e.g. Ryu and Famiglietti 2005; Choi and Jacobs 2007; Famiglietti et al. 2008), which are becoming increasingly available. Variability is also an important consideration in determining the best number of sampling points to estimate the spatial mean and reduce uncertainty (e.g. Hills and Reynolds 1969; Owe et al. 1982; Brocca et al. 2010a). Much of the previous research on the spatial characteristics of soil moisture has generally employed two different measurement approaches: (1) high resolution surface soil moisture campaigns over short time scales (e.g. Famiglietti et al. 2008), and (2) long-term networks of root-zone soil moisture with significantly fewer measurement locations (e.g. Takagi and Lin 2011; Kornelson and Coulibaly 2013). However, these two measurement techniques may provide different results for the exact same field site due to dissimilar trends in the variability-mean relationship which can exist for different observation depths.

The spatial variability of soil moisture changes in time due to spatial variations in hydrological fluxes (Albertson and Montaldo 2003), but can often be related to mean moisture content. The relationship between spatial variability and mean soil moisture is conceptually thought to follow a convex shape (Western et al. 2003), where spatial variability is highest for intermediate soil moisture conditions and lowest as the mean approaches wilting point or saturation. Field observations of the convex relationship (e.g. Owe et al. 1982; Choi and Jacobs 2007; Famiglietti et al. 2008; Rosenbaum et al. 2012; Kornelson and Coulibaly 2013) tend to be specific to surface soil moisture (0–5 cm), which is highly variable and often covers a wide range of moisture conditions. At deeper depths, trends of either increasing (e.g. Martínez-Fernández and Ceballos 2003; Takagi and Lin 2011) or decreasing (e.g. Hupet and Vanclooster 2002; Choi and Jacobs 2007; Kornelson and Coulibaly 2013) spatial variability with an increasing mean soil

moisture have been identified. The trends seen in these studies are generally still consistent with the conceptual convex variability-mean model; however, it is dependent upon whether the mean soil moisture is above or below a threshold that ultimately determines if the variability-mean relationship follows an increasing or decreasing trend (Pan and Peters-Liddard 2008). In general, trends of increasing variability with increasing mean soil moisture have been found in dry environments with low ranges of water content (i.e. 5-20% mean volumetric water content) (e.g. Martínez-Fernández and Ceballos 2003), while trends of decreasing variability with increasing mean soil moisture are found in wetter environments with high ranges of water content (i.e. 20-40% mean volumetric water content) (e.g. Hupet and Vanclooster 2002; Choi and Jacobs 2007; Kornelson and Coulibaly 2013). For a specific field site, the variability-mean relationship may also change with time, and has been shown to have a hysteresis effect (Ivanov et al. 2010; Rosenbaum et al. 2012), where different degrees of variability can exist for a single mean moisture content depending on whether the soil is in a wetting or drying phase.

Understanding the variability-mean relationship has been the focus of several modelling studies (Albertson and Montaldo 2003; Teuling and Troch 2005; Vereecken et al. 2007; Qu et al. 2015). Soil moisture variability can be either increased or decreased by considering the variability of hydrological fluxes and the initial soil moisture state (Albertson and Montaldo 2003). Teuling and Troch (2005) found observations of soil moisture variability and mean to be matched well using a simple physically-based model accounting for variations in vegetation, soil, and topography. Vereecken et al. (2007) demonstrated that the shape of the variability-mean relationship is largely controlled by the soil hydraulic properties and their spatial variability. Following up, Qu et al. (2015) compared estimates of the variability-mean relationship from a stochastic 1-D unsaturated flow model, using only soil properties, to field observations. The authors found the model provided a good estimate of the shape of the variability-mean relationship, but spatial variability was over or underestimated in some cases due to the importance of vegetation and topography in certain environments.

In addition to quantifying the spatial variability, understanding the temporal persistence of the spatial pattern of soil moisture, or the actual soil moisture representation in space can provide useful insight. A temporally stable spatial pattern is one where the ranking of soil moisture values for individual points in space remains constant with time (Vachaud et al. 1985).

Surface soil moisture is known to be highly variable, and the spatial pattern may have weak temporal stability even at short time scales (e.g. Mohanty et al. 2000; Mohanty and Skaggs 2001). However, spatial patterns of root-zone soil moisture have generally been found to display strong temporal stability (e.g. Kachanoski and de Jong 1988; Martínez-Fernández and Ceballos 2003; Biswas and Si 2011), sometimes over multiple years of measurement (Martínez-Fernández and Ceballos 2003; Biswas and Si 2011). A persistent soil moisture spatial pattern is expected when the dominant control on variability stays constant with time. For example, as a result of similar hydrological processes operating within a season (Martínez-Fernández and Ceballos 2003) spatial patterns may show intra-annual variability (e.g. Biswas and Si 2011), where stronger stability is seen when comparing spatial patterns from the same seasons, and less stability is seen when comparing the pattern from different seasons. Grayson et al. (1997) demonstrated the existence of two distinctly different preferred states that occur in areas with wet and dry seasons. The authors hypothesized that during wet seasons soil moisture is spatially organized due to non-local controls such as topography, and during dry seasons local controls such as soil properties and vegetation determine the spatial organization.

The main purpose of this study was to examine field-scale soil moisture dynamics at a pasture site in the Canadian prairies, focusing on: (1) the temporal stability of the soil moisture spatial pattern; (2) the relationship between the spatial variability and mean water content; and (3) the mechanism controlling these dynamics. Root-zone soil moisture is the main focus, but a brief comparison with data from surface soil moisture campaigns is provided to highlight how the spatial characteristics strongly depend on the depth of observation.

3.4 Materials and Methods

3.4.1 Field site

Data were collected from a grazing pasture (51° 22′ 54″ N, 106° 24′ 57″ W) located in central Saskatchewan, Canada. The prairie landscape is gently undulating, and the total topographic change over the 500^2 m^2 site is about 5 m (Figure 3.1b). The pasture is grazed during the warm months by cattle. Vegetation (Figure 3.1a) includes various Wheatgrasses (*Agropyron* sp.) and Needle grasses (*Stipa* sp.) with patches of Western Snowberry

(*Symphoricarpos occidentalis*), commonly referred to as Buckbrush. The climate is semi-arid and cold. Mean monthly air temperature (at Davidson, SK, 32 km east of field site) is -15.3 °C in January and 18.0 °C in July (Environment Canada 2014). Soils become frozen annually, and snow covers the ground for 5–6 months of the year. Average yearly precipitation is 377 mm, with 20% of this falling as snow (Environment Canada 2014).

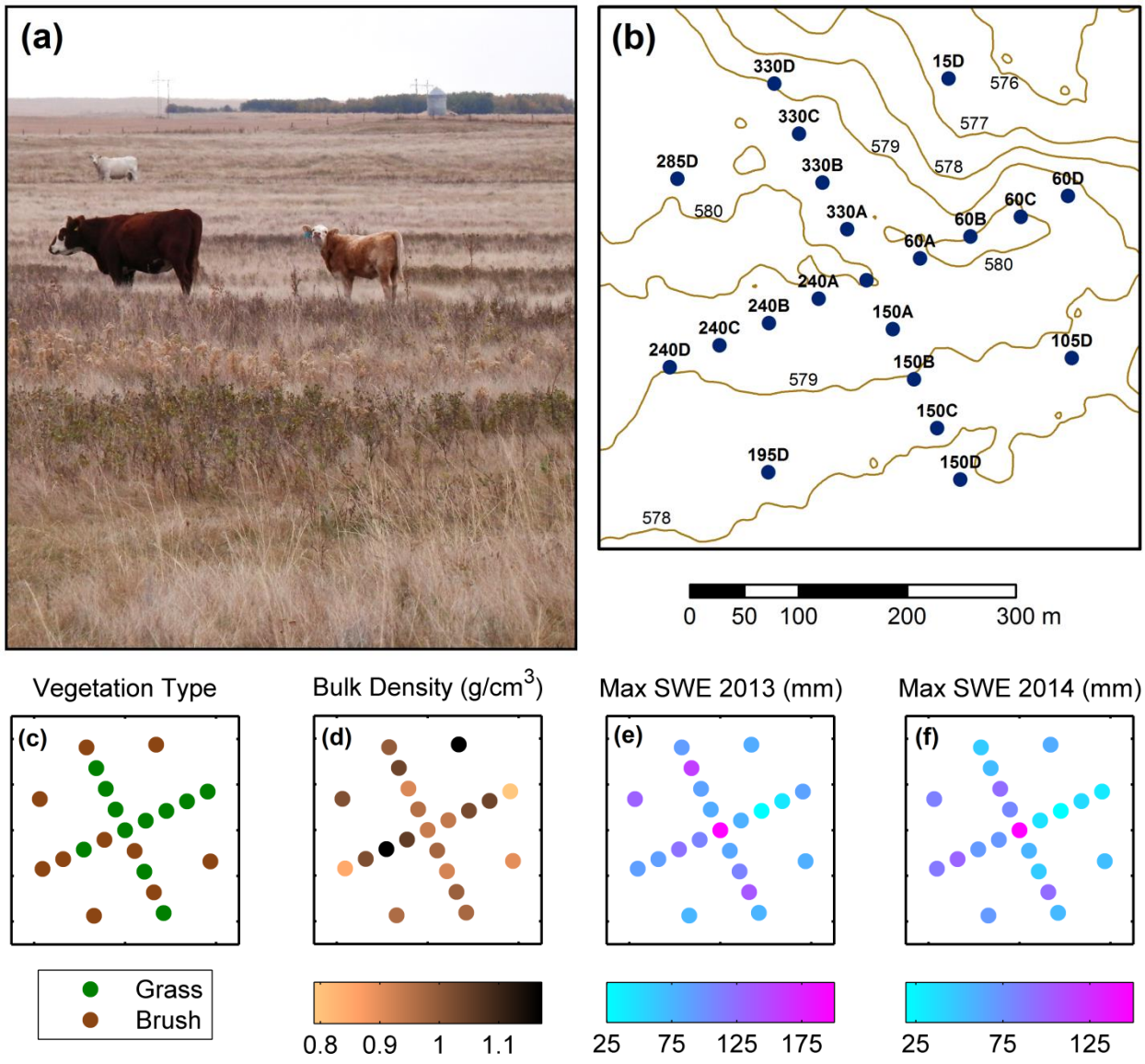

Figure 3.1 Description of pasture site and characteristics of neutron probe soil moisture monitoring locations, where (a) is a photo of pasture site, showing vegetation variability; (b) is a topography map showing soil moisture monitoring locations and names, contours are 1m; and (c-f) shows the vegetation type, average dry bulk density (0-80cm), and maximum snow water equivalent (SWE) of the monitored locations.

The soils of the pasture site and surrounding area are classified as part of the Rosemae Association (Ellis et al. 1970), which are predominantly dark brown Solonetzic soils that have been developed on medium to moderately fine textured glacial till. A recent review on Solonetzic soils was provided by Miller and Brierley (2011). The Solonetzic soil order has a distinctive high sodium and often clay-enriched B horizon with a prismatic or columnar structure that is of low permeability and very hard under dry conditions (Soil Classification Working Group 1998). Because of this dense B horizon, Solonetzic soils are often termed "claypan" soils (Sandoval and Reichman 1971). In the case of a thin A horizon, the hard claypan may be evident from randomly distributed barren or semi-barren patches on the landscape termed "scab-spots" (Sandoval and Reichman 1971); such "scab-spots" can also be seen at the pasture site. In Solonetzic soils, stunted vegetation may occur in spots due to a restricted rooting depth, and/or the nutritional deficiency of the soil (Cairns 1962). The Rosemae Association is often mapped in complex with the Chernozemic Weyburn Association (Ellis et al. 1970). In such cases, the Weyburn soils usually occur on the knolls and upper slopes. The local field soil has been classified, based upon a single soil pit in the center of the study site at a localized high spot in the landscape, as a dark brown Solonetzic Chernozem, in which the B horizon exhibits some of the features of a Solonetzic soil, but the structure is not fully characteristic of soils belonging to the Solonetzic Order. It is therefore likely that the pasture site has soils with both Solonetzic and Chernozemic characteristics, similar to the study site of Pennock et al. (1999), where soil heterogeneity is high and the low permeability Solonetzic B horizon is discontinuous or patchy across the landscape.

3.4.2 Data

Root-zone soil moisture was monitored at 21 locations (Figure 3.1b), with 50 m spacing along two transects. A neutron probe (CPN 503DR Hydroprobe, CPN International Inc., USA) was used to measure volumetric moisture content at 20 cm increments from 20–100 cm. A site specific calibration equation (RMSE = 0.018 cm^3/cm^3) was developed from soil samples taken during installation of the access tubes. The locations were given names containing a number and letter, which indicate the direction in degrees and distance from center respectively. Soil moisture was monitored from August 2012 to October 2014, on a bi-weekly (2012-2013) and

monthly (2014) basis. Measurements were taken only during the growing season (May-October), or warm months when soil was fully thawed.

Measurements were integrated over depth, and the average root-zone (0–110 cm) soil moisture for a single profile, $\theta_{(P)}$, is given by:

$$\theta_{(P)} = \frac{\sum_{j=1}^{n} \theta_j \cdot \Delta z_j}{z} \quad , \tag{3.1}$$

where θ_j is the volumetric water content for measurement depth j, Δz_j is the thickness of soil associated with the measurement depth, and z is the total averaging depth. Slightly more weighting was given to the soil moisture measurement at 20 cm, as it was used to represent a depth of 0–30 cm. All other measurement depths were set to represent a soil thickness of 20 cm. In addition to volumetric water content, moisture changes during the annual wetting and drying periods were also determined. The winter wetting period starts during the fall when soil moisture is at a minimum, and ends during spring when soil moisture reaches a maximum. By this definition, the wetting cycle includes changes due to snowmelt, as well as early spring and late fall rain. The summer drying period occurs between the wettest and driest soil moisture measurements within a year, where the majority of the change is due to evapotranspiration.

Characteristics of the root-zone monitoring locations are shown in Figures 3.1c–3.1f. Elevation was measured by differential, kinematic GPS (Leica GS-15, Leica Geosystems AG, Switzerland) during a topographic survey. Vegetation was assessed visually as grass or brush, and is descriptive a 2–3 m radius around the monitoring tube. Maximum snow water equivalent (SWE) was determined from snow depth and density measurements taken at the time of maximum accumulation using a snow core sampler (ESC30, Environment Canada, Canada). Dry bulk density for 0–80 cm was determined from volumetric samples taken during installation of the neutron probe access tubes. Soil resistance (results shown in section 3.5.5) was measured using a cone penetrometer (CP40II, Rimik, Australia) with a standard cone angle of 30° and a base surface cone of 1.3 cm^2 up to a depth of 75 cm. The resistance measurements were obtained on 1 May 2015 a couple weeks after snowmelt, when moisture conditions were high.

Surface soil moisture (0–6 cm) was measured over a 500 m by 500 m square grid, with a spacing of 20 m, using a dielectric moisture sensor (Hydra Probe II, Stevens Water Monitoring

Systems Inc., USA) connected to a data reader. The dielectric probes were attached to a pole that was carried to the monitoring location where it was inserted vertically into the soil to obtain a measurement. The factory supplied general loam calibration equation was used, which is expected to be accurate within ±0.04 cm^3/cm^3 (Seyfried et al. 2005). The center of the grid was located at the center of the neutron probe monitoring array. Measurements were taken on four different days to capture soil moisture under wet (1 May 2014), dry (14 August 2013), and intermediate (24 July 2013 and 27 July 2013) seasonal moisture conditions. Handheld GPS was used to locate the measurement positions. Due to the limited accuracy of the GPS, it is estimated that for a specific grid location the measurements taken at different times were within 5 m of each other.

3.4.3 Statistical analysis

Spatial patterns of soil moisture on different measurement days are compared against each other to determine their temporal stability. The strength of the temporal stability is measured using the Spearman rank correlation coefficient (Vachaud et al. 1985). This non-parametric coefficient is used to measure the strength of association between the ranking of two datasets that are non-linearly related, and/or are not normally distributed. It is defined as:

$$r_s = 1 - \frac{6 \cdot \sum_{i=1}^{n} \left(R_{i,t} - R_{i,k}\right)^2}{n \cdot (n^2 - 1)} \quad , \tag{3.2}$$

where n is the number of measurement points, $R_{i,t}$ is the rank of the observation value for point i, at measurement time t, and k represents a different measurement time. By this definition, temporal stability is a measure of the consistency of the rank order of observation points in terms of their wetness. High temporal stability indicates that the wettest locations remain the wettest, and the driest locations remain the driest.

The Spearman rank correlation coefficient was also used to examine the association between spatial patterns of soil moisture and possible controlling factors. In this case, the $R_{i,k}$ from Equation 3.2 is the rank of the observation value at point i for controlling factor k. The Spearman rank correlation coefficient ranges from 1 (perfect correlation or temporal stability) to -1 (perfect inverse correlation), with near zero indicating no association.

The spatial variability of soil moisture on a given measurement day is quantitatively described by the standard deviation. The relationship between spatial variability and mean water content was fit using a quadratic function. Changes in spatial variability with time were examined visually by comparing the spread of the distribution functions. Smoothed distribution functions were developed from sample histograms using a normal kernel function (Bowman and Azzalini 1997). This smoothing technique was applied to soil moisture distribution functions in the study by Ryu and Famiglietti (2005). The normal kernel function was found to provide a reasonable fit to histograms produced from the pasture data (Appendix B, Figure B.1).

3.5 Results

3.5.1 General patterns of variability

Depth (0–110 cm) and area (500 m diameter) averaged soil moisture, i.e. field-scale root-zone soil moisture, is shown in Figure 3.2a for the three growing seasons. The trend illustrated is typical of soil moisture in a semi-arid cold-region climate. Soil moisture is at a maximum at the start of the growing season due to infiltration of snowmelt and early spring rainfall events. Soil moisture decreases throughout the summer months, due to evapotranspiration, until it reaches a minimum in the fall. The rate of decrease, as well as variations between the three years, can be attributed to the frequency and magnitude of rainfall events (Figure 3.2b).

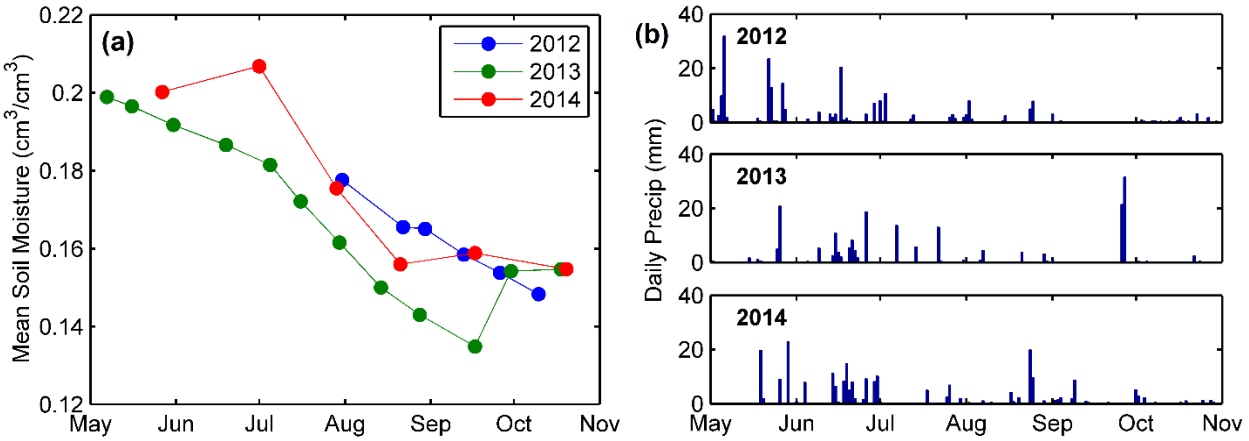

Figure 3.2 Mean root-zone soil moisture (0-110cm) and precipitation for 2012-2014.

Soil moisture variability with depth for individual monitoring locations and specific dates in 2013 are shown in Figure 3.3. Temporal variability of soil moisture is highest closer to the surface, and generally decreases with depth. Some locations show significant changes for all depths in the root-zone, while others (e.g. 60A, 60C, 240B, 330A, and 330C) only show temporal variability at shallow depths of 20–40 cm.

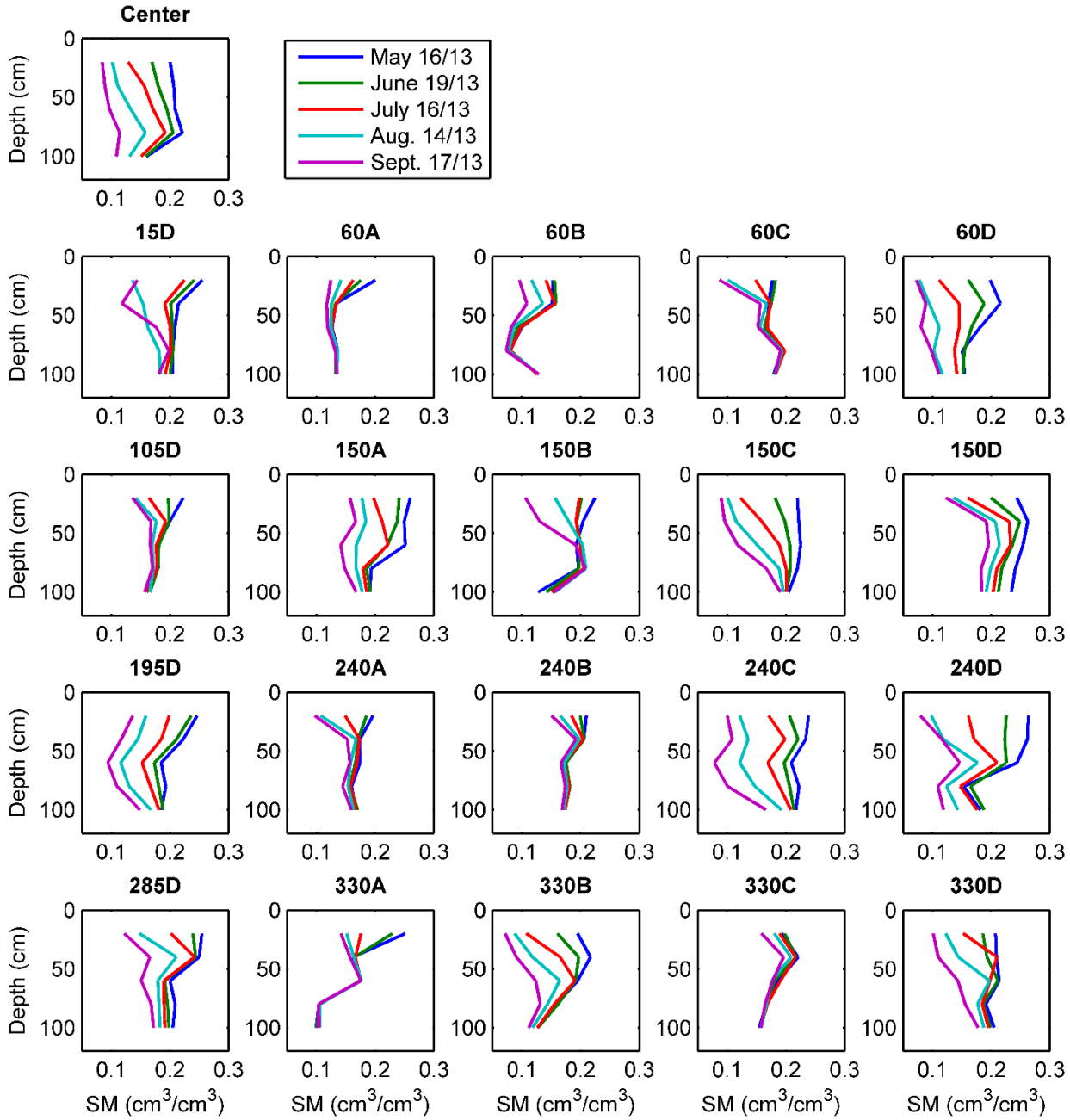

Figure 3.3 Spatial and temporal variability of soil moisture with depth, for select days in 2013.

Observations of surface (0–6 cm) soil moisture (Figure 3.4) are shown to be highly variable in space, with the highest variability occurring under intermediate conditions (24 July 2013) and the lowest variability occurring under extreme wet (1 May 2014) and dry (14 August 2013) conditions. Surface soil moisture is also more temporally variable than root-zone soil moisture (e.g. difference between 24 July 2013 and 27 July 2013) due to its high responsiveness to precipitation and evapotranspiration. It can also be seen from the maps that the spatial pattern of surface soil moisture has weak temporal stability. The only pattern that is stable is that the southeast corner appears to be consistently wetter than the rest of the field.

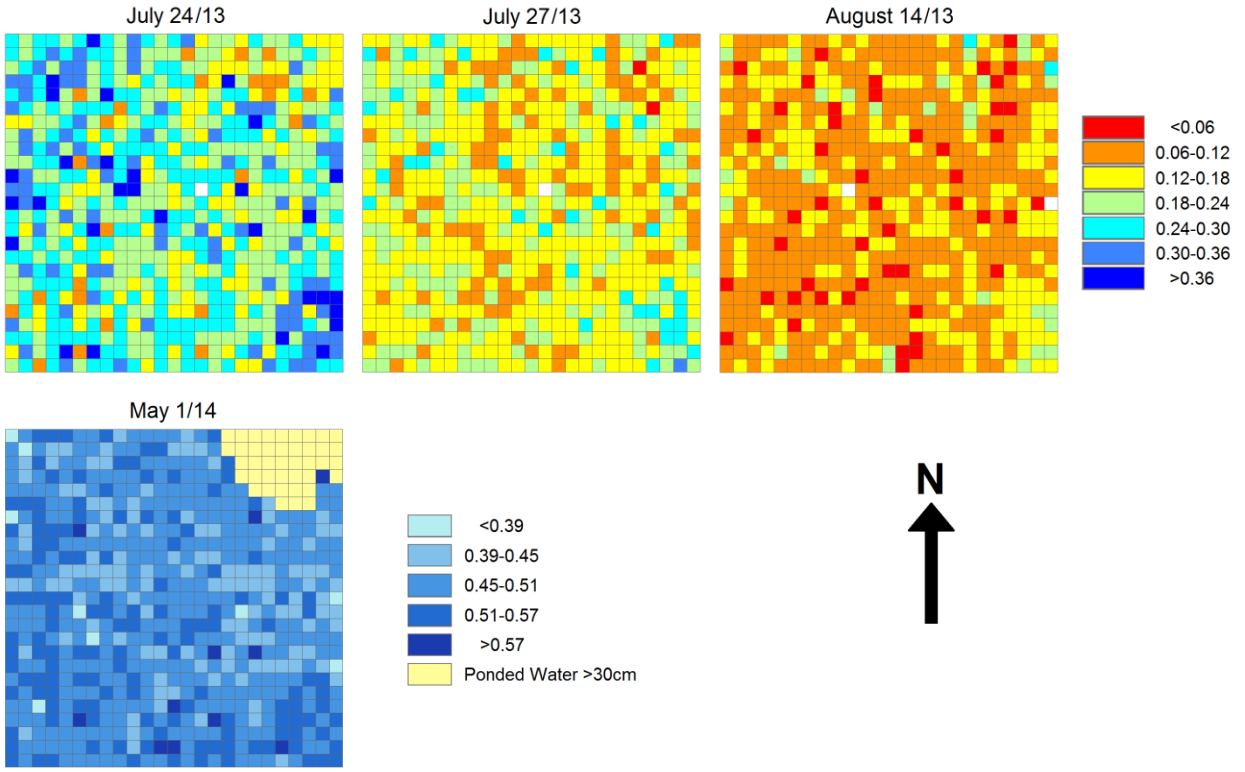

Figure 3.4 Maps of surface soil moisture (0-6cm) illustrating spatial variability of volumetric water content (cm^3/cm^3).

3.5.2 Temporal stability of spatial patterns

Large changes in volumetric water content occurred during the annual winter wetting and summer drying periods. By examining the spatial patterns of these soil moisture changes, areas of greater infiltration or transpiration can be identified. The temporal stability, or persistence of these patterns, was evaluated using the Spearman rank correlation coefficient (Table 3.1). Alternating signs are observed in the correlations, as the result of changes in adjacent seasons being in opposite directions (i.e. wetting is followed by drying). The strength of the correlations is high for all wetting and drying periods ($|r_s| > 0.7$), and statistically significant ($p < 0.01$). The strong positive correlations indicate similar spatial patterns of soil moisture changes during similar periods (i.e. both drying or both wetting). The strong negative correlations in adjacent seasons, i.e. those between a wetting and drying period, reveal that the locations with the largest increases or most positive changes during the wetting cycle also had the largest decreases or most negative changes during the drying cycle. These results imply persistence in the spatial ranking of the size of seasonal soil moisture changes.

Table 3.1 Temporal stability of the spatial pattern of soil moisture changes during the winter wetting (W) and summer drying (S) periods evaluated using the Spearman rank correlation coefficient.

	2012 S	12/13 W	2013 S	13/14 W	2014 S
2012 S	1				
12/13 W	**-0.74**	1			
2013 S	**0.76**	**-0.94**	1		
13/14 W	**-0.87**	**0.79**	**-0.90**	1	
2014 S	**0.91**	**-0.88**	**0.90**	**-0.93**	1

***p* < 0.01**

Diagrams of changes in root-zone soil moisture, ranked by magnitude of the change, are shown in Figure 3.5. Consistent with the correlation coefficient results, locations that have the smallest seasonal changes in soil moisture and those that have the largest changes were temporally stable over all wetting and drying periods. The locations with the small changes, i.e. those areas that experience minimal wetting in the spring, and minimal drying through the summer, are hereafter referred to as "non-participating" profiles. The non-participating profiles are: 60A, 60C, 240B, 330A, and 330C. The locations with large changes were termed "dynamic" profiles. The dynamic profiles are: Center, 60D, 150C, 195D, 240C, and 240D. The remaining locations had moderate seasonal soil moisture changes, and were placed in a separate category termed "medium" profiles. In Figure 3.3, the dynamic profiles are those that have notable soil moisture changes at all depths in the root-zone, while for the non-participating profiles soil moisture is shown to be relatively constant below a depth of 30 cm. This indicates that for non-participating profiles movement of water within the soil column in the up or down direction, i.e. through percolation or transpiration, is limited with depth. The change in volumetric water content for each monitoring location and season is shown in Figure 3.6, where considerable differences between each participation category are evident. In 2013 the total change of the non-participating profiles during the drying cycle was less than 4% volumetric water content, while the dynamic sites had a root-zone soil moisture change of 10% or more.

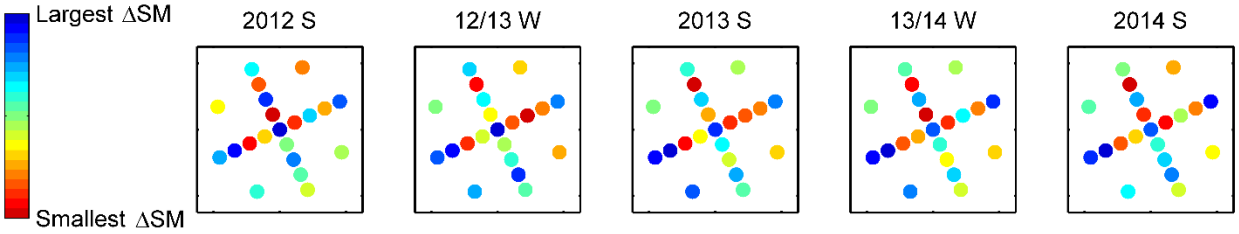

Figure 3.5 Maps of root-zone soil moisture changes ranked by magnitude, such that blue represents the largest soil moisture changes and red represents the smallest, for the winter (W) wetting and summer (S) drying periods.

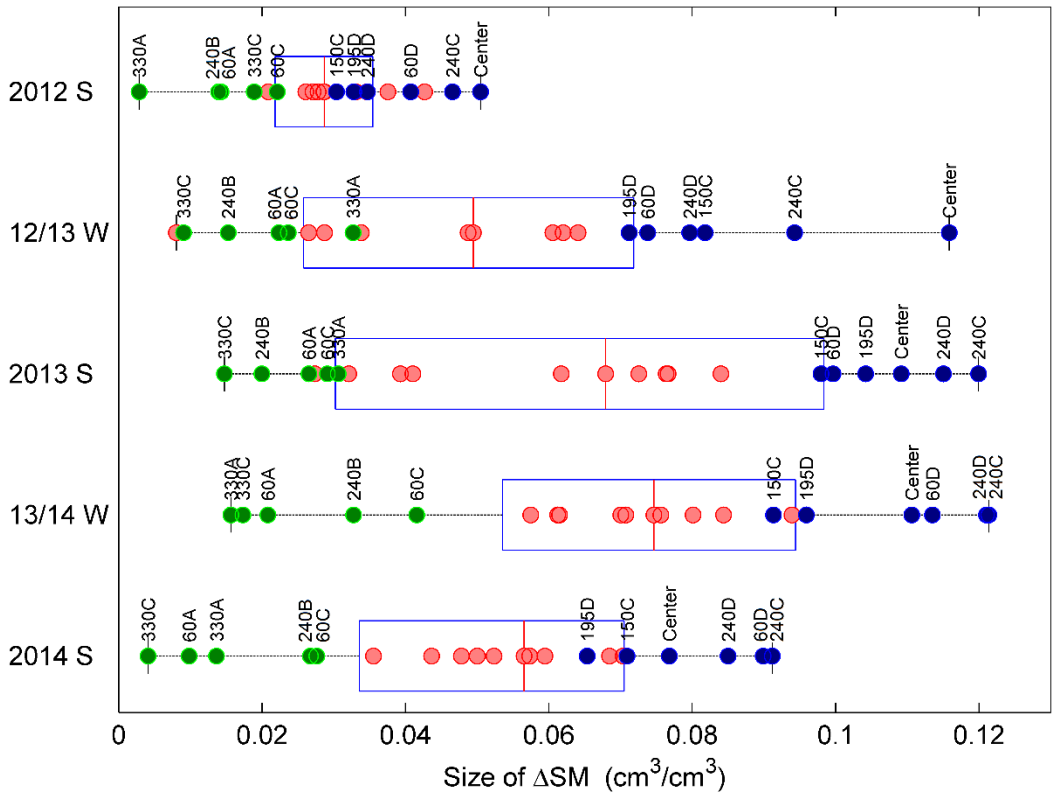

Figure 3.6 Seasonal soil moisture changes for the individual soil profiles, categorized as non-participating (green), medium (red), and dynamic (blue). Winter (W) changes are positive and summer (S) changes are negative, but here they are plotted on the same axis using the absolute value. The boxplot indicates the median (red line), 25th and 75th percentile (edges of the box), and minimum and maximum (extent of whiskers) values.

The temporal stability of the spatial patterns of volumetric water content was assessed for individual measurement dates using the Spearman rank correlation coefficients shown in Table 3.2. The correlation coefficients indicate strong seasonal spatial patterns or intra-annual variability. Dates have been categorized into early and late growing season, which also represent wet and dry moisture conditions, respectively. The switch between wet and dry conditions usually occurred mid-July. Shaded areas compare the same seasons (i.e. early growing season compared with early growing season, or late growing season compared with late growing season), and show strong correlation usually greater than 0.7. The non-shaded areas compare different seasons (i.e. comparing spatial patterns between early and late in the growing season), and generally show only moderate or weak correlation.

Table 3.2 Temporal stability of the spatial pattern of volumetric water content for early (blue) and late (red) in growing season evaluated using the Spearman rank correlation coefficient.

	Jul. 31/12	Aug. 22/12	Aug. 30/12	Sep. 13/12	Sep. 26/12	Oct. 10/12	May 7/13	May 16/13	May 31/13	Jun. 19/13	Jul. 5/13	Jul. 16/13	Jul. 30/13	Aug. 14/13	Aug. 28/13	Sep. 17/13	Sep. 30/13	Oct. 18/13	May 27/14	Jul. 1/14	Jul. 29/14	Aug. 21/14	Sep. 17/14	Oct. 20/14
Jul. 31/12	1																							
Aug. 22/12	**0.97**	1																						
Aug. 30/12	**0.96**	**0.99**	1																					
Sep. 13/12	**0.94**	**0.99**	**0.99**	1																				
Sep. 26/12	**0.92**	**0.98**	**0.99**	**0.99**	1																			
Oct. 10/12	**0.92**	**0.98**	**0.98**	**0.99**	**1.00**	1																		
May 7/13	**0.65**	**0.57**	*0.52*	*0.51*	*0.46*	*0.48*	1																	
May 16/13	**0.72**	**0.66**	**0.61**	**0.60**	*0.54*	*0.56*	**0.96**	1																
May 31/13	**0.74**	**0.68**	**0.63**	**0.62**	**0.57**	**0.59**	**0.95**	**0.99**	1															
Jun. 19/13	**0.84**	**0.80**	**0.76**	**0.75**	**0.71**	**0.72**	**0.92**	**0.97**	**0.97**	1														
Jul. 5/13	**0.85**	**0.82**	**0.79**	**0.78**	**0.74**	**0.74**	**0.87**	**0.93**	**0.94**	**0.98**	1													
Jul. 16/13	**0.87**	**0.86**	**0.84**	**0.83**	**0.80**	**0.80**	**0.69**	**0.78**	**0.79**	**0.88**	**0.93**	1												
Jul. 30/13	**0.82**	**0.84**	**0.84**	**0.84**	**0.82**	**0.82**	*0.54*	**0.64**	**0.66**	**0.77**	**0.83**	**0.96**	1											
Aug. 14/13	**0.70**	**0.75**	**0.76**	**0.78**	**0.76**	**0.76**	0.34	*0.45*	*0.47*	**0.58**	**0.63**	**0.82**	**0.93**	1										
Aug. 28/13	**0.70**	**0.78**	**0.79**	**0.82**	**0.81**	**0.81**	0.25	0.37	0.39	*0.53*	**0.58**	**0.78**	**0.90**	**0.97**	1									
Sep. 17/13	**0.69**	**0.78**	**0.81**	**0.82**	**0.84**	**0.84**	0.19	0.29	0.33	*0.46*	*0.52*	**0.72**	**0.85**	**0.92**	**0.97**	1								
Sep. 30/13	**0.67**	**0.73**	**0.73**	**0.75**	**0.74**	**0.74**	0.28	0.40	*0.43*	*0.54*	**0.60**	**0.79**	**0.91**	**0.93**	**0.94**	**0.93**	1							
Oct. 18/13	**0.69**	**0.75**	**0.75**	**0.77**	**0.76**	**0.76**	0.32	0.42	*0.46*	**0.57**	**0.62**	**0.81**	**0.92**	**0.94**	**0.95**	**0.94**	**0.99**	1						
May 27/14	**0.77**	**0.69**	**0.64**	**0.62**	**0.57**	**0.58**	**0.93**	**0.96**	**0.96**	**0.95**	**0.92**	**0.80**	**0.67**	*0.49*	0.40	0.34	0.43	*0.45*	1					
Jul. 1/14	**0.71**	**0.62**	**0.58**	**0.57**	*0.51*	*0.52*	**0.95**	**0.95**	**0.95**	**0.93**	**0.88**	**0.72**	**0.59**	0.36	0.28	0.25	0.37	0.39	**0.95**	1				
Jul. 29/14	**0.94**	**0.90**	**0.89**	**0.87**	**0.84**	**0.84**	**0.71**	**0.80**	**0.82**	**0.89**	**0.90**	**0.88**	**0.81**	**0.65**	**0.62**	**0.62**	**0.63**	**0.65**	**0.84**	**0.81**	1			
Aug. 21/14	**0.88**	**0.93**	**0.95**	**0.95**	**0.96**	**0.95**	0.42	*0.53*	**0.56**	**0.69**	**0.73**	**0.84**	**0.88**	**0.84**	**0.87**	**0.89**	**0.80**	**0.82**	*0.55*	*0.48*	**0.85**	1		
Sep. 17/14	**0.87**	**0.93**	**0.94**	**0.95**	**0.96**	**0.96**	0.41	*0.49*	*0.52*	**0.66**	**0.69**	**0.82**	**0.88**	**0.86**	**0.89**	**0.92**	**0.84**	**0.85**	*0.51*	*0.45*	**0.80**	**0.98**	1	
Oct. 20/14	**0.88**	**0.94**	**0.95**	**0.96**	**0.97**	**0.97**	0.40	*0.49*	*0.52*	**0.66**	**0.69**	**0.80**	**0.85**	**0.83**	**0.86**	**0.89**	**0.80**	**0.82**	*0.51*	*0.45*	**0.81**	**0.99**	**0.99**	1

$p < 0.01$ *$p < 0.05$*

3.5.3 Controls on spatial patterns

Spatial patterns of volumetric water content were compared with spatial patterns of a few of the potential controlling factors; again, using the Spearman rank correlation coefficient (Figure 3.7). The controlling factors considered were elevation, dry bulk density (0–80 cm average), and maximum snow water equivalent (max SWE). Elevation displayed the strongest correlation, between -0.7 and -0.6, but only in the spring when soil moisture was highest. The negative correlation indicates that locations with the lowest elevation tend to have the highest soil moisture. The strength of the correlation decreases as soil moisture is depleted throughout the growing season. Bulk density shows the opposite trend, where strength is weakest in the spring, and highest in the fall when soil moisture is driest. It was expected that there would be a high correlation between max SWE and water content at the beginning of the growing season, just after snowmelt. A high correlation in spring would suggest that meltwater from the snowpack had infiltrated where it accumulated, resulting in higher water contents at these locations. In 2014 the rank correlation between volumetric water content and max SWE was moderate in the spring, and decreased over the growing season. This decreasing trend was expected, because snowfall does not occur during the growing season and its association should decrease as the time from snowmelt increases. The expected trend was not seen in 2013. The rank correlation was weak in spring and changed very little over the growing season.

Spatial patterns between the magnitude of the soil moisture changes and potential controlling factors was assessed using the Spearman rank correlation coefficients in Table 3.3. Soil moisture changes from the winter wetting cycle had relatively equal correlation strength with elevation, dry bulk density, and max SWE. This indicates that these factors tend to have equal influences on spring infiltration at the pasture site. The magnitude of soil moisture changes from the drying cycle showed greater correlation with bulk density than with elevation. The negative bulk density correlation indicates that the locations with the largest changes in soil moisture tend to have the lowest bulk densities.

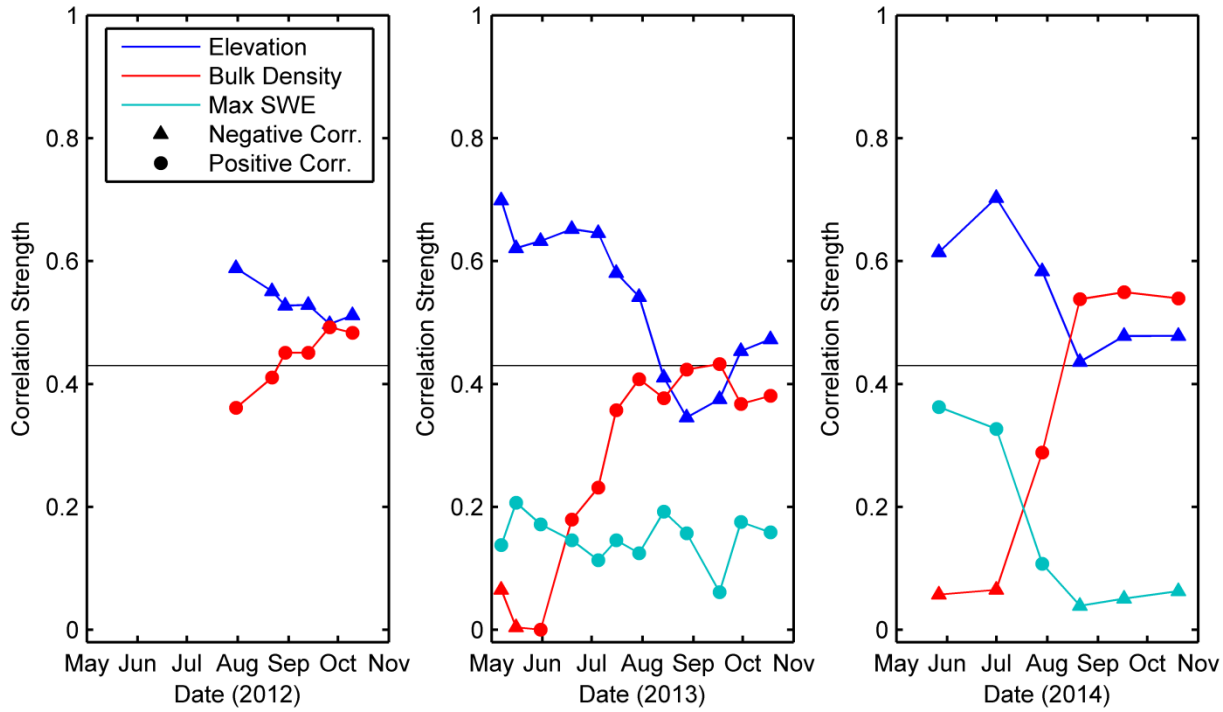

Figure 3.7 Seasonal changes in correlation strength between soil moisture and potential controlling factors, where correlation strengths above the black line are significant ($p < 0.05$).

Table 3.3 Spearman rank correlation between the size of soil moisture changes and possible controlling factors during the winter (W) wetting and summer (S) drying periods.

	12/13 W	13/14 W	2012 S	2013 S	2014 S
Elevation	-0.28	-0.17	-0.03	-0.31	-0.17
Dry Bulk Density	***-0.47***	-0.36	***-0.50***	***-0.44***	***-0.50***
Max SWE	0.35	0.36			

p < 0.05

3.5.4 Variability-mean relationship

The frequency distributions of root-zone volumetric water content for all measurement days are shown in Figure 3.8a. The frequency distributions display similar evolution each year. Standard deviation is smallest for intermediate soil moisture conditions, and largest under wet and dry conditions. This pattern is contrary to previously published patterns (e.g. Hupet and Vanclooster 2002; Martínez-Fernández and Ceballos 2003; Choi and Jacobs 2007; Takagi and Lin 2011; Kornelson and Coulibaly 2013). The anomalous behavior of these patterns were further investigated by considering the three previously described participation categories: non-participating, medium, and dynamic. The volumetric water content distribution of each category is shown against the distribution of all measurements in Figure 3.8b, for select days in 2014. The non-participating locations have mid-range soil moisture values that stay fairly constant in all soil moisture conditions. The dynamic profiles go from having high soil moisture to being some of the driest locations. All participation levels reach intermediate soil moisture at a similar time, and appear to contribute to the observation that soil moisture variability is smallest at intermediate range soil moisture conditions.

The frequency distributions of surface soil moisture from the hydra probe surveys (Figure 3.9) show an opposite seasonal evolution. Variability of surface soil moisture is smallest under extreme wet and dry conditions, and largest for intermediate conditions.

The temporal variability of the soil moisture patterns can be further explored by plotting the standard deviation of water content against the mean. Figure 3.10 shows the spatial variability-mean trends for different depths. The red lines show the best quadratic fit for the data. For 0–6 cm the relationship is convex, with the largest variability observed under intermediate soil moisture conditions. At 20 cm there is an almost linear negative relationship, with standard deviation increasing with decreasing moisture content. For depths greater than or equal to 40 cm the relationship is concave, with the smallest variability observed at mid-range soil moisture conditions. Concave relationships between standard deviation and mean moisture content are unusual, and are assumed to be due to the non-participating profiles. Soil moisture in the non-participating profiles are static at 40 cm (and deeper), which is the first depth that the concave relationship is seen.

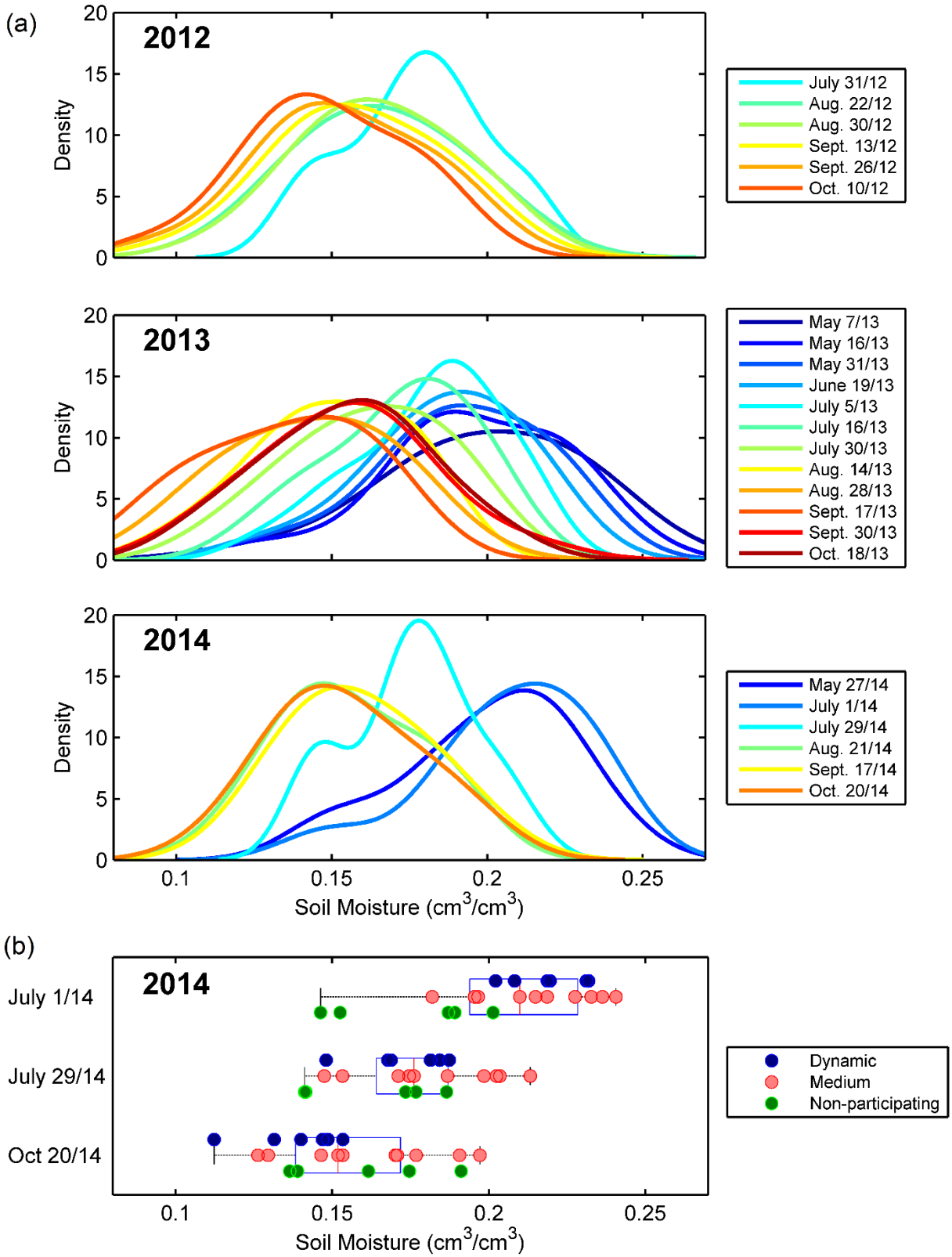

Figure 3.8 Kernel densities of root-zone soil moisture (n=21), showing (a) consistent patterns from 2012-2014, and (b) seasonal evolution connected to participation level.

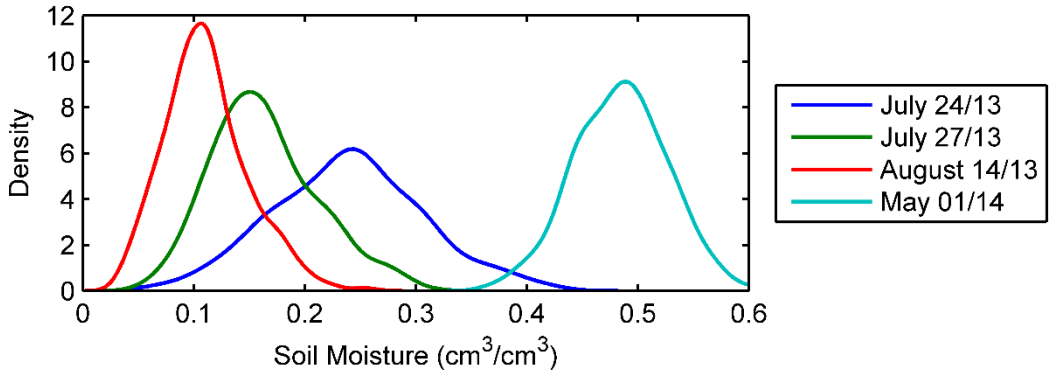

Figure 3.9 Kernel densities of surface soil moisture (n=625).

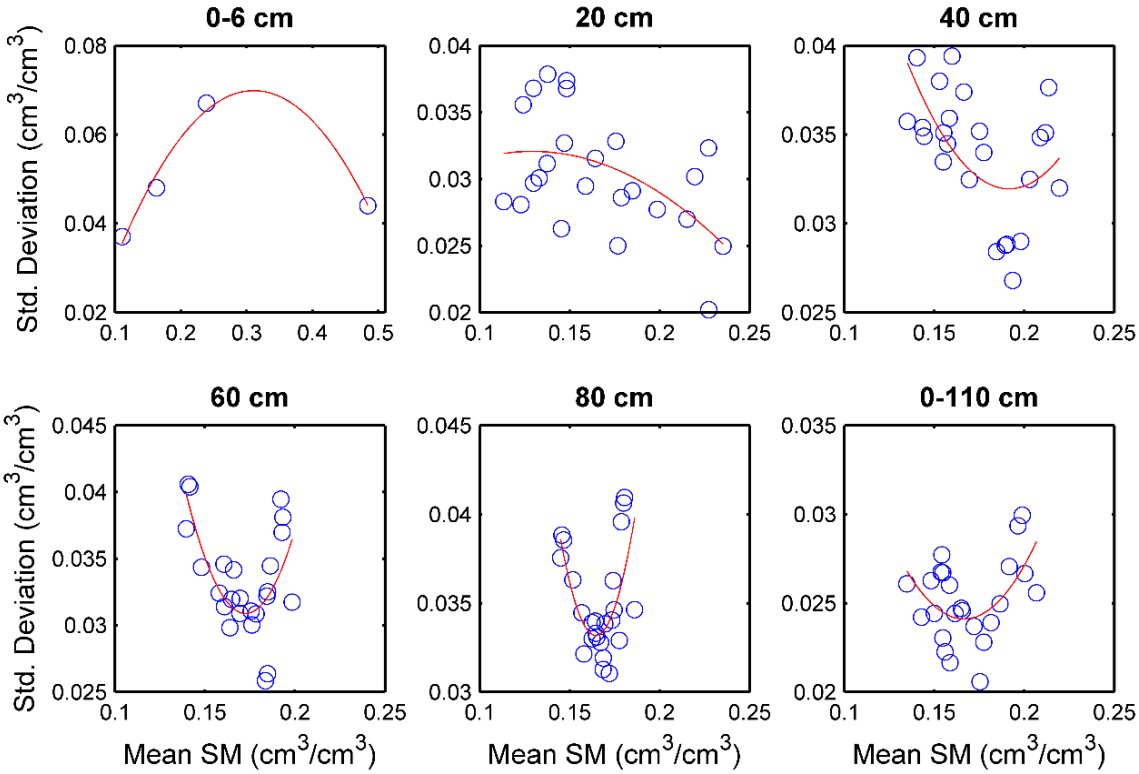

Figure 3.10 Relationship between spatial variability and mean water content with depth. Data was fit with a quadratic function to illustrate trend.

3.5.5 Characteristics of "non-participating" profiles

The non-participating profiles found at this field have a notable impact on the frequency distributions and temporal stability of the spatial patterns of root-zone soil moisture. The characteristics of the non-participating profiles, as compared to the rest of the profiles, are shown

in Figure 3.11. The characteristics measured at each location were vegetation type, dry bulk density (0–80 cm), elevation, and max SWE. These attributes may affect participation level at a specific location by influencing transpiration rates, soil water holding capacity and porosity, and infiltration of ponded and accumulated water, respectively. There is no clear separation of the locations based on these characteristics, but some clustering exists. The non-participating sites are shown to generally be at higher elevation than the dynamic sites (Figure 3.11). However, this may also partially be due to vegetation type, with grass vegetation tending to be associated with the higher topographic positions (Figure 3.1). All five of the non-participating sites are grass, while the majority of the dynamic sites (4 of 6) are brush. The other two dynamic sites are grass. One of these sites is at the center location, where a fence and additional instrumentation led to anomalously large accumulation of snow (Figure 3.11), and reduced grazing (due to fenced area) led to taller grass and higher transpiration losses. The other dynamic grass site, 60D, has the lowest bulk density of all the monitoring locations (Figure 3.11).

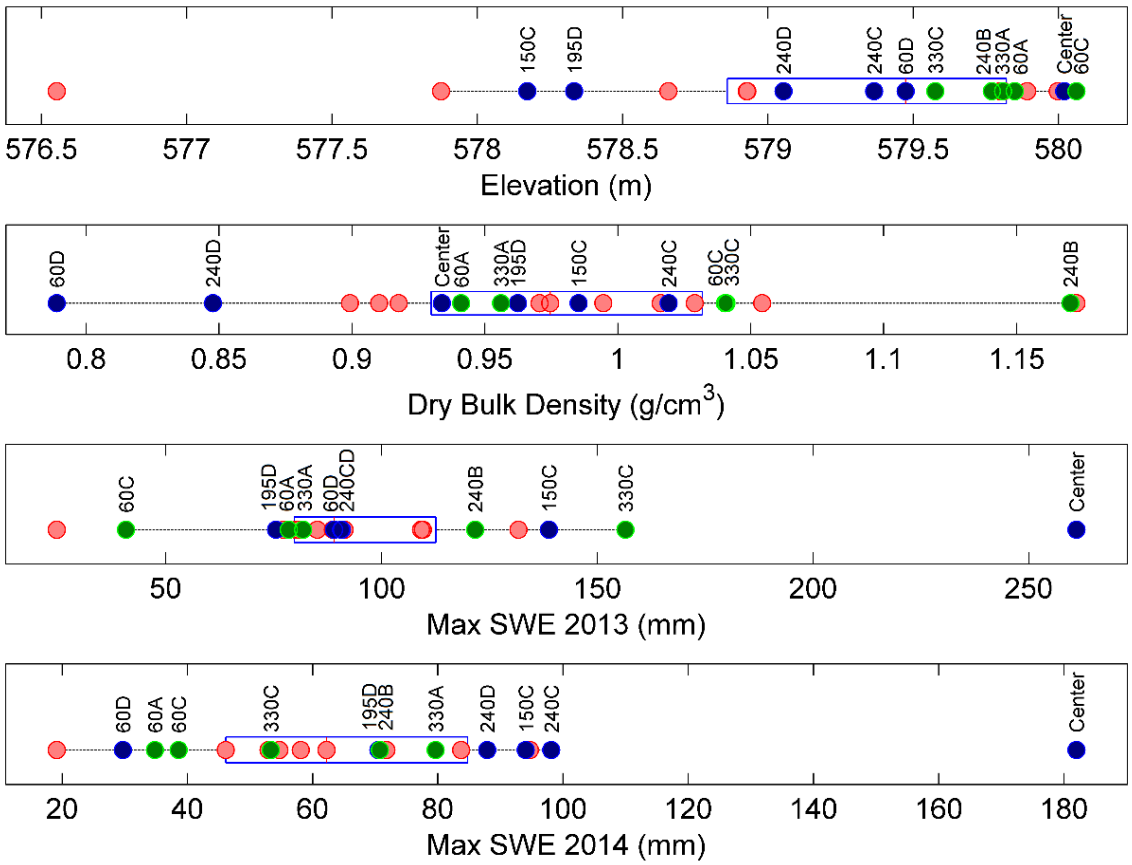

Figure 3.11 Characteristics of the soil moisture profiles grouped by participation level. The groups are non-participating (green), medium (red), and dynamic (blue).

The characteristics discussed so far provide limited insight into what makes a profile non-participating or dynamic at this field site. The ease of water transmission through the soil column is not well captured by using a profile average bulk density. Soil penetration resistance with depth for each of the profiles is shown in Figure 3.12. A high soil resistance would suggest a barrier to water. Solonetzic soils are known to have a higher penetration resistance than Chernozemic soils (Ayres et al. 1973; Pennock et al. 1999), and the amount of resistance can be linearly related to the sodium content of the B horizon (Pennock et al. 1999). Auguring tests (results not shown) were done in combination with the penetrometer measurements to provide further information. Hard claypans (dense Solonetzic B horizons) were present at locations 60C and 330A, with strong resistance seen at 20–30 cm (Figure 3.12). At the hard claypan, soil was dry and cracked. The locations of the hard claypans were found to be associated with patches of abnormally short stunted vegetation, termed scab-spots. The remaining non-participating profiles (60A, 240B, and 330C) were found to be comprised of clay, and sharp structural changes were evident at 240B (Figure 3.12). Half the dynamic profiles, particularly Center, 150C, and 195D, show low penetration resistance (< 2000 kPa) with depth. However, several profiles classified as medium participation, and one classified as non-participating (330C), also showed low resistance. Location 330C, although having low resistance at the tube itself, is on the edge of a scab-spot and moving towards the center yielded measurements of high resistance similar to 60C. In summary, the structure and composition of the soil profiles has a strong influence on which locations are non-participating, but profiles that are most dynamic may be due to a combination of factors.

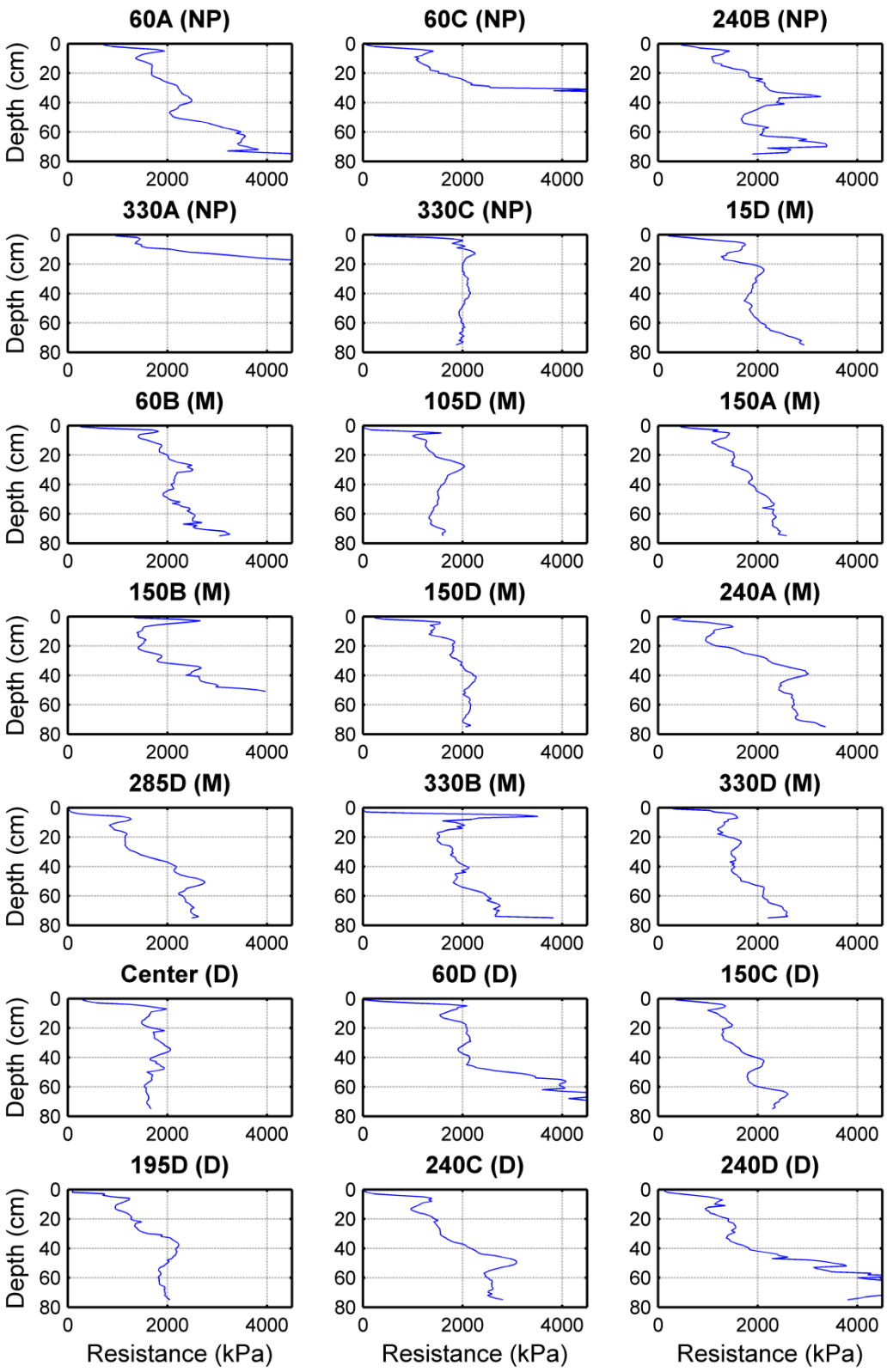

Figure 3.12 Soil resistance with depth for individual profiles. Results are an average of 3-5 measurements taken within a couple meters of the neutron probe tube. The profiles are grouped by their participation level and labeled as NP for non-participating, M for medium, and D for dynamic.

3.6 Discussion

The spatial pattern of volumetric water content exhibited strong temporal stability within seasons (Table 3.2). The spatial organization of spring moisture from 2013 was strongly correlated with 2014 spring patterns and weakly correlated with 2013 fall patterns. Biswas and Si (2011) identified similar intra-annual stability for root-zone soil moisture. However, they found strong temporal stability over the entire record (all $r_s > 0.75$); so although there would have been differences in the spatial pattern between spring and fall, they were minor. At the pasture site, the spatial pattern in the spring (wet conditions) was most strongly correlated with topographic controls, while the fall pattern (dry conditions) was most strongly associated with dry bulk density, which may be considered a proxy to other soil properties (such as texture and water holding capacity and porosity). In this way, these findings appear to support the hypothesis by Grayson et al. (1997), that a non-local control (i.e. topography) determines the spatial organization of soil moisture for wet conditions, while local controls (e.g. soil, vegetation) have the most influence during dry conditions. It is important to note that correlation between water content and the examined potential controlling factors is only moderate at best, with the highest observed correlation strength to topography and bulk density being -0.7 and 0.5, respectively (Figure 3.7). Indeed, great care needs to be taken when examining controlling factors as correlation does not necessarily mean causation. The correlation trends and values, in this case, may be influenced by the existence of the non-participating profiles. At this field site, monitored non-participating profiles tended to be at higher elevations (Figure 3.11), and their volumetric water content was generally lowest in spring (Figure 3.8b). The perceived influence of topography on spring soil moisture patterns, from the calculated correlation coefficient, may therefore be over exaggerated. The same conclusion about bulk density and max SWE cannot be made because the monitored non-participating profiles did not show a similar clustering of these attributes towards high or low values. In summary, the topographic (non-local) control is not likely as strong as initial results would indicate. The temporal persistence of the non-participating and dynamic soil profiles themselves, as opposed to the switch between non-local and local controls, provides a better explanation for the two distinct spatial patterns and persistent intra-annual variability.

The spatio-temporal variability of root-zone soil moisture was found to be quite different from surface soil moisture. Surface soil moisture measurements covered a range of moisture contents from extreme dry to extreme wet conditions. For surface soil moisture, the relationship between spatial variability and mean had the expected convex shape, with spatial variability highest at mean intermediate soil moisture conditions and lowest in extreme wet and dry moisture conditions. Root-zone soil moisture varied over a much smaller moisture range (0.1–0.25 cm^3/cm^3), and illustrated a quite different concave variability-mean relationship, with spatial variability smallest for mid-range moisture conditions. Differences amongst the trend of the variability-mean relationship between surface and deeper measurements in the root-zone were also found by others (Choi and Jacobs 2007; Rosenbaum et al. 2012; Kornelson and Coulibaly 2013); however none found a concave variability-mean relationship. It is important to note again that a concave shaped variability-mean relationship is different from many previously published trends (e.g. Hupet and Vanclooster 2002; Martínez-Fernández and Ceballos 2003; Choi and Jacobs 2007; Takagi and Lin 2011; Rosenbaum et al. 2012; Kornelson and Coulibaly 2013). However, there has been at least one study where concave variability-mean trends were seen (i.e. Figure 6 of Famiglietti et al. 2008). The trend was for surface soil moisture, and it is unclear what the cause of this may have been. The idea of a concave shaped trend describing the true relationship between soil moisture spatial variability and spatial mean does not exist at present, which may be the main reason it is not seen very often, or is not well discussed, in published literature.

In the current study, root-zone soil moisture had a consistent concave variability-mean trend each year, with the spatial variability being smallest at mid-range moisture content (~0.18 cm^3/cm^3) and largest for wet (~0.22 cm^3/cm^3) and dry (~0.14 cm^3/cm^3) conditions (this is most clearly shown for the 2014 data; Figure 3.8). At the pasture site, the main reason for this consistent trend is the presence of the non-participating profiles. The dynamic profiles tend to have high volumetric water content in the spring and low volumetric water content in the fall (Figure 3.8b). The non-participating locations stay at very similar volumetric water content throughout the whole year. Hence, as the dynamic profiles dry, they "cross-over" the water content of the non-participating profiles, leading to a temporary suppression of field-scale variability.

Locations of strong and weak soil moisture dynamics were persistent over multiple years for both the winter wetting and summer drying period. This explained the strong intra-annual variability and two distinct spatial patterns, as well as the unique concave shape of the spatial variability-mean relationship. The hypothesis is made that other environments or land uses with similar spatio-temporal moisture characteristics as the ones seen here may also have a significant number of both dynamic and non-participating soil moisture profiles. In order to create long-term differences in participation amongst soil profiles, soil heterogeneity must be high. The pasture site in this study has high soil heterogeneity and may be particularly susceptible to having non-participating profiles, due to grazing and the presence of Solonetzic soils. Non-participating profiles are those that have limited infiltration and evapotranspiration at all points in the year. Trampling from grazing is known to increase bulk density and soil strength (Chanasyk and Naeth 1995) and reduce soil organic carbon (Zhao et al. 2007), which both lead to reduced infiltration (Naeth et al. 1990; Zhao et al. 2007). Solonetzic soils are particularly heterogeneous in nature (e.g. Carter and Pearen 1985; Sandoval and Reichman 1971; Pennock et al. 1999). Weak spatial dependence was found amongst 5 m sampling intervals by Carter and Pearen (1985), in terms of the thickness of the A horizon and the extractable sodium in the B horizon. Related to the thickness of the A horizon, infiltration rates over Solonetzic soils are also variable within short distances (Sandoval and Reichman 1971).

In this study, non-participating locations were associated with poor soil structure, particularly hard claypans, poorly drained clays, or sharp structural changes. The persistent differences in participation amongst the soil profiles at the pasture site were largely due to the presence of Solonetzic soils, while grazing likely only had a minor influence. Field sites located ~100 km north in Chernozemic soils (Kachanoski and de Jong 1988; Biswas and Si 2011) did not have similar spatio-temporal soil moisture characteristics. With only one distinct spatial pattern of root-zone soil moisture present over time periods of one (Kachanoski and de Jong 1988) and four (Biswas and Si 2011) years, it can be assumed there were no major differences in participation level amongst the soil moisture profiles. The spatio-temporal characteristics of root-zone soil moisture seen in the present study, that is intra-annual spatial patterns and a unique concave shape for the variability-mean relationship, may be specific to Solonetzic soils. Solonetzic soils account for 11–13 million ha in the Great Plains Region of Canada and the United States (Sandoval and Reichman 1971; Miller and Brierley 2011). This soil type has been

given other names, such as Solonetz, alkali soils, and sodic soils. Solonetzic soils cover 135 million ha worldwide (Driessen et al. 2001), with major areas also present in Australia, Ukraine, and Russia. It is possible that the results of this study may be applicable to other soils as well, such as those with an impeding or low permeability layer due to other reasons besides sodicity.

3.7 Conclusion

Soil moisture variability was examined at a prairie pasture site using two and a half years of data. The main spatio-temporal characteristics of root-zone soil moisture at the site were found to be: (1) intra-annual variability, with two distinct spatial patterns representing early and late in the growing season (and/or wet and dry moisture conditions); and (2) an unusual concave variability-mean relationship, where spatial variability was highest at mid-range mean water content. Changes in the spatial patterns of soil moisture with time were explained by distinct differences in participation amongst the soil profiles; specifically, the presence of highly dynamic profiles alongside those where the water content was practically static. The latter were termed non-participating, due to their limited soil water dynamics. The depth of soil examined proved to be important. Non-participating locations were first noticeable in moisture measurements at 40cm depth, and shallower layers did not exhibit the same spatio-temporal characteristics. The persistence of the dynamic and non-participating soil profiles for both the winter wetting and summer drying period were demonstrated as the dominant control on the temporal evolution of the spatial moisture patterns. The long-term differences in participation are due to the high soil heterogeneity associated with Solonetzic soils. The non-participating profiles were found to have poor soil structure, particularly a dense claypan, poorly drained clays, or sharp structural changes. Other locations exhibiting the same spatio-temporal characteristics may also have significant differences in participation level. Further research is needed to better understand the influence of non-participating profiles on soil moisture spatial and temporal variability, and determine the extent of their existence in other environments.

CHAPTER 4: ESTIMATING MEAN SOIL MOISTURE[1]

4.1 Preamble

This manuscript addresses the second objective, which was to compare field scale soil moisture determination methods with respect to the quality of the estimate. The cosmic-ray neutron probe was identified in Section 2.2 as the instrument with the most potential for measuring field scale soil moisture. This manuscript builds upon the material presented in Chapter 2, by evaluating different field-scale root-zone estimation methods that utilize the shallow moisture measurements from the cosmic-ray neutron probe.

4.2 Abstract

Many practical hydrological, meteorological and agricultural management problems require estimates of soil moisture with an areal footprint equivalent to field scale, integrated over the entire root-zone. The cosmic-ray neutron probe is a promising instrument to provide mean field-scale soil moisture, but these observations are shallow and require depth scaling in order to be considered representative of the entire root zone. A study to identify appropriate depth-scaling techniques was conducted at a grazing pasture site in central Saskatchewan, Canada over a two year period. Area-averaged soil moisture was assessed using a cosmic-ray neutron probe. Root zone soil moisture was measured at 21 locations within the 500^2 m^2 area, using a down-hole neutron probe. The cosmic-ray neutron probe was found to provide accurate estimates of field scale surface soil moisture, but accounted for less than 40% of the seasonal change in root zone storage due to its shallow measurement depth. The root zone estimation methods evaluated were: (1) the coupling of the cosmic-ray neutron probe with a time stable neutron probe

[1] This manuscript has been published in Peterson, A. M., Helgason, W. D., and Ireson, A. M. 2015. Estimating field scale root zone soil moisture using the cosmic-ray neutron probe. Hydrology and Earth System Sciences Discussions, 12: 12789-12826. doi:10.5194/hessd-12-12789-2015. Minor modifications have been made.

monitoring location, (2) coupling the cosmic-ray neutron probe with a representative landscape unit monitoring approach, and (3) convolution of the cosmic-ray neutron probe measurements with the exponential filter. The time stability method provided the best estimate of root zone soil moisture (RMSE = 0.004 cm^3/cm^3), followed by the exponential filter (RMSE = 0.012 cm^3/cm^3). The landscape unit approach, which required no calibration, had a negative bias but estimated the cumulative change in storage reasonably. The feasibility of applying these methods to field sites without existing instrumentation is discussed. It is concluded that the exponential filter method has the most potential for estimating root zone soil moisture from cosmic-ray neutron probe data.

4.3 Introduction

Root-zone soil moisture stored in the top meter of the unsaturated zone is an important regulator of both the hydrological and energy cycle. It places an important control on evapotranspiration in water limited environments, and influences the partitioning of latent and sensible heat, having a marked effect on the near-surface state of the atmosphere. Soil moisture is a state variable in the water balance equations of many hydrological, meteorological, and agricultural models; thus accurate observations of root-zone soil moisture over large spatial extents are indispensable for model validation (Grayson and Western 1998), and for run-time assimilation (e.g. Brocca et al. 2010b). At very large scales, active and passive remote sensing instruments attached to satellites (e.g. the Soil Moisture and Ocean Salinity (SMOS) mission) have the potential to measure soil moisture globally (Kerr et al. 2010), but have coarse resolutions (35–50 km). Soil moisture observations at finer scales, such as field scale (0.1–1 km^2), are often required for understanding hydrological processes (e.g. water balance studies) or for use in agricultural applications (irrigation scheduling, crop water use monitoring, etc.). The cosmic-ray neutron probe uniquely fills the measurement scale gap between remote sensing techniques and point-scale observing methods, providing observations of average soil moisture for a ~300 m radius footprint (Zreda et al. 2008). Cosmic-ray neutron probes have been shown to be successful in measuring field-scale soil moisture in a variety of environments and regions (e.g. Rivera Villarreyes et al. 2011; Franz et al. 2012b; Bogena et al. 2013; Hawdon et al. 2014), and have potential for validating remote sensing data (Crow et al. 2012; Hornbuckle et al. 2012; Dong et al. 2014). The cosmic-ray neutron probe holds great promise; however the effective

measurement depth is less than 30 cm for most soils (Franz et al. 2012a), requiring upscaling with depth to be representative of the entire root-zone.

In this study, the depth of the field-scale cosmic-ray neutron probe measurements is extended by coupling with an estimate of the deeper root-zone soil moisture that has been determined by two main approaches: (1) upscaling point measurements, and (2) modeling.

The three methods considered to upscale the deeper point-scale measurements to the same areal extent as the cosmic-ray neutron probe were: (1) averaging of multiple point-scale measurements, (2) using a single time stable measurement location to represent the large-scale spatial average, and (3) disaggregating the larger area into a few landscape units which can be represented by single monitoring locations. Multi-point averaging is the simplest way to upscale a network of point measurements. With a large number of measurement points this method can be accurate; however, to implement such a monitoring scheme in practice is often not feasible. The other methods allow soil moisture to be monitored from a reduced amount of locations. In the time stability approach, a single site having a soil moisture response similar to that of the areal average is used to estimate the field-scale moisture content. Since the method was first proposed by Vachaud et al. (1985), time stable sites have been found in a variety of environments (e.g. Grayson and Western 1998; Mohanty and Skaggs 2001; Teuling et al. 2006; Brocca et al. 2010a; Zhao et al. 2010; Gao et al. 2013). However, this approach often requires extensive investigation in order to identify a time stable soil moisture location (Teuling et al. 2006). In the landscape monitoring approach, the number of point measurements needed to estimate field-scale soil moisture is reduced to the number of representative landscape units. Landscape features that influence the spatial variability of soil moisture, such as vegetation and topography, are relatively easy to visually assess (Hawley et al. 1983) and form a convenient conceptual model from which to build a simplified soil moisture monitoring strategy. However, the usefulness of this method may be limited due to a number of factors: (1) soil properties may be the dominant control (e.g. Western et al. 2004; Biswas et al. 2012), and they are hard to measure spatially; (2) topography may also be of limited use, as Western et al. (1999) determined that terrain indices will only be able to predict up to 50% of the spatial variability of soil moisture; and (3) quite often the use of multiple influential factors is needed to explain soil moisture variability (e.g. Western et al. 1999; Mohanty and Skaggs 2001; Biswas et al. 2012).

The assimilation of remotely sensed near surface soil moisture data into water balance models to obtain profile soil moisture has been frequently studied (e.g. Ragab 1995; Calvet and Noilhan 2000; Walker et al. 2001; Heathman et al. 2003). Some of these models were shown to provide good results, but often require meteorological data as well as information on soil properties and vegetation cover. Cosmic-ray neutron probe data has also been assimilated into models with similar complexity, such as the NOAH land surface model (Shuttleworth et al. 2013; Rosolem et al. 2014), Community Land Model (Han et al. 2015), and HYDRUS-1D (Rivera Villareyes et al. 2014). In the present study, the cosmic-ray neutron probe data was combined with a simpler modeling approach, termed the exponential filter method or soil water index (SWI) method. This method, introduced by Wagner et al. (1999), is based on a two layer soil water balance. The soil moisture of the deeper layer (layer 2) is estimated as a function of the previous layer 2 estimate and the current surface (layer 1) soil moisture measurement; the importance of these two terms are determined by an exponential filter. The exponential filter model has been applied to data from: the ERS Scatterometer (Wagner et al. 1999; Ceballos et al. 2005), ASCAT (Albergel et al. 2009) and SMOS (Ford et al. 2014).

The following sections describe the experimental approach used to apply and validate the depth-scaling techniques considered. Performance of the techniques in terms of estimating field-scale volumetric water content and moisture changes were evaluated using two years of data collected from a prairie pasture in central Saskatchewan, Canada. The feasibility of applying the methods at locations without existing instrumentation is also discussed. A conclusion is reached on which of the methods is most suitable for estimating root zone soil moisture from cosmic-ray neutron probe data.

4.4 Methods

4.4.1 Study site

The study site is within a grazing pasture (51° 22′ 54″ N, 106° 24′ 57″ W), located an hour south of Saskatoon, SK in the Brightwater Creek watershed. The perennial vegetation primarily consists of Wheatgrasses (*Agropyron* sp.) and Needle grasses (*Stipa* sp.) with patches of Western Snowberry (*Symphoricarpos occidentalis*) (Figure 4.1). The areal fractions of grass and shrub were surveyed to be 54% and 46% respectively. Topography is of low relief, varying ~5 m over the 500^2 m^2 study area (Figure 4.1). The dominant soil type is dark brown Solonetzic of the Rosemae association (Ellis et al. 1970). The climate is semi-arid, and the winters are characterized as cold. The regional average yearly precipitation is 298 mm rain and 78 mm snow water equivalent; and average daily temperatures are -15.3 °C in January and 18.0 °C in July (climate normals from Davidson, a community 32 km from the site (Environment Canada 2014)). The period of interest for this study is the warm months (May-October) when the soil is unfrozen and significant changes in soil moisture occur.

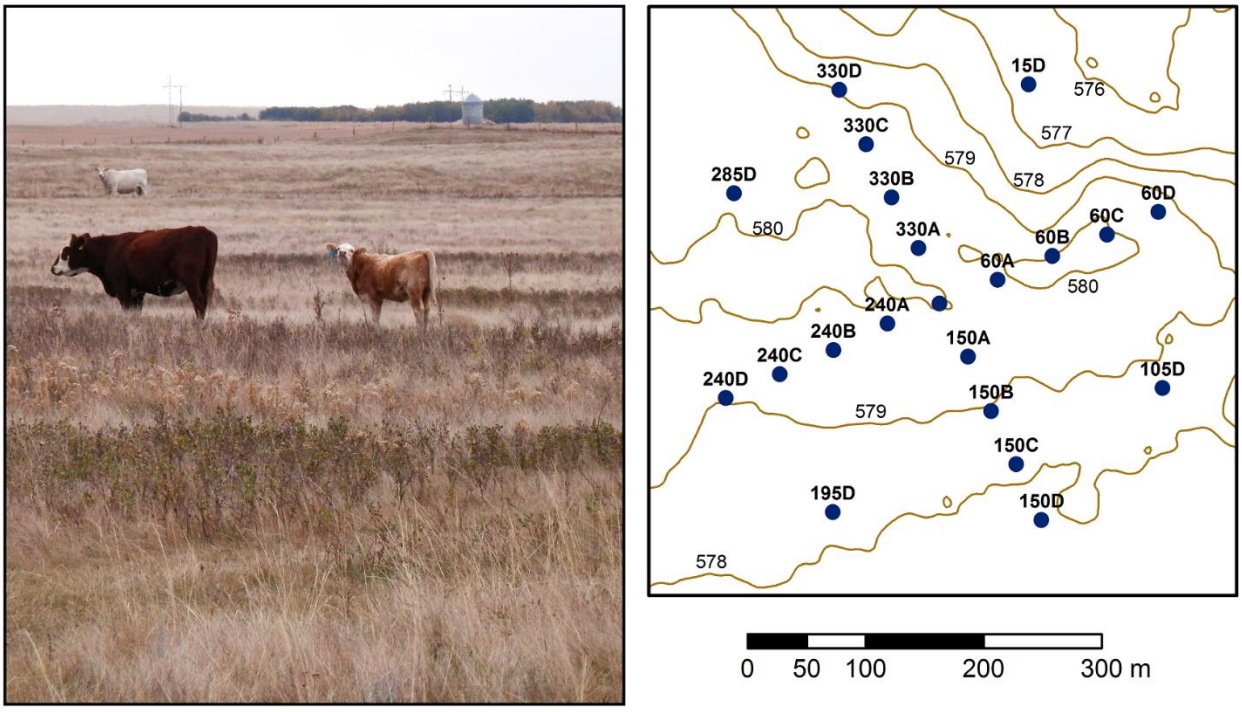

Figure 4.1 Vegetation heterogeneity at the prairie pasture site, and topography map showing neutron probe monitoring locations. Elevation contours are presented in 1 m intervals.

4.4.2 Ground-based observations

a. Cosmic-ray neutron probe

Continuous measurements of field average surface soil moisture were obtained using a cosmic-ray neutron probe (Model CRS-1000, Hydroinnova LLC, USA). Cosmic-ray neutron probes monitor the levels of cosmic-ray fast neutrons (naturally produced background radiation) found near the earth's surface. Fast neutrons are most effectively slowed by hydrogen, and therefore the quantity of fast neutrons detected by the probe can be related to soil moisture. The neutron counts detected by the probe were converted to gravimetric soil moisture (θ_g) using the equation for a general silica soil (Desilets et al. 2010),

$$\theta_g = \frac{0.0808}{\left(\frac{N_{corr}}{N_o}\right)-0.372} - 0.115 \quad , \tag{4.1}$$

where N_o is the neutron intensity over dry soil, and N_{corr} is the corrected neutron counts. The neutron counts were corrected for air pressure, atmospheric water vapor, and incoming neutron intensity using the method outlined in Zreda et al. (2012). Soil samples were taken on 3 July 2013 to calibrate N_o and determine site specific parameters necessary to calculate measurement depth. The average dry bulk density (ρ_{bd}) of the soil samples was used to convert from θ_g to volumetric water content (θ). The effective measurement depth (z^*) varies with changes in volumetric water content and uses site specific soil properties as per the relationship provided by Franz et al. (2012a),

$$z^* = \frac{5.8}{\rho_{bd} \cdot \tau + \theta + 0.0829} \quad , \tag{4.2}$$

where τ is the weight fraction of lattice water (tightly bound water adhered to the mineral crystals present in soil, which cannot be removed through evaporation or oven drying).

Neutron counts were integrated over a period of 1 hour, and the 12 hour running averages of soil moisture were created as a way to smooth the noisy data signal (Zreda et al. 2012). Daily values of soil moisture from the cosmic-ray neutron probe are used in this study, and defined as the 12 hour running average at noon. To validate the cosmic-ray neutron probe, gravimetric samples of the top 0–20 cm were taken on four measurement dates (August 9, September 11,

September 30, and October 23 of 2013). On each measurement day, 20 different randomly selected sampling locations within the cosmic-ray neutron probe footprint were chosen.

b. Neutron probe array

Point measurements of root-zone soil moisture were taken using a down-hole neutron moisture meter (CPN 503DR Hydroprobe ,CPN International Inc., USA) at 50 m spacing in a wheel and spoke pattern (Figure 4.1), to coincide with the radial footprint of the cosmic-ray neutron probe. For each of the 21 locations, soil moisture was measured at 20 cm increments from 20–160 cm. A site specific calibration (RMSE = 0.018 cm^3/cm^3) was developed from soil cores taken in 20 cm increments during the installation of the aluminum access tubes. Soil moisture, at all locations within the array, were measured bi-weekly in 2013 and monthly in 2014.

c. Meteorological data

Precipitation was measured using an all-weather precipitation gauge (T-200B, Geonor, Inc., USA). Ancillary meteorological instrumentation, including air temperature and pressure, are located beside the center neutron probe location, along with the cosmic-ray neutron probe.

4.4.3 Estimation techniques

The methods used to estimate field-scale root-zone soil moisture are described in this section. In all the methods, soil moisture is integrated over a 110 cm depth. The first three methods involve coupling the shallow soil moisture measured by the cosmic-ray neutron probe with the deeper area-scaled estimates from the neutron probe array. The fourth method only requires measurements from the cosmic-ray neutron probe after calibration. The performance of the methods for estimating field-scale volumetric water content and changes in storage will be assessed using four metrics: Pearson correlation coefficient (R), root mean square error (RMSE), bias (BIAS), and Nash-Sutcliffe efficiency coefficient (NSE).

a. Neutron probe spatial average

This approach couples the cosmic-ray neutron probe with the average of all available (21) point-scale measurements from the neutron probe array. Measurements are integrated over depth, and the field-scale soil moisture, $\theta_{(F)}$, is given by:

$$\theta_{(F)} = \frac{\sum_{j=1}^{n}\sum_{i=1}^{m}\frac{\theta_{i,j}}{m}\cdot\Delta z_j}{z_n} \quad , \tag{4.3}$$

where $\theta_{i,j}$ is the volumetric water content for location i and measurement depth j, m is the number of measurement locations, n is the number of measurement depths, Δz_j is the thickness of the soil represented by the measurement depth, and z_n is the total measurement depth.

The accuracy of this method is dependent on the estimates of field-scale soil moisture from both the cosmic-ray neutron probe and neutron probe array being accurate. Applying the statistical method found in Jacobs et al. (2004), the error in using 21 point measurements will be less than ±0.014 cm^3/cm^3 (Appendix B, Figure B.2). By using a large number of point measurements it is assumed that the error between actual field-scale soil moisture and the value estimated by averaging has been minimized. This method is assumed to provide the best field-scale estimate and will be used to measure the performance of the other methods.

b. Upscaling by time stability

This approach couples the cosmic-ray neutron probe with a single time-stable location in the neutron probe array. The concept of time stability is the idea that throughout time there will be sites that maintain their ranking in a distribution function, i.e. sites that continually exhibit field averages or extremes. The mean relative difference (MRD) method, demonstrated by Vachaud et al. (1985) to be a successful method in determining time stable sites, is defined as:

$$MRD_{i,j} = \frac{\theta_{i,j} - \overline{\theta_j}}{\overline{\theta_j}} \quad , \tag{4.4}$$

where $\theta_{i,j}$ is the soil moisture measured at location i and time j, and $\overline{\theta}_j$ is the average of all soil moisture measurements at time j. The measurement point with the smallest standard deviation in MRD over the monitoring period is considered the most time stable. However, the most time stable point is not necessarily representative of field average unless the average MRD for that

point is zero. An offset (δ) is therefore needed to convert soil moisture measured at the time stable site (θ_{TS}) to field average ($\theta_{(F)}$):

$$\theta_{(F)} = \theta_{TS} + \delta \ , \tag{4.5}$$

in which δ is the average of the MRD numerator for the time stable site.

c. Upscaling by landscape unit

This approach couples the cosmic-ray neutron probe measurements with deeper soil moisture measurements upscaled using a representative landscape unit, which in this case is based on vegetation type. It assumes that all soil moisture under a particular vegetation type is similar. A single monitoring site representing each vegetation type is used and field-scale moisture storage, $\theta_{(F)}$, can be calculated as:

$$\theta_{(F)} = \sum_{i=1}^{n} (A_i \cdot \theta_i) \ , \tag{4.6}$$

where A_i and θ_i are the area fraction and depth weighted soil moisture of vegetation type i. To apply the landscape unit monitoring approach at the study site, a single grass and brush monitoring location were chosen by subjectively picking the location that visually appears to be most representative of each vegetation type. Location 60A was chosen as the grass monitoring site, and location 150C was chosen as the brush monitoring site. Both sites are typical of the distinct high-density grass and brush patches that can be seen in Figure 4.1. A two-tailed independent samples t-test was used to determine whether the mean soil moisture and moisture changes between the two vegetation groups were statistically different.

d. Extrapolation by exponential filter

This approach uses the field-scale surface soil moisture measurements of the cosmic-ray neutron probe to model root-zone soil moisture. This model, developed by Wagner et al. (1999), considers the water balance of a two-layer soil profile: where layer 1 is the surface layer in which field-scale soil moisture is measured, and layer 2 is the lower soil layer of interest for modelling. Soil moisture of layer 1 (θ_1) and layer 2 (θ_2) are related in a simple water balance as,

$$L \frac{d\theta_2}{dt} = C(\theta_1 - \theta_2) \ , \tag{4.7}$$

where t is time, L is the depth of layer 2, and C is a proportionality constant. This approach assumes that transpiration and drainage losses from the lower layer are negligible, and that hydraulic diffusivity (i.e. the ratio of hydraulic conductivity to specific storage) between the soil layers is constant (Wagner et al. 1999). The recursive formulation of the solution for Equation 4.7 using an exponential filter (Albergel et al. 2008) can be rearranged as,

$$SWI_{2(t)} = SWI_{2(t-1)} \cdot (1 - K_t) + SWI_{1(t)} \cdot K_t \quad , \tag{4.8}$$

where SWI_2 and SWI_1 are the soil water index of layer 2 and layer 1 respectively, t is a time index, and K_t is the gain. Soil water index is the volumetric water content scaled from 0–1 using assumed minimum and maximum values. For layer 1, the volumetric water content is bounded by the minimum and maximum of the observations. For layer 2, water content can be bounded using wilting point as the minimum value, and the mid-point between field capacity and total water storage as the maximum value (Wagner et al. 1999). Soil data is therefore a necessary model input. The gain (K_t), which ranges from 0–1, is calculated as:

$$K_t = \frac{K_{t-1}}{K_{t-1} + \exp(-(\Delta t)/T)} \quad , \tag{4.9}$$

where K_{t-1} is the gain of the previous time, Δt is the time step, and T is a characteristic time length (equal to L/C from Equation 4.7). The filter is initialized by setting $K_1 = 1$ and $SWI_{2(1)} = SWI_{1(1)}$. The characteristic time length (T) is dependent on a variety of factors, including thickness of layer 2, and soil properties (i.e. hydraulic conductivity, texture, density) that may influence evaporation and infiltration rates (Albergel et al. 2008); and therefore requires calibration. For this study, layer 2 minimum and maximum also needed calibration, as the soil data from a large scale survey (Ellis et al. 1970) proved to be unsatisfactory (reasoning described in Section 4.5.3c). A Monte Carlo simulation was used to calibrate the three parameters simultaneously. A range for each parameter was first assumed, and 100,000 random combinations were generated. The optimum parameters were the set that had the highest Nash-Sutcliffe efficiency (NSE). A perfect model would have a NSE of 1, whereas a NSE of 0 or less indicates that modeled layer 2 SWI is no better than using the season average of the neutron probe array.

4.4.4 Data selection

Soil moisture data is available for the months of May-November in 2013 and 2014. Calibration was required for upscaling by time stability and the use of the exponential filter. For these methods, 2013 is used as the calibration period; whereas 2014 represents the validation period, and allows us to determine the temporal transferability of the methods. Meteorological data from the site showed that 2014 was wetter and cooler than 2013. May-August precipitation was 141 mm in 2013 and 206 mm in 2014, and average air temperature was 15.8 °C and 15.0 °C, respectively.

4.5 Results and Discussion

4.5.1 Near-surface soil moisture measured by the cosmic-ray neutron probe

The soil moisture measured by the cosmic-ray neutron probe is shown in Figure 4.2 for the 2013 and 2014 growing seasons, along with the measured daily precipitation and modeled depth of influence. The soil moisture, calculated using Equation 4.1, was based on the single calibration date (3 July 2013). To provide validation of these measurements gravimetric samples were taken on 4 occasions during summer of 2013, and are presented in Figure 4.2 as the mean value ±1 standard deviation (n = 20). The general trend of the mean surface soil moisture from the gravimetric samples is well matched by the cosmic-ray neutron probe. Differences in soil moisture between the cosmic-ray neutron probe and the point measurement averages may be in part due to differences in measurement depth. The gravimetric samples were of the top 20 cm. The effective depth of the cosmic-ray neutron probe ranged between 10 and 23 cm, with a mean depth of 17 cm in 2013 and 16 cm in 2014. Agreement between the cosmic-ray neutron probe and the gravimetric samples are strongest when the measurement depths coincide with each other, which occurred on 9 August and 11 September 2013. The array average of the 20 cm down-hole neutron probe measurements compared poorly with the cosmic-ray neutron probe measurements (Appendix B, Figure B.3), due to differences in measurement depth. Given the radius of influence of the neutron probe (equation from Kristensen 1973), the 20 cm measurements from the neutron probe array are actually representative of the moisture in the top 50 cm (Appendix A, Figure A.3).

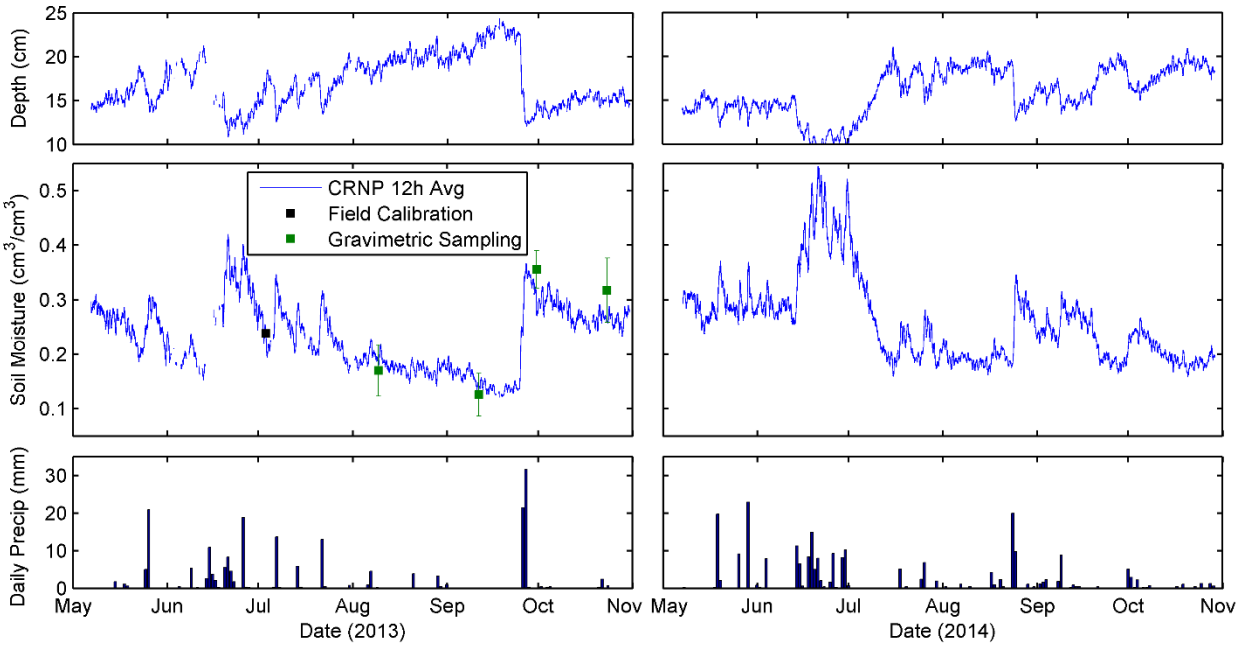

Figure 4.2 Field average soil moisture measured by cosmic-ray neutron probe (CRNP) as compared to gravimetric soil samples (average ± 1 standard deviation) and precipitation for 2013 and 2014. The changing measurement depth is shown in the top graph.

4.5.2 Soil moisture variability with depth

The spatial variability of soil moisture with depth is examined in Figure 4.3a-4.3b using the observations from the neutron probe array. The boxplots show consistent spatial variability of volumetric water content with depth, with the average moisture content difference between the 25th and 75th percentile being 0.05 cm^3/cm^3. When looking at the season change in soil moisture with depth (Figure 4.3c), it can be seen that the temporal variability is high for shallower soil moisture, and low for deeper soil moisture. This indicates that, although the spatial variability is similar for all depths, there is very little change in soil moisture below 100 cm. The 2014 data showed similar variability characteristics with depth.

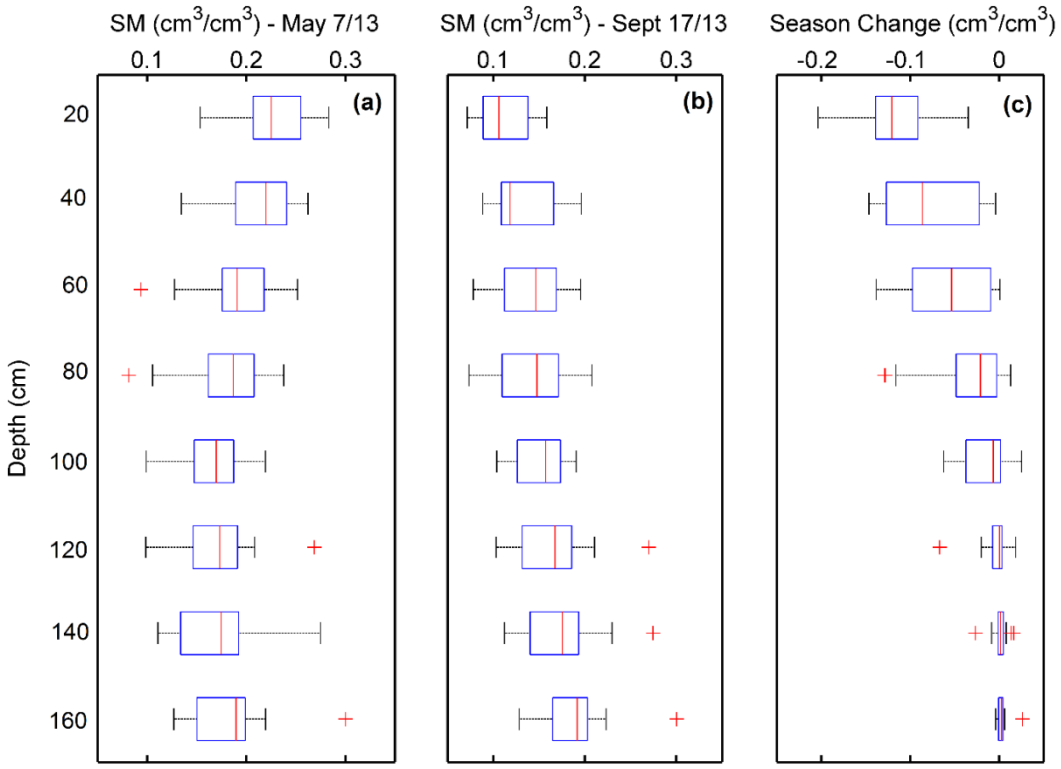

Figure 4.3 Spatial variability of soil moisture with depth; volumetric water content for 7 May and 17 September 2013, and season change (difference between 17 September and 7 May 2013). The boxplot indicates the median (red line), 25th and 75th percentile (edges of the box), and minimum and maximum (extent of whiskers) values.

Next, the shallow soil moisture observations from the cosmic-ray neutron probe were combined with the deeper 21-point averaged neutron probe observations to construct a time series of field-scale water content with depth. The cumulative change in soil moisture storage over different depth intervals is shown in Figure 4.4. The majority of the temporal change in moisture storage over the 2013 and 2014 growing seasons was captured within the top 110 cm of the soil profile, with negligible changes below this. The change in soil moisture measured by the cosmic-ray neutron probe, represented as the 0–17 cm interval, was highly variable but accounted for less than 40% of the total seasonal change in moisture storage (Figure 4.4, fraction of total cumulative storage change for 0–17 cm on 17 September 2013 and 20 October 2014).

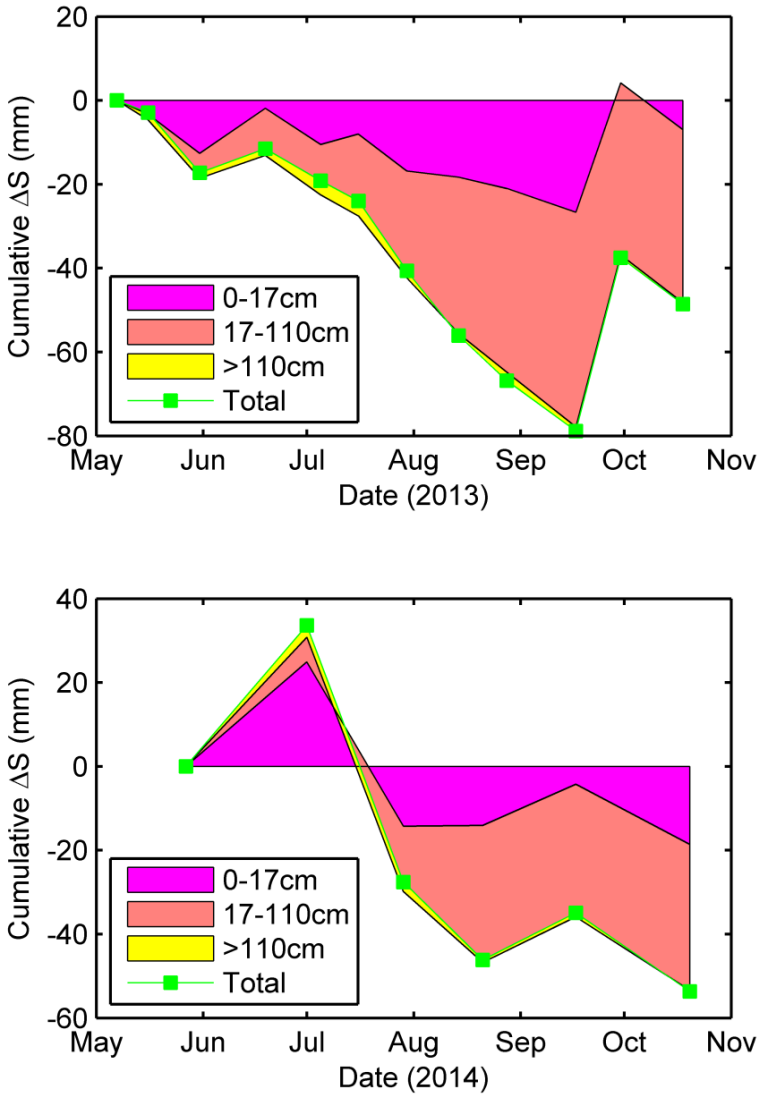

Figure 4.4 Cumulative change in storage with depth; 0–17 cm represents the cosmic-ray neutron probe measurements.

4.5.3 Upscaling methods

a. Time stability

The time stability of soil moisture at each neutron probe location was evaluated by examining the MRD (Equation 4.4) during the 2013 season (Figure 4.5). The locations which are most similar to field mean soil moisture content are those with an MRD near zero (e.g. 195D, 240D, and 240C). However, given that they have relatively large standard deviations, they cannot be considered time stable. Rather, location 285D is shown to be the most time stable

location as it has the smallest MRD standard deviation (2.8%), closely followed by 330D (3.0%), 150D (3.1%), and 60B (3.1%). To upscale the soil moisture from 285D to field scale, a constant offset of 0.025 cm^3/cm^3 was applied.

Several authors (e.g. Grayson and Western 1998; Vachaud et al. 1985) have suggested that time stable sites, in particular those that are also average representative (MRD near 0), may have average physical properties, i.e. topography, soil, or vegetation characteristics. However, at the pasture site none of the locations were considered both time stable and average representative (Figure 4.5). Figure 4.6 examines the elevation and dry bulk density (0–80 cm average) of the time stable and average representative sites, with respect to all monitored locations. The time stable locations, those that have similar changes in soil moisture as the field mean, were found to have a bulk density near field average (clustered near the median value in Figure 4.6), but no relation with elevation. The average representative sites showed no relation with either elevation or bulk density.

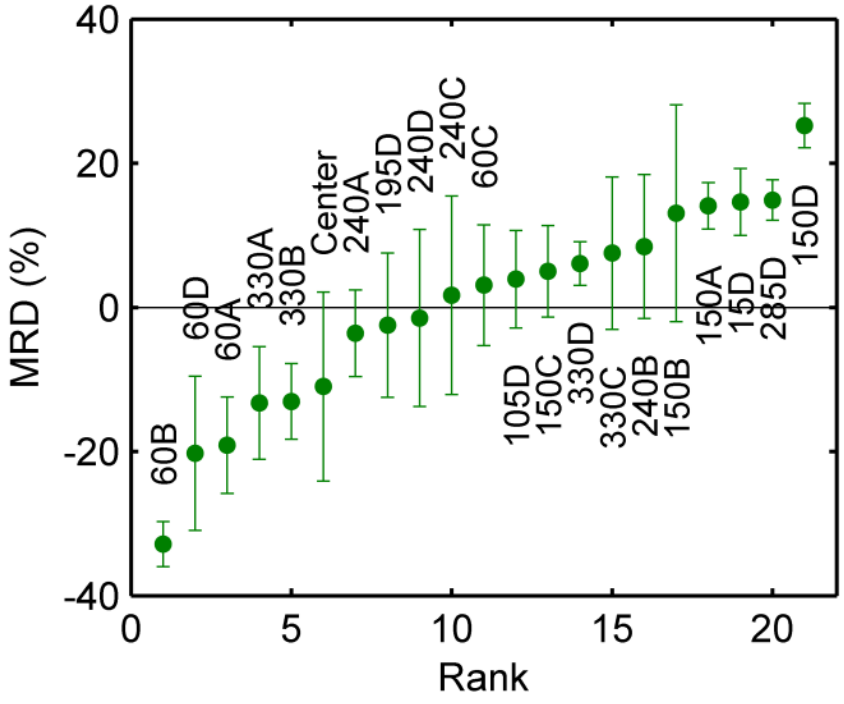

Figure 4.5 Average mean relative difference (MRD) ±1 standard deviation for each neutron probe monitoring location.

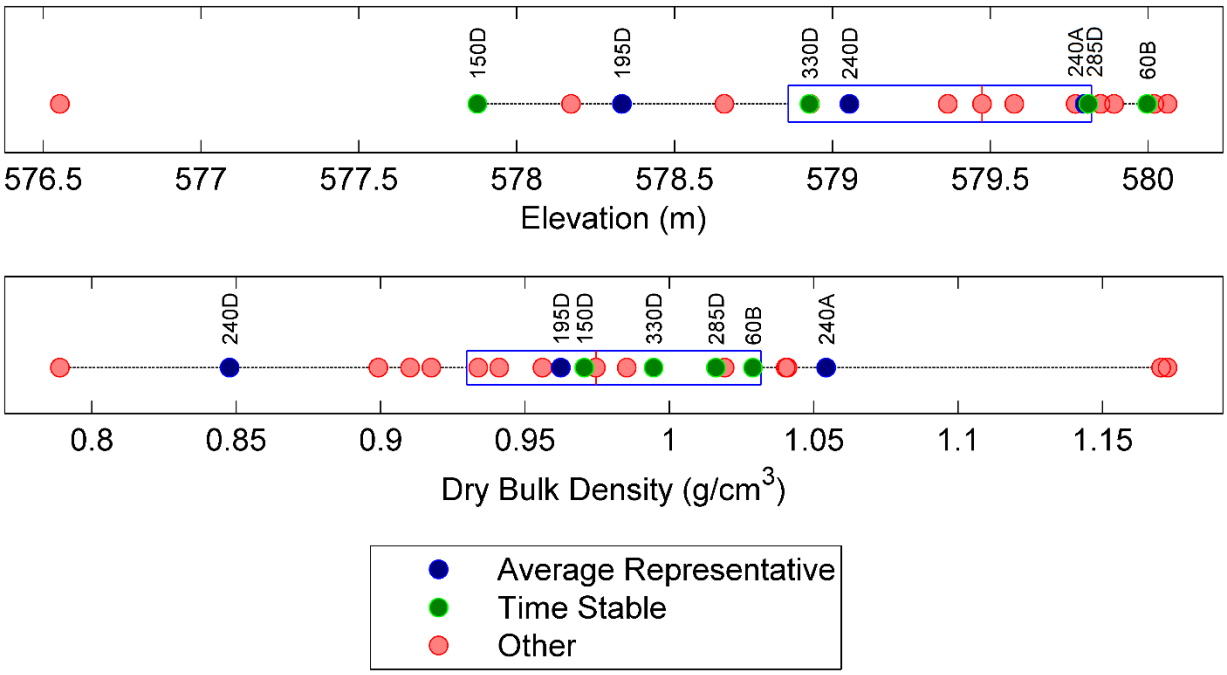

Figure 4.6 Physical characteristics of the time stable and average representative sites. The boxplot indicates the median (red line), 25th and 75th percentile (edges of the box), and minimum and maximum (extent of whiskers) values.

b. Representative landscape units

The premise of using vegetation type to define similar response units for soil moisture depends on whether the units actually display differences in their mean values and in the variability of soil moisture. Box and whisker plots for select dates in 2013 (Figure 4.7) show that for half the dates a very noticeable difference in the median soil moisture storage between brush and grass units exists, but for the other plots the interquartile ranges overlap. A two-tailed independent samples t-test was used to determine if the means were different. The p-value of the t-tests (displayed at the top of each graph in Figure 4.7) indicates the likeliness that the means are statistically similar. During the earlier months, when soil moisture is higher, the means between the two vegetation types are statistically different at 95% confidence (P-value <0.05). In the later months, under drier soil moisture conditions, the means are statistically similar, as indicated by the large p-values. The means of the season change in storage between the two vegetation groups were found to be statistically different at 98% confidence. By the mixed results, it is

unclear whether vegetation type is the best way to group the soil moisture measurements at this particular site.

The locations chosen to represent grass and brush, which were 60A and 150C respectively, are indicated by the blue-dots in Figure 4.7. For the brush vegetation, location 150C represents the median soil moisture of this vegetation group well. However, for the grass vegetation group, location 60A represents the median change in soil moisture fairly well, but soil moisture values measured at this site are lower than the majority of the other grass sites. This suggests that the estimate of field-scale volumetric water content using this method, and these representative sites, is expected to be consistently low.

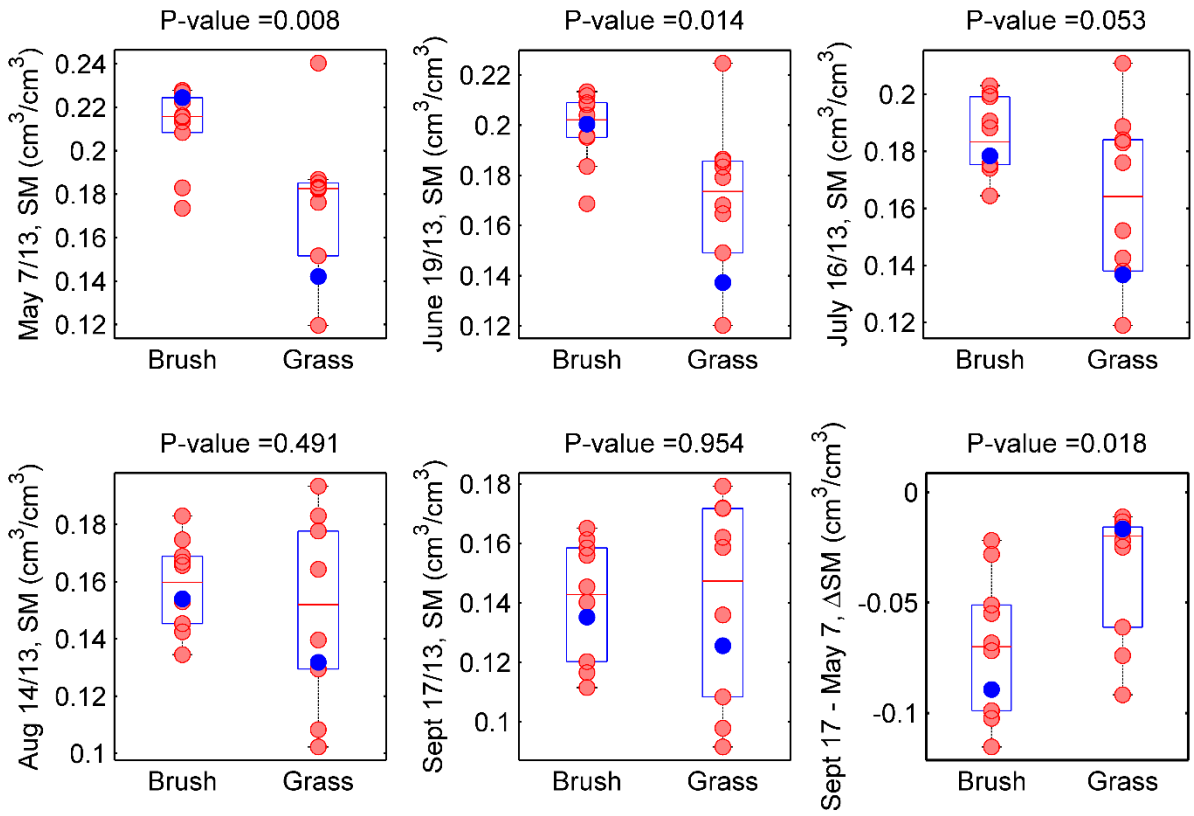

Figure 4.7 Variability of soil moisture storage for the two different vegetation groups shown by box and whisker plot, with the p-value from the t-test indicating the chance of similar means. The number of grass and brush locations are both 10. Blue dots indicate the chosen grass and brush monitoring sites; 60A and 150C.

c. Extrapolation by exponential filter

Wilting point, field capacity, and total water capacity were not measured at the field site. These properties were available from a government agency soil survey (Ellis et al. 1970). However, the wilting point given was higher than some of the field average measurements of the neutron probe array. Using these soil properties would therefore yield significantly higher layer 2 soil moisture than the measured values. To get better results, both the minimum and maximum layer 2 bounds were calibrated in addition to the T parameter. The Monte Carlo simulations (Figure 4.8), shows that layer 2 minimum and maximum water contents are very sensitive, whereas the *T* parameter is less sensitive, with values ranging from 40-70 days giving similar results.

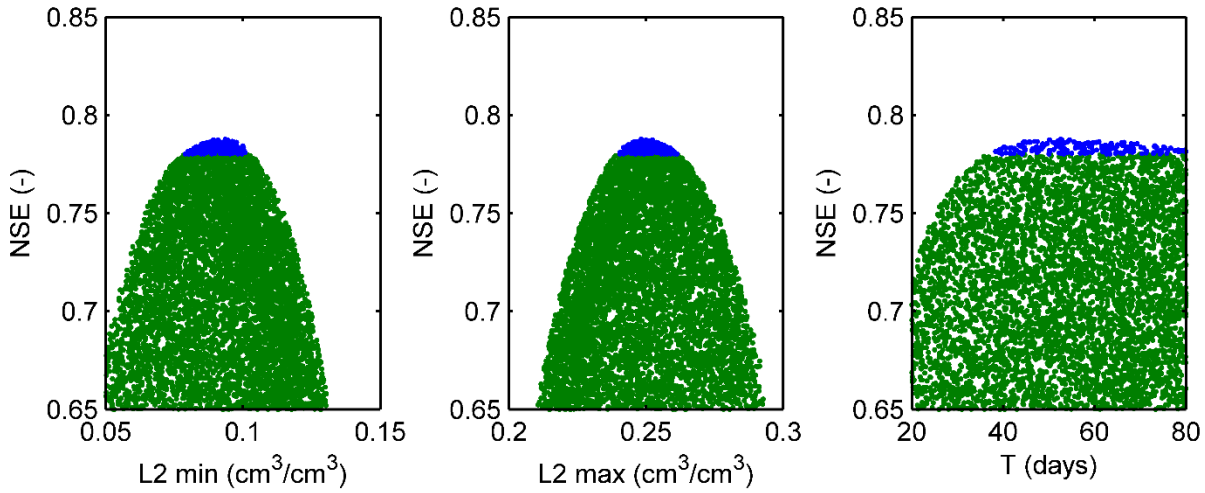

Figure 4.8 Sensitivity of the exponential filter parameters. Parameters were optimized based on the Nash-Sutcliffe efficiency (NSE) coefficient. The blue dots indicate the top 200 combinations with the highest NSE, giving an indication of the sensitivity.

The optimum value of *T*, and layer 2 soil moisture bounds are shown in Table 4.1. Layer 1 minimum and maximum were based on the 2013 cosmic-ray neutron probe data. The problem with this approach is that the layer 1 minimum and maximum bounds may not be assessed correctly when only using one year of data. For example, Wagner et al. (1999) used observations from 6 years to define layer 1 soil moisture bounds. It should be noted that the layer 1 minimum and maximum bounds have a high impact on the optimum layer 2 minimum and maximum bounds found through calibration.

Table 4.1 Exponential filter parameter values found from layer 1 observations and calibration.

Parameters	Value
Observation Based:	
min(L1)	0.12
max(L1)	0.37
Calibrated:	
min(L2)	0.09
max(L2)	0.25
T	54

Input and output signals of the exponential filter, using the optimum parameters, are shown in Figure 4.9. The gain is shown to exponentially decay from its initialized value of 1, and stay at a constant level (Figure 4.9a). The gain is controlled by the *T* parameter, as seen in Equation 4.9. At lower *T* values, the gain will level out quicker at a higher value. Comparison of the measured and modelled layer 2 SWI (SWI_2) is shown in Figure 4.9b. A smaller gain produces a more damped SWI_2 signal. Modelled SWI_2 provides a better fit to the measured values starting at the end of June, after the gain becomes constant. The poorer performance in May and June may be related to higher gain values (caused by initializing the model at a gain of 1), which makes the model more sensitive to layer 1 soil moisture (SWI_1) measurements during this time period.

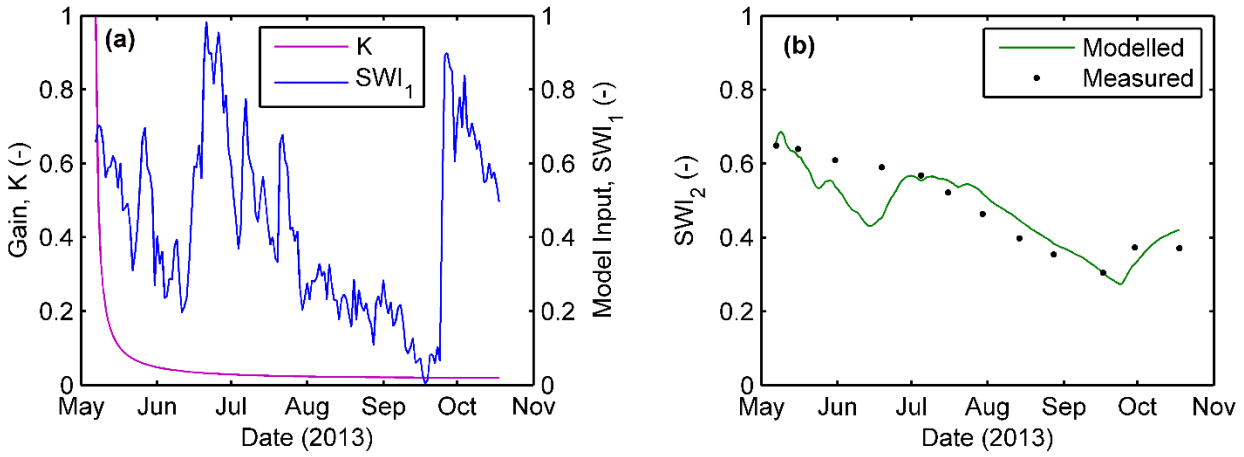

Figure 4.9 Input and output signals of the exponential filter using the optimized parameters from Table 4.1. SWI_1 is the soil water index of the cosmic-ray neutron probe measurements.

4.5.4 Method performance

The cumulative change in root-zone storage and mean volumetric water content for the 2013 and 2014 growing seasons are shown in Figure 4.10. Absolute values of volumetric water content provide a more rigorous test of the performance of the methods, while the cumulative change in storage is insensitive to systematic errors in the magnitude, but will be adequate for assessing annual water balances. The benchmark, neutron probe spatial average combined with the cosmic-ray neutron probe measurements, is shown in green as mean soil moisture ± 1 standard deviation, which is based upon the spatial variability of soil moisture measured by the neutron probe array. Method performance of estimating field-scale volumetric water content was evaluated using the Pearson correlation coefficient (R), root mean square error (RMSE), bias (BIAS), and Nash-Sutcliffe efficiency coefficient (NSE). The results are shown in Table 4.2.

The time stability approach performed well in estimating both field-scale volumetric water content and changes in soil moisture, and had the highest performance metrics in both 2013 and 2014. The RMSE for both years was 0.004 cm^3/cm^3.

The landscape unit approach provided good estimates of field-scale change in soil moisture for both 2013 and 2014. The pattern of soil moisture change was accurately captured ($R > 0.98$), but the method exhibited a negative bias, where estimates of field-scale volumetric water content were consistently lower than the benchmark average. This result is consistent with Figure 4.7, where it was shown that the chosen locations, 60A and 150C, represented the change in soil moisture. The soil moisture measurements from 60A were consistently lower than the median value for grass, and it was expected that the estimate of volumetric water content would be low.

The exponential filter provided good estimates of both field scale volumetric water content and change in soil moisture over both years, with the metrics showing slightly poorer performance in 2014 (RMSE = 0.012 cm^3/cm^3; NSE = 0.714) due to the poor match with spatial average on 1 July 2014. This RMSE is lower than previous studies (RMSE of 0.022 cm^3/cm^3 in Ceballos et al. (2005); RMSE of 0.049 cm^3/cm^3 in Wagner et al. (1999)) most likely because the method is being applied on a smaller scale (<1 km^2) and the bounds of layer 2 have been calibrated. The cosmic-ray neutron probe also has a deeper measurement depth than satellite

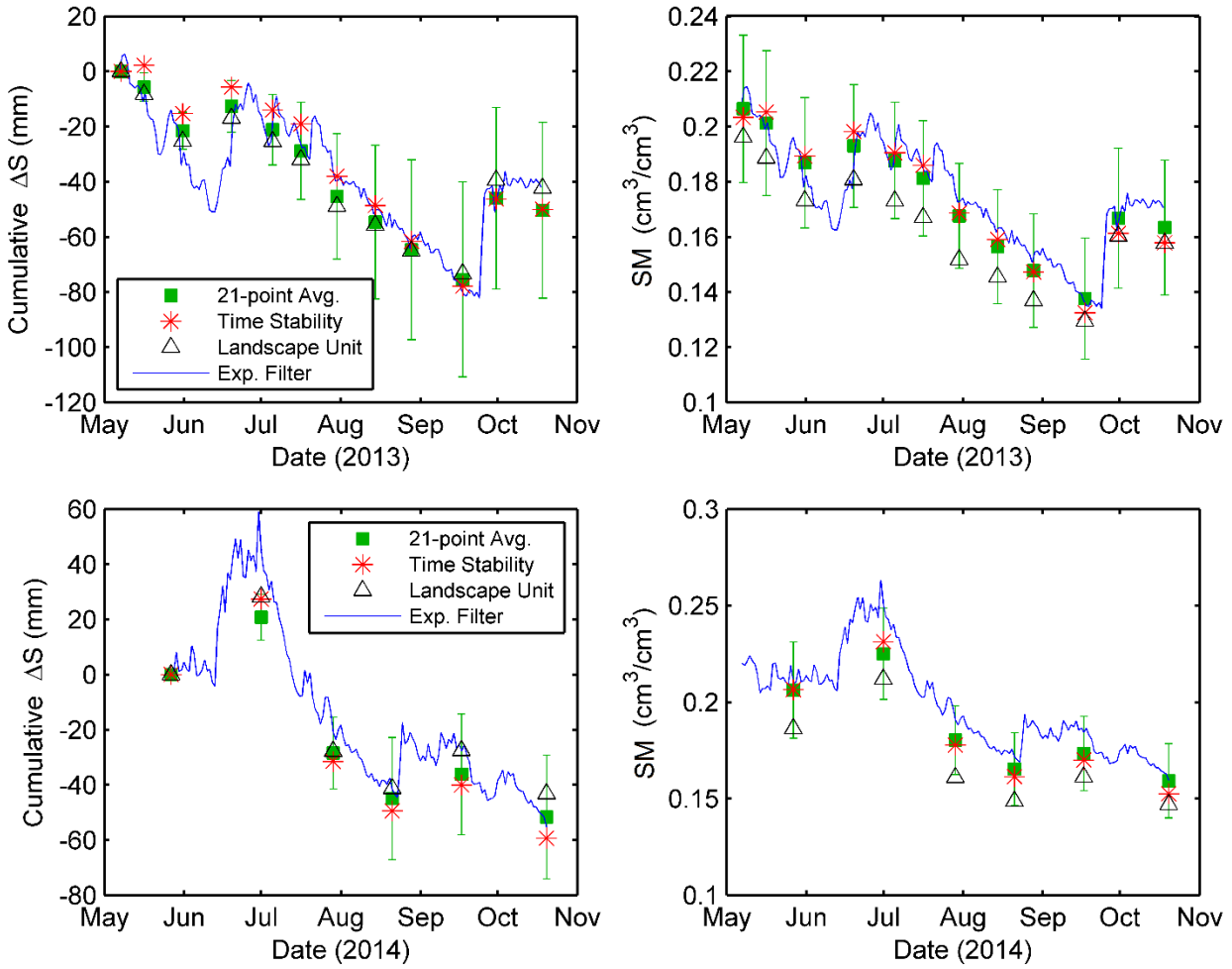

Figure 4.10 Comparison of field scale root-zone soil moisture estimates, in terms of volumetric water content (cm^3/cm^3) and cumulative change in storage (mm).

Table 4.2 Performance metrics of root-zone estimation methods using instrumentation average as the control. Units of RMSE and BIAS are cm^3/cm^3.

	R	RMSE	BIAS	NSE
2013 (n=12)				
Time Stability	0.988	0.004	0.000	0.964
Landscape Unit	0.989	0.012	-0.011	0.676
Exponential Filter	0.951	0.006	-0.001	0.903
2014 (n=6)				
Time Stability	0.999	0.004	-0.002	0.964
Landscape Unit	0.990	0.016	-0.016	0.537
Exponential Filter	0.981	0.012	0.009	0.714

remote sensing instruments, and therefore less of the root-zone needs to be modelled. An inherent advantage of the exponential filter method is that the estimates are of the same temporal resolution as the cosmic-ray neutron probe measurements, whereas estimates from the other methods are dependent on how frequently down-hole neutron probe measurements are taken.

Based on the similarities in performance between 2013 and 2014, all methods can be considered stable at this prairie pasture over the two year period. The time stability and the representative landscape unit approach rely on the spatial pattern of soil moisture staying constant with time. The consistent performance of these methods may be due to no physical changes to the environment occurring, i.e. the spatial pattern of vegetation stayed constant over the two years. Han et al. (2012) compared several upscaling methods, including time stability, and determined they were not temporally transferable at an agricultural site due to differences in rainfall and crop type between the two years. It is important to note that the 2014 season (May-August) received 46% more rain than the 2013 season. Despite the differences in precipitation the methods perform consistently

4.5.5 Spatial transferability

The results of this study suggest that both the time stable site and the exponential filter method would provide reliable estimates of field scale soil moisture at the study site in subsequent years. However, these methods require calibration. In order for the methods to be applied more widely they must be able to be used at other locations with no calibration, or at least reduced calibration. The spatial average method comprised of observations from a 21-point neutron probe array. Although this method was assumed to be the most accurate, the averaging of many point observations is often not a logistically feasible long term option for estimating field-scale soil moisture. In this section, suggestions are provided on how or if the remaining methods can be spatially transferred.

a. Time stability

In order for this method to be transferred to another site, the user would need to be able to locate the most time stable site with only a small amount of work, or be able to identify the location of the site based on its physical characteristics. Studies (e.g. Grayson and Western 1998; Jacobs et al. 2004; Teuling et al. 2006) have mainly focused on locating time stable sites

that are already representative of the average moisture conditions so that an offset is not required. Teuling et al. (2006) found high uncertainty in the spatial mean estimate (~75% of spatial variability) when a single survey was used to locate the average representative time stable site, as opposed to a general uncertainty of ~40% of the spatial variability when the seasonal dynamics were understood. There have also been mixed results in field studies on if average representative sites have average physical characteristics. Teuling et al. (2006) examined time stability of root-zone soil moisture and did not find average representative sites to have field average elevation or leaf area index. At the pasture site, the average representative locations were not time stable (Figure 4.5) and did not have field average elevation or bulk density characteristics (Figure 4.6). However, the locations that were time stable had field average bulk density (Figure 4.6). For surface soil moisture, Jacobs et al. (2004) determined average representative sites were found at mid hillslopes under specific soil textures. In general, root-zone soil moisture may be more difficult than surface soil moisture to relate to physical characteristics, as it may incorporate an average from multiple soil layers. A study on the variability of root-zone soil moisture in the Canadian prairies (Biswas et al. 2012), found root-zone soil moisture to be strongly influenced by the depth of the A and C horizons, in addition to soil texture and bulk density. For root-zone soil moisture, these studies show that time stable sites may not be easily identified from their physical characteristics or with a single soil moisture survey. The time stability upscaling method would therefore be difficult to implement at sites lacking existing instrumentation.

b. Landscape unit

The landscape unit monitoring approach is one of the most feasible methods to implement in practice, requiring soil moisture instrumentation to be installed at only a single measurement location per vegetation type. This method is non-calibrated and large variability of soil moisture could potentially exist within the vegetation groups. Therefore, the performance of this method is largely dependent on which locations are chosen to subjectively represent the vegetation types. In this study, the sites chosen represented the change in soil moisture well, but the chosen grass site provided consistently low water content estimates (Figure 4.7). The landscape unit approach will be most effective in places where vegetation is the dominant control on soil moisture variability. The reliability of this method in general may be limited as other

factors such as topography or soil properties may be of greater importance (e.g. Hawley et al. 1983; Western et al. 2004; Biswas et al. 2012).

c. Exponential filter

The exponential filter method may be the most promising in providing root zone soil moisture for fields where profile soil moisture is not monitored. The question is then how to parameterize the exponential filter on such a large scale. Soil hydraulic properties will need to be estimated in order to determine layer 1 and layer 2 soil moisture bounds, given that previous layer 1 measurements most likely will not exist and layer 2 cannot be calibrated as performed in this study. The regional soil hydraulic properties of the area available from soil survey data (Ellis et al. 1970) were not accurate for the pasture site studied here, most likely due to the map resolution. It may therefore be necessary to measure the local soil hydraulic properties to obtain higher accuracy. The effect of soil property errors was shown by Wagner et al. (1999) to cause a bias in the estimate that is dependent on soil type. Also, consideration of how to establish a suitable characteristic time length (T) needs to be given. Several studies (Ceballos et al. 2005; Albergel et al. 2008; de Lange et al. 2008) have examined controls on T. The most important control on T is modelling depth, with larger T values being more suitable for greater modelling depths (Wagner et al. 1999; Ceballos et al. 2005; Albergel et al. 2008). Soil texture (de Lange et al. 2008) and climate (Albergel et al. 2008) were also found to have an influence on T. Although T may be affected by a number of factors, the results of this study and others (e.g. Wagner et al. 1999; Ceballos et al. 2005; Albergel et al. 2008) show that the parameter has relatively low sensitivity when considering the entire root zone. Because the acceptable range of T values is usually relatively large, accurate parameterization may not be necessary to obtain suitable soil moisture estimates.

4.6 Conclusion

In this study, the cosmic-ray neutron probe was used along with different depth-scaling methods to estimate field-scale root-zone soil moisture. The cosmic-ray neutron probe was found to provide good estimates of surface soil moisture for this site through comparison with precipitation events and gravimetric sampling. The effective measurement depth generally

ranged from 10–20 cm, which was determined to account for less than 40% of the seasonal change in soil water storage. This illustrates that depth-scaling is necessary for the cosmic-ray neutron probe measurements to be representative of root zone soil moisture.

Three different depth-scaling methods were used to estimate field scale soil moisture over the entire root zone. Their performance, in terms of estimating volumetric water content and changes in moisture storage, was evaluated against the 21-point spatial average. The time stability method provided the best estimates of field scale root zone soil moisture (RMSE = 0.004 cm^3/cm^3) during both the calibration and validation years, followed by the exponential filter (RMSE of 0.006 and 0.012 cm^3/cm^3 for the calibration and validation years respectively). The landscape unit approach, based on the monitoring locations chosen, showed a consistent negative bias and was only able to estimate moisture changes well. The ease of applying these methods to sites without existing instrumentation was discussed. Intensive soil moisture monitoring is necessary to determine the time stable location, making application of the time stability method difficult. The exponential filter may be easier to apply given that the main parameter, the characteristic time length, has relatively low sensitivity. Soil hydraulic properties, which are also important for the exponential filter method, can be obtained from regional soil survey data; however, they may need to be measured locally for better accuracy. Considering both performance and ease of spatial transferability, the exponential filter method is the most suitable for scaling cosmic-ray neutron probe data. Further studies are necessary to understand the full potential of the exponential filter method in estimating root-zone soil moisture from cosmic-ray neutron probe data.

CHAPTER 5: SYNTHESIS AND CONCLUSION

The findings of this thesis are of use to those interested in the measurement or modelling of soil moisture at the field scale. Estimates of variability and mean soil moisture at this scale are useful for applications relating to hydrology, land-atmosphere interactions, and agriculture. The main objectives were to: (1) examine soil moisture spatial patterns and variability within the field scale, and (2) compare field-scale soil moisture determination methods. This study involved the examination, analysis, and interpretation of soil moisture data collected over two and a half growing seasons from a prairie pasture site in central Saskatchewan.

The spatial variability of root-zone soil moisture was measured by a 21-point neutron probe array on a bi-weekly basis. Chapter 3 focused on understanding the spatial patterns of soil moisture at the prairie pasture site. The specific sub-objectives were: (1) examine the temporal stability of the spatial pattern, (2) investigate the relationship between soil moisture spatial variability and the mean, and (3) explain the results. The spatial pattern of root-zone soil moisture displayed seasonal stability. Distinct patterns were seen for early and late growing season, which corresponds to the wet and dry periods. For root-zone soil moisture, the relationship between the spatial variability and mean was best described by a concave trend, where the spatial variability was lowest under mid-range moisture conditions. These results were persistent over the two and a half years of data. The existence of two unique patterns pertaining to wet and dry periods is not unusual (e.g. Grayson et al. 1997). What is unusual is the concave variability-mean relationship. Through analysis of the spatial pattern of soil moisture changes, it became evident that this was caused by differences in participation level amongst the soil profiles. Participation refers to how responsive the profiles are to precipitation or drying. Dynamic soil moisture profiles experience large changes in soil moisture over a season, while non-participating ones have very little or almost negligible changes. The non-participating profiles maintain mid-range soil moisture content, while the dynamic profiles move from high to low water content over the growing season. This causes a suppression of variability

at mid-range moisture contents, and appears to be the reason for the concave variability-mean relationship. The differences in participation level are also assumed to be responsible for the seasonal stability of the soil moisture patterns at the pasture site. These unique soil moisture variability characteristics are the result of high soil heterogeneity, such as that typical of Solonetzic soils (e.g. Carter and Pearen 1985; Sandoval and Reichman 1971; Pennock et al. 1999). Non-participating profiles were associated with slow draining clays and the presence of a low permeability Solonetzic B horizon. Surveys of surface soil moisture (0–6 cm) did not reach the B horizon, yielding the common convex spatial variability-mean relationship where variability was highest mid-range. The depth of interest is therefore important when considering soil moisture variability.

The cosmic-ray neutron probe provided a field-scale soil moisture measurement for the top 20 cm of the soil profile. Although this instrument has the deepest measurement depth, when considering current field-scale instruments, it is still only able to cover a small portion of the root-zone. Chapter 4 compared different techniques that could be used to scale the shallow cosmic-ray neutron probe measurements up to a root-zone average. The methods to estimate lower root-zone soil moisture were: (1) a single time stable location from the neutron probe array, (2) a representative landscape unit approach, where a single soil moisture profile was monitored for each vegetation type, and (3) modelling by exponential filter. The performance of these methods was evaluated against the average of the 21 point monitoring locations in the neutron probe array. The time stability method provided the best estimate, followed closely by the exponential filter. The representative landscape unit approach performed the poorest in terms of providing an estimate of volumetric water content, but was able to accurately mimic soil moisture changes. Although the time stability method provided the best estimate of mean root-zone soil moisture at the field scale, this method is difficult to apply to new field sites. Intensive soil moisture monitoring is necessary to find a time stable location suitable for representing the mean, and there is little that can be done in the way of reducing this time consuming and costly procedure. In contrast, the exponential filter approach has great potential for being applied to areas without existing instrumentation. At the pasture site, calibration of the exponential filter was crucial in achieving accurate estimates for two main reasons: (1) available soil hydraulic properties from survey data were unreliable, and (2) the main controls on the remaining parameter, that is the characteristic time length, are not yet fully understood. However, if these

two issues are able to be addressed calibration may be eliminated. In particular, when considering the entire root-zone, the characteristic time length was found to have low sensitivity in this study and those by others (e.g. Wagner et al. 1999; Ceballos et al. 2005; Albergel et al. 2008), meaning that accurate parameterization may not be necessary. Also, in the case where information on soil hydraulic properties are unavailable or unrepresentative, local measurement may be a suitable substitute for calibration.

The findings of this research make a contribution to the large body of literature on soil moisture variability and scaling that currently exists. Additionally, the results of this project point towards much further work to be done. In particular, this research was focused around a prairie pasture site. This is just one of many different environments that exist throughout the world. It would therefore be useful to conduct a similar field study in other types of land uses and climatic regions.

A hypothesis can be made that the unique soil moisture variability characteristics seen at the pasture; that is the temporal persistence of the concave variability-mean relationship and seasonal spatial patterns of root-zone soil moisture, may be present in other regions with Solonetzic soils. Additional testing at other field sites may be necessary to provide confirmation. A concave shape needs to be recognized as being able to describe the "true" variability-mean relationship in some cases. Researchers that find a concave fit for their data need to be aware that the trend is real, and likely not instrument or sampling errors (i.e. Famiglietti et al. 2008). Care should be taken to understand the factors controlling this trend. It is entirely possible that differences in participation level could occur under circumstances other than the ones seen here. The concave spatial variability-mean relationship may also be seen at other measurement depths or time scales (e.g. Famiglietti et al. 2008).

The exponential filter has the most potential for estimating field-scale root-zone soil moisture from cosmic-ray neutron probe data. An increased understanding of method performance and model parameterization are necessary. The grounds to evaluate the exponential filter on a large scale may already be available. Networks of cosmic-ray neutron probes exist in both the United States (COSMOS, Zreda et al. 2012) and Australia (CosmOz, Hawdon et al. 2014). Many researchers are currently conducting studies to understand soil moisture within the cosmic-ray neutron probe footprint. In a lot of cases there may already be point measurement

sensors installed that can be used to provide mean root-zone soil moisture. It may therefore not be too much work to test the exponential filter at these locations and gain further insights.

REFERENCES

Albergel, C., Rüdiger, C., Pellarin, T., Calvet, J.-C., Fritz, N., Froissard, R., Suquia, D., Petitpa, A., Piguet, B., and Martin, E. 2008. From near-surface to root-zone soil moisture using an exponential filter: an assessment of the method based on in-situ observations and model simulations. Hydrology and Earth System Sciences, **12**: 1323-1337. doi:10.5194/hessd-5-1603-2008.

Albergel, C., Rüdiger, C., Carrer, D., Calvet, J.-C., Fritz, N., Naeimi, V., Bartalis, Z., and Hasenauer, S. 2009. An evaluation of ASCAT surface soil moisture products with in-situ observations in Southwestern France. Hydrology and Earth System Sciences, **13**: 115-124. doi:10.5194/hess-13-115-2009.

Albertson, J.D., and Montaldo, N. 2003. Temporal dynamics of soil moisture variability: 1. Theoretical basis. Water Resources Research, **39**(10): 1274. doi:10.1029/2002WR001606.

Ayres, K.W., Button, R.G., and de Jong, E. 1973. Soil morphological and soil physical properties. II. Mechanical impedance and moisture retention and movement. Canadian Journal of Soil Science, **53**: 9-19.

Biswas, A., and Si, B.C. 2011. Scales and locations of time stability of soil water storage in a hummocky landscape. Journal of Hydrology, **408**: 100-112. doi:10.1016/j.hydrol.2011.07.027.

Biswas, A., Chau, H.W., Bedard-Haughn, A.K., and Si, B.C. 2012. Factors controlling soil water storage in the hummocky landscape of the Prairie Pothole Region of North America. Canadian Journal of Soil Science, **92**: 649-663. doi:10.4141/cjss2011-045.

Bogena, H.R., Huisman, J.A., Baatz, R., Hendriks Franssen, H.-J., and Vereecken, H. 2013. Accuracy of the cosmic-ray soil water content probe in humid forest ecosystems: The worst case scenario. Water Resources Research, **49**: 5778-5791. doi:10.1002/wrcr.20463.

Bowman, A.W., and Azzalini, A. 1997. Applied Smoothing Techniques for Data Analysis: the Kernel Approach with S-Plus Illustrations. Oxford University Press Inc., New York.

Brocca, L., Melone, F., Moramarco, T., and Morbidelli, R. 2010a. Spatial-temporal variability of soil moisture and its estimation across scales. Water Resources Research, **46**: W02516. doi:10.1029/2009WR008016.

Brocca, L., Melone, F., Moramarco, T., Wagner, W., Naeimi, V., Bartalis, Z., and Hasenauer, S. 2010b. Improving runoff prediction through the assimilation of the ASCAT soil moisture product. Hydrology and Earth System Sciences, **14**: 1881-1893. doi:10.5194/hess-14-1881-2010.

Cairns, R.R. 1962. Soil moisture relations in a Solonetzic soil complex. Canadian Journal of Soil Science, **42**: 17-22.

Calvet, J.-C., and Noilhan, J. 2000. From near-surface to root-zone soil moisture using year-round data. Journal of Hydrometeorology, **1**(5): 393-411.

Carter, M.R., and Pearen, J.R. 1985. General and spatial variability of Solonetzic soils in north central Alberta. Canadian Journal of Soil Science, **65**: 157-167.

Ceballos, A., Scipal, K., Wagner, W., and Martínez-Fernández, J. 2005. Validation of ERS scatterometer-derived soil moisture data in the central part of the Duero Basin, Spain. Hydrological Processes, **19**: 1549-1566. doi:10.1002/hyp.5585.

Chanasyk, D.S., and Naeth, M.A. 1995. Grazing impacts on bulk density and soil strength in the foothills fescue grasslands of Alberta, Canada. Canadian Journal of Soil Science, **75**: 551-557.

Chanasyk, D.S., Naeth, M.A. 1996. Field measurement of soil moisture using neutron probes. Canadian Journal of Soil Science, **76**: 317-323.

Choi, M., and Jacobs, J.M. 2007. Soil moisture variability of root-zone profiles within SMEX02 remote sensing footprints. Advances in Water Resources, **30**: 883-896. doi:10.1016/j.advwatres.2006.07.007.

Crow, W.T., A.A. Berg, M.H. Cosh, A. Loew, B.P. Mohanty, R. Panciera, P. de Rosnay, D. Ryu, and J.P. Walker. 2012. Upscaling sparse based soil moisture observations for the validation of coarse-resolution satellite soil moisture products. Review of Geophysics, **50**: RG2002. doi:10.1029/2011RG000372.

de Lange, R., Beck, R., van de Giesen, N., Fiesen, J., de Wit, A., and Wagner, W. 2008. Scatterometer-derived soil moisture calibrated for soil texture with a one-dimensional water-flow model. IEEE Transactions on Geoscience and Remote Sensing, **46**(12): 4041-4049. doi:10.1109/TGRS.2008.2000796.

Desilets, D., and Zreda, M. 2001. On scaling cosmogenic nuclide production rates for altitude and latitude using cosmic-ray measurements. Earth and Planetary Science Letters, **193**(1): 213-225.

Desilets, D., Zreda, M., and Ferré, T.P.A. 2010. Nature's neutron probe: Land surface hydrology at an elusive scale with cosmic rays. Water Resources Research, **46**: W011505. doi:10.1029/2009WR008726.

Dong, J., Ochsner, T.E., Zreda, M., Cosh, M.H., and Zou, C.B. 2014. Calibration and validation of the COSMOS rover for surface soil moisture measurement. Vadose Zone Journal, **13**(4). doi:10.2136/vzj2013.08.0148.

Driessen, P., Deckers, J., and Nachtergaele, F. 2001. Lecture notes on the major soils of the world. World Soil Resources Reports 94, Food and Agriculture Organization of the United Nations, Rome.

Ellis, J.G., Acton, D.F., and Moss, H.C. 1970. The Soils of the Rosetown Map Area, 72-O Saskatchewan. Saskatchewan Institute of Pedology, Saskatoon, SK. Publ. S3.

Environment Canada. 2014. Canadian climate normals: 1980-2010 for Davidson, Saskatchewan. Available from http://climate.weather.gc.ca/climate_normals/ [accessed 28 November 2014].

Famiglietti, J.S., Ryu, D., Berg, A.A., Rodell, M., and Jackson, T.J. 2008. Field observations of soil moisture variability across scales. Water Resources Research, **44**: W01423. doi:10.1029/2006WR005804.

Ford, T.W., Harris, E., and Quiring, S.M. 2014. Estimating root-zone soil moisture using near-surface observations from SMOS. Hydrology and Earth System Sciences, **18**: 139-154. doi:10.5194/hess-18-139-2014.

Franz, T.E., Zreda, M., Ferré, T.P.A., Rosolem, R., Zweck, C., Stillman, S., Zeng, X., and Shuttleworth, W.J. 2012a. Measurement depth of the cosmic ray soil moisture probe affected by hydrogen from various sources. Water Resources Research, **48**: W08515. doi:10.1029/2012WR011871.

Franz, T.E., Zreda, M., Rosolem, R., and Ferré, T.P.A. 2012b. Field validation of a cosmic-ray neutron sensor using a distributed sensor network. Vadose Zone Journal, **11**(4). doi:10.2136/vzj2012.0046.

Gao, X., Wu, P., Zhao, W., Zhang, B., Wang, J., and Shi, Y. 2013. Estimating the spatial means and variability of root-zone soil moisture in gullies using measurements from nearby uplands. Journal of Hydrology, **276**: 28-41. doi:10.1016/j.jhydrol.2012.10.030.

Gómez-Plaza, A., Martínez-Mena, M., Albaladejo, J., and Castillo, V.M. 2001. Factors regulating spatial distribution of soil water content in small semiarid catchments. Journal of Hydrology, **253**: 211-226.

Grayson, R.B., Western, A.W., Chiew, H.S., and Blöschl, G. 1997. Preferred states in spatial soil moisture patterns: local and non-local controls. Water Resources Research, **33**(12): 2897-2908.

Grayson, R.B., and Western, A.W. 1998. Towards areal estimation of soil water content from point measurements: Time and space stability of mean response. Journal of Hydrology, **207**(1-2): 68-82.

Han, E., Heathman, G.C., Merwade, V., and Cosh, M.H. 2012. Application of observation operators for field scale soil moisture averages and variances in agricultural landscapes. Journal of Hydrology, **444-445**: 34-50. doi:10.1016/j.hydrol.2012.03.035.

Han, X., Franssen, H.-J. H., Rosolem, R.., Jin, R., Li, X., and Vereecken, H. 2015. Correction of systematic model forcing bias of CLM using assimilation of cosmic-ray neutrons and land surface temperature: a study in the Heihe Catchment, China. Hydrology and Earth System Sciences, **19**: 615-629. doi:10.5194/hess-19-615-2015.

Hawdon, A., McJannet, D., and Wallace, J. 2014. Calibration and correction procedures for cosmic-ray neutron soil moisture probes located across Australia. Water Resources Research, **50**: 5029-5043. doi:10.1002/2013WR015138.

Hawley, M.E., Jackson, T.J., and McCuen, R.H. 1983. Surface soil moisture variation on small agricultural watersheds. Journal of Hydrology, **62**: 179-200.

Heathman, G.C., Starks, P.J., Ahuja, L.R., and Jackson, T.J. 2003. Assimilation of surface soil moisture to estimate profile soil water content. Journal of Hydrology, **279**: 1-17. doi:10.1016/S0022-1694(03)00088-X.

Henninger, D.L., Peterson, G.W., and Engman, E.T. 1976. Soil moisture within a watershed – variations, factors influencing, and relationship to surface runoff. Soil Science Society of America Journal, **40**(5): 773-776.

Hills, R.C., and Reynolds, S.G. 1969. Illustrations of soil moisture variability in selected areas and plots of different sizes. Journal of Hydrology, **8**: 27-47.

Hornbuckle, B., Irvin, S., Franz, T., Rosolem, R., and Zweck, C. 2012. The potential of the COSMOS network to be a source of new soil moisture information for SMOS and SMAP. *In* Proceedings of the IEEE International Geoscience Remote Sensing Symposium, Munich, Germany, pp. 1243-1246.

Hupet, F., and Vanclooster, M. 2002. Intraseasonal dynamics of soil moisture variability within a small agricultural maize cropped field. Journal of Hydrology, **261**: 86-101.

Ivanov, V.Y., Fatichi, S., Jenerette, G.D., Espeleta, J.F., Troch, P.A., and Huxman, T.E. 2010. Hysteresis of soil moisture spatial heterogeneity and the "homogenizing" effect of vegetation. Water Resources Research, **46**: W09521. doi:10.1029/2009WR008611.

Jackson, T.J., Le Vine, D.M., Hsu, A.Y., Oldak, A., Starks, P.J., Swift, C.T., Isham, J.D., and Haken, M. 1999. Soil moisture mapping at regional scales using microwave radiometry: The Southern Great Plains Hydrology Experiment. IEEE Transaction on Geoscience and Remote Sensing, **37**(5): 2136-2151.

Jacobs, J.M., Mohanty, B.P., Hsu, E.-C., and Miller, D. 2004. SMEX02: Field scale variability, time stability and similarity of soil moisture. Remote Sensing of Environment **92**: 436-446. doi:10.1016/j.rse.2004.02.017.

Kachanoski, R.G., and de Jong, E. 1988. Scale dependence and the temporal persistence of spatial patterns of soil water storage. Water Resources Research, **24**(1): 85-91.

Kerr, Y.H., Waldteufel, P., Wigneron, J.P., Delwart, S., Cabot, F., Boutin, J., Escorihuela, M., Font, J., Reul, N., Gruhier, C., Juglea, S., Drinkwater, M., Hahne, A., Martín-Neira, M., and Mecklenburg, S. 2010. The SMOS mission: New tool for monitoring key elements of the global water cycle. Proc. IEEE, **98**: 666–687. doi:10.1109/JPROC.2010.2043032.

Kodama, M., Kudo, S., and Kosuge, T. 1985. Application of atmospheric neutrons to soil moisture measurement. Soil Science, **140**(4): 237-242.

Kodama, M., Nakai, K., Kawasaki, S., and Wada, M. 1979. An application of cosmic-ray neutron measurements to the determination of the snow-water equivalent. Journal of Hydrology, **41**: 85-92.

Kornelsen, K.C., and Coulibaly, P. 2013. McMaster Mesonet soil moisture dataset: description and spatio-temporal variability analysis. Hydrology and Earth System Sciences, **17**: 1589-1606. doi:10.5194/hess-17-1589-2013.

Kristensen, K.J. 1973. Depth intervals and topsoil moisture measurements with the neutron depth probe. Nordic Hydrology, **4**: 77-85.

Larson, K.M., Braun, J.J., Small, E.E., Zavorotny, V.U., Gutmann, E.D., Bilich, A.L. 2010. GPS multipath and its relation to near-surface soil moisture content. IEEE Journal Selected Topics in Applied Earth Observations and Remote Sensing, **3**: 91-99. doi:10.1109/JSTARS.2009.2033612.

Martínez-Fernández, J., and Ceballos, A. 2003. Temporal stability of soil moisture in a large-field experiment in Spain. Soil Science Society of America Journal, **67**: 1647-1656.

Miller, J.J., and Brierley, J.A. 2011. Solonetzic soils of Canada: Genesis, distribution and classification. Canadian Journal of Soil Science, **91**:889-902. doi:10.4141/CJSS10040.

Mohanty, B.P., Skaggs, T.H., and Famiglietti, J.S. 2000. Analysis and mapping of field-scale soil moisture variability using high resolution, ground-based data during the Southern Great Plains 1997 (SGP97) Hydrology Experiment. Water Resources Research, **36**(4): 1023-1031.

Mohanty, B.P., and Skaggs, T.H. 2001. Spatio-temporal evolution and time-stable characteristics of soil moisture within remote sensing footprints with varying soil, slope, and vegetation. Advances in Water Resources, **24**: 1051-1067.

Naeth, M., Rothwell, R.L., Chanasyk, D.S., and Bailey, AW. 1990. Grazing impacts on infiltration in mixed prairie and fescue grassland ecosystems of Alberta. Canadian Journal of Soil Science, **70**: 593-605.

Ochsner, T.E., Cosh, M.H., Cuenca, R.H., Dorigo, W.A., Draper, C.S., Hagimoto, Y., Kerr, Y.H., Larson, K.M., Njoku, E.G., Small, E.E., and Zreda, M. 2013. State of the art in large-scale soil moisture monitoring. Soil Science Society of America Journal. doi:10.2136/ssaj2013.03.0093.

Owe, M., Jones, E.B., and Schmugge, T.J. 1982. Soil moisture variation patterns observed in hand county, South Dakota. Water Resources Bulletin, **18**(6): 949-954.

Pan, F., and Peters-Liddard, C.D. 2008. On the relationship between mean and variance of soil moisture fields. Journal of the American Water Resources Association, **44**(1): 235-242.

Pennock, D.J., McCann, B.L., de Jong, E., and Lemmen, D.S. 1999. Effects of soil redistribution on soil properties in a cultivated Solonetzic-Chernozemic landscape of southwestern Saskatchewan. Canadian Journal of Soil Science, **79**: 593-601.

Qu, W., Bogena, H.R., Huisman, J.A., Vanderborght, J., Schuh, M., Priesack, E., and Vereecken, H. 2015. Predicting subgrid variability of soil water content from basic soil information. Geophysical Research Letters, **42**: 789-796. doi:10.1002/2014GL062496.

Ragab, R. 1995. Towards a continuous operational system to estimate the root-zone soil moisture from intermittent remotely sensed surface moisture. Journal of Hydrology, **173**: 1-25.

Reynolds, S.G. 1970. The gravimetric method of soil moisture determination part III: An examination of factors influencing soil moisture variability. Journal of Hydrology, **11**: 288-300.

Rivera Villarreyes, C.A., Baroni, G., and Oswald, S.E. 2011. Integral quantification of seasonal soil moisture changes in farmland by cosmic-ray neutrons. Hydrology and Earth System Sciences, **15** (12): 3843-3859. doi:10.5194/hess-15-3843-2011.

Rivera Villarreyes, C.A., Baroni, G., and Oswald S.E. 2014. Inverse modelling of cosmic-ray soil moisture for field-scale soil hydraulic parameters. European Journal of Soil Science, **65**: 876-886. doi:10.1111/ejss.12162.

Robinson, D.A., Campbell, C.S., Hopmans, J.W., Hornbuckle, B.K., Jones, S.B., Knight, R., Ogden, F., Selker, J., and Wendroth, O. 2008. Soil moisture measurement for ecological and hydrological watershed-scale observatories: A review. Vadose Zone Journal, **7**: 358-389. doi:10.2136/vzj2007.0143.

Rodriguez-Iturbe, I., D'Odorico, P., Porporato, A., and Ridolfi, L. 1999. On the spatial and temporal links between vegetation, climate, and soil moisture. Water Resources Research, **35**(12): 3709-3722.

Rosenbaum, U., Bogena, H.R., Herbst, M., Huisman, J.A., Peterson, T.J., Weuthen, A., Western, A.W., and Vereecken, H. 2012. Seasonal and event dynamics of spatial soil moisture patterns at the small catchment scale. Water Resources Research, **48**: W10544. doi:10.1029/2011WR011518.

Rosolem, R., Hoar, T., Arellano, A., Anderson, J.L., Shuttleworth, W.J., Zeng, X., and Franz, T.E. 2014. Translating aboveground cosmic-ray neutron intensity to high-frequency soil moisture profiles at sub-kilometer scale. Hydrology and Earth System Sciences, **18**: 4363-4379. doi:10.5194/hess-18-4363-2014.

Ryu, D., and Famiglietti, J.S. 2005. Characterization of footprint-scale surface soil moisture variability using Gaussian and beta distribution functions during the Southern Great Plains 1997 (SGP97) hydrology experiment. Water Resources Research, **41**: W12433, doi:10.1029/2004WR003835.

Sandoval, F.M., and Reichman, G.A. 1971. Some properties of Solonetzic (sodic) soils in western North Dakota. Canadian Journal of Soil Science, **51**: 143-155.

Schmugge, T., Gloerson, P., Wilheit, T., and Geiger, F. 1974. Remote sensing of soil moisture with microwave radiometers. Journal of Geophysical Research, **79**: 317-323.

Schmugge, T.J., Jackson,T.J., and McKim, H.L. 1980. Survey of methods for soil moisture determination. Water Resources Research, **16**(6): 961-979.

Seneviratne, S.I., Corti, T., Davin, E.L., Hirschi, M., Jaeger, E.B., Lehner, I., Orlowsky, B., and Teuling, A.J. 2010. Investigating soil moisture-climate interactions in a changing climate: A review. Earth-Science Reviews, **99**: 125-161. doi:10.1016/j.earscirev.2010.02.004.

Seyfried, M.S., Grant, L.E., Du, E., and Humes, K. 2005. Dielectric loss and calibration of the Hydra Probe Soil Water Sensor. Vadose Zone Journal, **4**: 1070-1079. doi:10.2136/vzj2004.0148.

Sheldrick, B.H., and Wang, C. 1993. Particle size distribution. *In* Soil sampling and methods of analysis. *Edited by* M.R. Carter. Canadian Soil Science Society, Bocca Raton: Lewis Publishers, Ann Arbor, MI. pp. 499-512.

Shiklomanov, I.A., and Sokolov, A.A. 1983. Methodological basis of world water balance investigation and computation. *In* New approaches in water balance computations. *Edited by* van der Beken, A., and Herrmann, A. International Association for Hydrological Sciences, Publ. 148.

Shuttleworth, J., Rosolem, R., Zreda, M., Franz, T. 2013. The Cosmic-ray Soil Moisture Interaction Code (COSMIC) for use in data assimilation. Hydrology and Earth System Sciences, **17**: 3205-3217. doi: 10.5194/hess-17-3205-2013.

Simpson, J.A. 1951. Neutrons produced in the atmosphere by the cosmic radiations. Physical Review, **83**: 1175-1188.

Soi1 Classification Working Group. 1998. The Canadian System of Soil Classification. Agriculture and Agri-Food Canada, Publ. 1646 (Revised).

Striegl, A.M., and Loheide, A.P. 2012. Heated distributed temperature sensing for field scale soil moisture monitoring. Ground Water, **50**(3): 340-347. doi:10.1111/j.1745-6584.2012.00928.x.

Takagi, K., and Lin, H.S. 2011. Temporal dynamics of soil moisture spatial variability in the Shale Hills. Vadose Zone Journal, **10**: 832-842. doi:10.2136/vzj2010.0134.

Teuling, A.J., and Troch, P.A. 2005. Improved understanding of soil moisture variability dynamics. Geophysical Research Letters, **32**: L05404. doi:10.1029/2004GL021935.

Teuling, A.J., Uijlenhoet, R., Hupet, F., van Loon, E.E., and Troch, P.A. 2006. Estimating spatial mean root-zone soil moisture from point-scale observations. Hydrology and Earth System Sciences, **10**: 755-767. doi:10.5194/hess-10-755-2006.

Vachaud, G., Passerat de Silons, A., Balabanis, P., and Vauclin, M. 1985. Temporal stability of spatially measured soil water probability density function. Soil Science Society of America Journal, **49**: 822-828.

Vereecken, H., Kamai, T., Harter, T., Kasteel, R., Hopmans, J., and Vanderborght, J. 2007. Explaining soil moisture variability as a function of mean soil moisture: A stochastic unsaturated flow perspective. Geophysical Research Letters, **34**: L22402. doi:10.1029/2007/GL031813.

Vereecken, H., Huisman, J.A., Bogena, H., Vanderborght, J., Vrugt, J.A., and Hopmans, J.W. 2008. On the value of soil moisture measurements in vadose zone hydrology: A review. Water Resources Research, **44**: W00D06. doi:10.1029/2008WR006829.

Vereecken, H., Huisman, J.A., Pachepsky, Y., Montzka, C., van der Kruk, J., Bogena, H., Weihermüller, L., Herbst, M., Martínez, G., and Vanderborght, J. 2014. On the spatio-temporal dynamics of soil moisture at the field scale. Journal of Hydrology, **516**: 76-96. doi:10.1016/j.jhyrol.2013.11.061.

Wagner, W., Lemoine, G., and Rott, H. 1999. A method for estimating soil moisture from ERS scatterometer and soil data. Remote Sensing Environment, **70**: 191-207.

Walker, J.P., Willgoose, G.R., and Kalma, J.D. 2001. One-dimensional soil moisture profile retrieval by assimilation of near-surface observations: a comparison of retrieval algorithms. Advances in Water Resources, **24**: 631-650.

Western, A.W., Grayson, R.B., Blöschl, G., Willgoose, G.R., and McMahon, T.A. 1999. Observed spatial organization of soil moisture and its relation to terrain indices. Water Resources Research, **35**(3): 797-810.

Western, A.W., R.B. Grayson, and G. Blöschl. 2002. Scaling of soil moisture: A hydrologic perspective. Annual Reviews Earth Planetary Science, **30**: 149-180.

Western, A.W., Grayson, R.B., Blöschl, G., and Wilson, D.J. 2003. Spatial variability of soil moisture and its implications for scaling. *In* Scaling methods in soil physics. *Edited by* Y. Pachepsky, D.E. Radcliffe, and H.M. Selim. CRC Press, Boca Raton, Florida. pp. 119-142.

Western, A.W., Zhou, S.L., Grayson, R.B., McMahon, T.A., Blöschl, G., and Wilson, D.J. 2004. Spatial correlation of soil moisture in small catchments and its relationship to dominant spatial hydrological processes. Journal of Hydrology, **286**: 113-134. doi:10.1016/j.jhydrol.2003.09.014.

Williams, C.J., McNamara, J.P., and Chandler, D.G. 2009. Controls on the temporal and spatial variability of soil moisture in a mountainous landscape: the signature of snow and complex terrain. Hydrology and Earth System Sciences, **13**: 1325-1336.

Zhao, Y., Peth, S., Krümmelbein, J., Horn, R., Wang, Z., Steffens, M., Hoffmann, C., and Peng, X. 2007. Spatial variability of soil properties affected by grazing intensity in Inner Mongolia grassland. Ecological Modelling, **205**: 241-254. doi:10.1016/j.ecolmodel.2007.02.019.

Zhao, Y., Peth, S., Wang, X.Y., Lin, H., and Horn, R. 2010. Controls of surface soil moisture spatial patterns and their temporal variability in a semi-arid steppe. Hydrological Processes, **24**: 2507-2519. doi:10.1002/hyp.7665.

Zielinski, J. 2002. Watershed vulnerability analysis. Center for Watershed Protection, Ellicot City, MD 21043. Available from http://www.cwp.org/ [accessed 19 June 2013].

Zreda, M., Desilets, D., Ferré, T.P.A., and Scott, L. 2008. Measuring soil moisture content non-invasively at intermediate spatial scale using cosmic-ray neutrons. Geophysical Research Letters, **35**: L21402. doi:10.1029/2008GL035655.

Zreda, M., Shuttleworth, W.J., Zeng, X., Zweck, C., Desilets, D., Franz, T., and Rosolem, R. 2012. COSMOS: The COsmic-ray Soil Moisture Observing System. Hydrology and Earth System Sciences, **16**: 1-21. doi:10.5194/hess-16-1-2012.

APPENDIX A: SOIL MOISTURE DATA SUMMARY AND CALIBRATION

This section contains supplemental information on the soil moisture data. It includes a summary of the data collection, measurement errors/difficulties, and the calibration equations used. Soil moisture measurement methods included a cosmic-ray neutron probe, surveys of surface soil moisture by hydra probe, and a 21-point neutron probe array. All soil moisture data was taken at a prairie pasture site in the Brightwater Creek watershed (51° 22′ 54″ N, 106° 24′ 57″ W). The measurement footprints of the instrumentation techniques overlap as per Figure A.1.

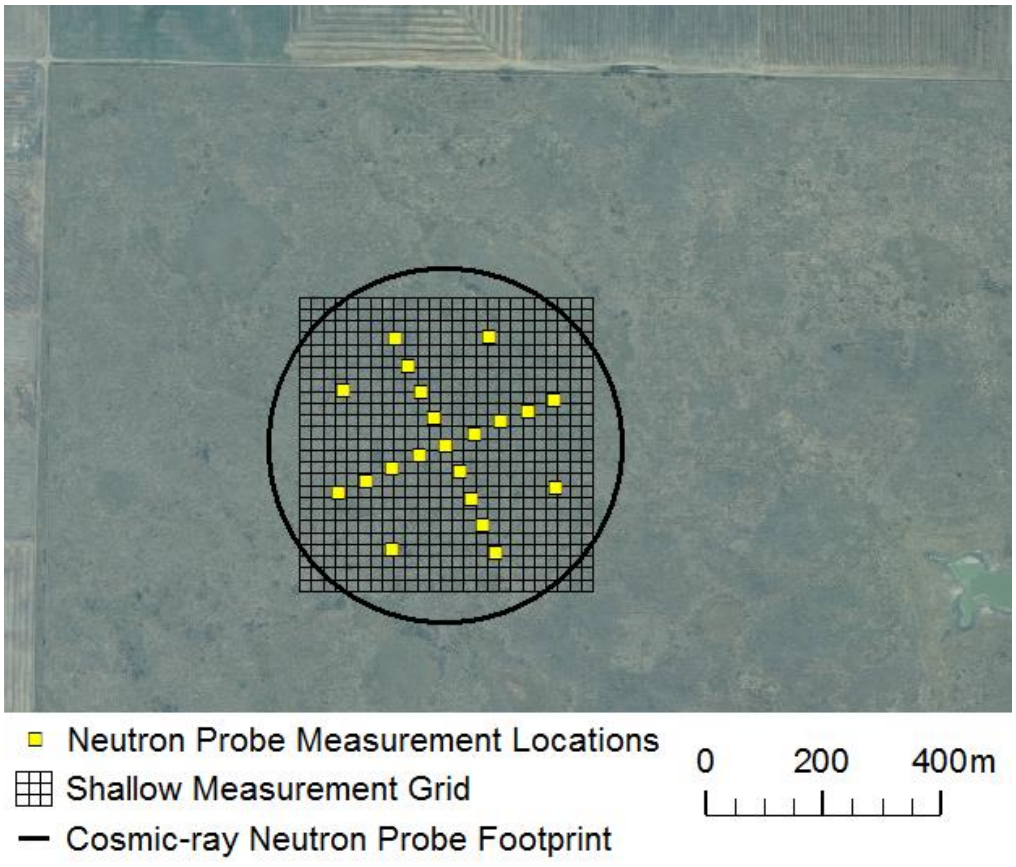

Figure A.1 Arial view of the pasture site showing soil moisture monitoring locations.

A.1 Cosmic-ray Neutron Probe

A.1.1 Summary of data collection

A cosmic-ray neutron probe, model CRS-1000 manufactured by Hydroinnova (USA), was installed at the pasture site at the beginning of August 2012. Hourly counts of fast and thermal neutrons are collected by neutron detectors within the device. Sensors that measure relative humidity, air pressure, and air temperature are also included with the instrument for quality control and to be used in the correction of neutron counts. The device uses changing levels of naturally produced background radiation, termed cosmic-ray neutrons, to calculate soil moisture. The soil moisture measurement of the cosmic-ray neutron probe is representative of the average soil moisture for a 300 m radius footprint (Zreda et al. 2008) and a measurement depth of the top 15–20 cm at the pasture site (Figure 4.2).

A.1.2 Measurement errors and difficulties

Some of the measurement errors and difficulties encountered using the cosmic-ray neutron probe were:

1) *Battery issues* – Batteries for the cosmic-ray neutron probe are charged using solar panels. Due to the northern latitude of this site, more solar panels than recommended were needed to keep the battery charged.

2) *Changes in water storage* – Fast neutrons are most effectively slowed by hydrogen, and therefore the neutron counts are affected by all sources of hydrogen, such as soil moisture, atmospheric water vapor, ponded water, and water stored in biomass (Desilets et al. 2010). Calibration of the cosmic-ray neutron probe is very important in separating soil moisture from other hydrogen sources within the footprint. In using the same calibration equation over the whole time period, one makes the assumption that there are no changes in storage of the other hydrogen sources.

3) *Measurement depth* – The measurement depth of the cosmic-ray neutron probe varies with time, being inversely affected by the volumetric water content (θ_v) of the shallow soil. For the case of no surface water, the formula for estimating the effective measurement depth (Z^*) was determined by Franz et al. (2012a) to be:

$$Z^* = \frac{5.8}{\rho_{bd}\tau + \theta_v + 0.0829} \quad \text{(A.1)}$$

Where ρ_{bd} is the bulk density of the soil, and τ is the weight fraction of lattice water. Both ρ_{bd} and τ are variables that can be measured from soil samples taken at the field site.

A.1.3 Quality control and calculation of water content

Only the fast neutron counts are used to calculate soil moisture. The cosmic-ray neutron probe measures the fast neutrons in counts per interval. The counts per interval must be converted to counts per hour and quality controlled. As per Zreda et al. (2012), data was removed from the record if:

1) Neutron counts differ from the previous value by more than 20%;
2) Relative humidity is greater than 80% inside the probe box, or;
3) Battery voltage is less than 11.8 V.

These quality controlled fast neutron counts were corrected for pressure effects, atmospheric water vapour, and variations in neutron intensity using the methods described in Zreda et al. (2012). The pressure coefficient (*PRESS*) is calculated as:

$$PRESS = exp\big(\beta(P - P_o)\big) \quad , \quad \text{(A.2)}$$

where, β is the pressure coefficient (mb^{-1}), P is the measured pressure (mb), and P_o is the average pressure (mb) of the entire record. The water vapor coefficient (*VAPOR*) is calculated as:

$$VAPOR = 1 + 0.0054 * (\rho_v - \rho_{v\,o}) \quad , \quad \text{(A.3)}$$

where ρ_v is the density of the water vapor, and $\rho_{v\,o}$ is the average water vapor density of the entire record. The neutron intensity coefficient (*INTEN*) is calculated as:

$$INTEN = \frac{I_m}{I_o} \quad , \tag{A.4}$$

where I_m is the intensity of incoming neutrons from the neutron monitor at Jungfraujoch (*JUNG*), Switzerland, and I_o is the reference intensity, which is the intensity on 1 May 2011 at the *JUNG* station. A record of the neutron counts for the *JUNG* station are kindly provided by the Cosmic Ray Group, Physikalisches Institut (University of Bern, Switzerland) at http://cosray.unibe.ch/. The ranges for the correction coefficients (Zreda et al. 2012) are: 0.9 to 1.1 for *PRESS*, 0.99 to 1.07 for *VAPOR*, and 0.95 to 1.05 for *INTEN*.

Three scaling factors are also applied to the data (Appendix A of Zreda et al. 2012). These are *SCALE*, *PROBE*, and *SANPE*. *SCALE* is a scaling factor to account for differences in cosmic-ray intensity as a result of the elevation and cutoff rigidity at the site, and can be calculated at http://cosmos.hwr.arizona.edu/Util/calculator.php. *PROBE* is a scaling factor for different probe types. For the CRS-1000, *PROBE* is equal to 1. *SANPE* is the scaling factor of the San Pedro site (2.486).

The corrected neutrons (CORR) can be calculated using the quality controlled raw neutron counts ($N_{raw\ QC}$), the correction factors, and the scaling factors. The equation from Zreda et al. (2012) is:

$$CORR = N_{raw\ QC} * PROBE * \left(\frac{PRESS}{SCALE}\right) * \left(\frac{SANPE}{INTEN}\right) * VAPOR \quad . \tag{A.5}$$

The soil moisture can be calculated using the equation from Desilets et al. (2010):

$$\theta_g = \frac{a_o}{\left(\frac{CORR}{N_o}\right) - a_1} - a_2 \qquad , \tag{A.6}$$

where θ_g is the gravimetric water content, N_o is the count rate over dry soil, and a_o, a_1, and a_2 are fitting parameters. The fitting parameters can be assumed to be 0.0808, 0.372, and 0.115 respectively for a general silica soil (Desilets et al. 2010). The count rate over dry soil (N_o) is the variable that needs to be calibrated.

A.1.4 Calibration and validation

Field calibration was carried out on 3 July 2013 via the procedure in Zreda et al. (2012), where volumetric measurements of 5 cm increments for 0–30 cm depth were taken at distances of 0, 25, 75, and 150 m from the device every 60°. This shows that the soil moisture measurements from the cosmic-ray neutron probe are more heavily weighted towards the center. The value for N_o can then be calculated using Equation A.6. Further validation of the cosmic-ray neutron probe was conducted at the pasture through comparison with precipitation and subsequent gravimetric samples. The gravimetric samples used for validation were collected using a different method than that described for calibration. In particular, the samples were collected from 20 randomly selected locations on a grid, covering the cosmic-ray neutron probe footprint. This provides a more robust test for the probe as weighting, or distance from the probe, is not considered. A soil auger was used to collect each 0–20 cm soil sample, and gravimetric moisture content was determined by oven drying. The validation samples were collected on four different dates (9 August, 11 September, 30 September, and 23 October 2013), with each measurement day using a different set of 20 locations for sampling.

A.2 Hydra Probe Surveys

A.2.1 Summary of data collection

Data was collected using Stevens Hydra Probes (Hydra Probe II, Stevens Water Monitoring Systems Inc., USA) connected to data readers. Surface measurements were taken over a 500 m by 500 m area with a grid spacing of 20 m. The probes were attached to metal rods and inserted vertically into the soil at each location. This equaled 625 measurements, with each survey taking three people 6–8 hours to complete. Data was collected on 24 July 2013, 27 July 2013, 14 August 2013, and 1 May 2014. There was a large rainfall event (13.6 mm) on 21 July 2013. Therefore, 24 July and 27 July are representative of a single drying event. 14 August and 1 May illustrates the variability of soil moisture under extreme dry and wet conditions, respectively.

A.2.2 Measurement errors and difficulty

The major operational difficulty with the data readers was that they would sometimes all of a sudden start displaying volumetric water contents of 0.00%. When this occurred measurement was stopped and either the batteries would be changed or a new combination of hydra probe and data reader was used. Measurements would not continue until probes were reading reliable levels again.

Sources of error to the soil moisture values obtained during surveys could be due to heterogeneity of soil texture, and the presence of roots at the surface. Calibration equations are important, and are quite variable between different soil types. Roots and other organic material can also cause changes in the dielectric constant.

A.2.3 Calibration

Options for calibration are to use one of the factory calibrations or fit a curve based on lab data. Environment Canada has a site specific equation for their permanent sensors installed at the pasture site. This equation was developed in the lab using a soil sample taken directly from the field. The procedure involved lab controlled wetting and drying of the soil sample, with continuous measurement from a Stevens Hydra Probe. The best fit to their data was a third order polynomial. Their calibration equation to determine volumetric water content (θ_v) is:

$$\theta_v = 5.2459 + 0.6285 * RDC\_tc + 0.0613 * RDC\_tc^2 - 0.0012 * RDC\_tc^3; \quad \text{(A.7)}$$

where *RDC_tc* is the temperature corrected real dielectric constant. The error was found to be small ($R^2 = 0.997$), for a range of 0.14–0.47 cm^3/cm^3. The soil texture of the sample used in their calibration was sandy loam. There are two main concerns that must be addressed before this equation is used. The first is that the hydra probe was not in thermal equilibrium with the soil during the surveys; with movement from location to location there was no time for this to occur. The temperature read by the probe during the surveys was more representative of air temperature than soil temperature. The second concern is the heterogeneity of soil texture over the entire measurement grid.

The other option is to use the general loam calibration equation developed by Seyfried et al. (2005), which is:

$$\theta_v = 0.109\sqrt{RDC} - 0.179; \quad \text{(A.8)}$$

where RDC is the non-temperature corrected real dielectric constant.

a. Temperature effect

To examine the effect of temperature the soil moisture values calculated using the temperature and non-temperature corrected real dielectric contents for all soil moisture surveys are plotted in Figure A.2. It can be seen that the difference between using temperature corrected and non-temperature corrected is small, at most ~0.01 cm^3/cm^3. Temperature, in this case, was not found to have much effect on soil moisture.

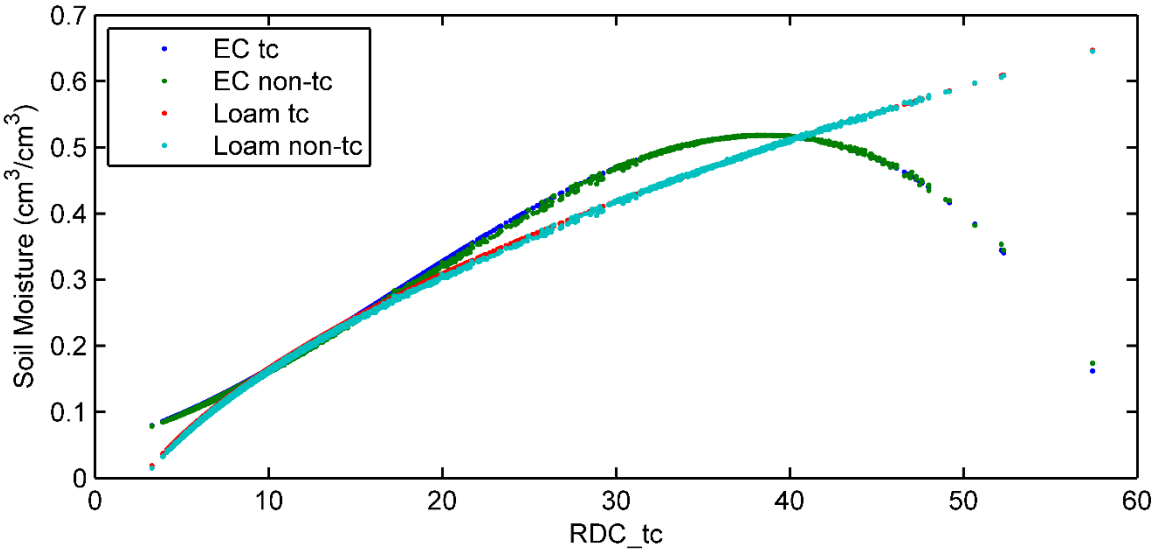

Figure A.2 Comparison of volumetric water content computed using temperature corrected and non-temperature corrected real dielectric constants, for both the Environment Canada (Eqn A.7) and general loam (Eqn. A.8) calibration equations.

b. Soil texture variability

Soil samples of the top 0–20 cm were taken at 60 randomly selected locations within the hydra probe survey grid. Initially, the gravimetric water content from these soil samples was determined from oven drying and the average was compared to that of the cosmic-ray neutron probe. Later, soil texture analysis was completed for these samples using the hydrometer method in Sheldrick and Wang (1993). Soil texture was determined from the measured silt, sand, and clay components. The breakdown of the soil texture results is shown in Table A.1. The majority of the soil samples were considered a type of loam (52 of 60), while the remaining 8 were clay. None of the soil textures were sandy loam, which was the texture of the soil sample that Environment Canada used for their lab calibration. It was therefore assumed that the general loam equation would provide better accuracy than the site specific equation from Environment Canada. The general loam equation is expected to be accurate within ±0.04 cm^3/cm^3 (Seyfried et al. 2005), and is more suitable for high water contents (Figure A.2).

Table A.1 Breakdown of soil texture samples (0-20cm) taken at 60 locations.

Soil Texture	Frequency
Silty Loam	26
Loam	10
Clay Loam	9
Silty Clay Loam	7
Silty Clay	5
Clay	3

A.3 Neutron Probe Array

A.3.1 Measurement description

Root-zone soil moisture was measured by neutron probe (CPN 503DR Hydroprobe, CPN International Inc., USA). Detailed information on the use of neutron probes for soil moisture

measurement is given in Chanasyk and Naeth (1996). Down-hole neutron probes measure point-scale soil moisture. The radius of influence (R [cm]) is a function of volumetric water content (θ_v [%]), defined by Kristensen (1973) as:

$$R = 100/(1.4 + 0.1 \cdot \theta_v) \quad . \tag{A.9}$$

This relationship is illustrated in Figure A.3. The radius decreases as volumetric water content increases.

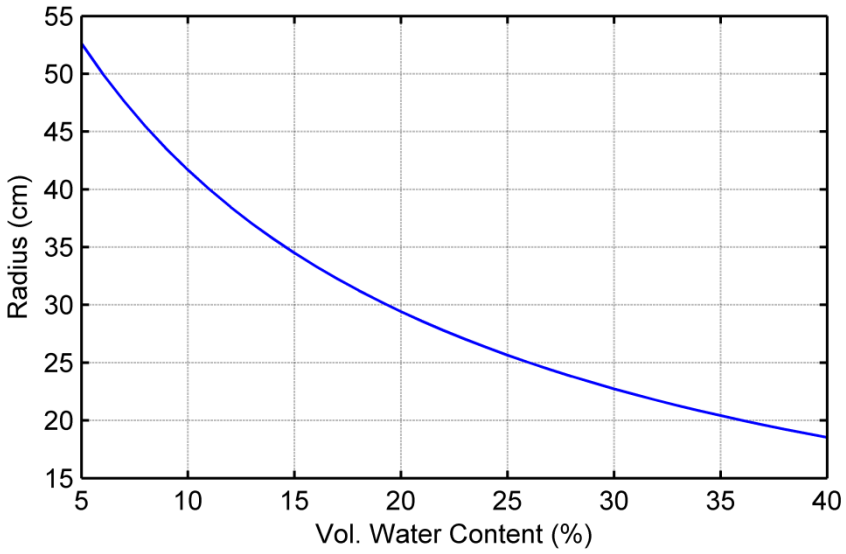

Figure A.3 Neutron probe radius of influence as a function of volumetric water content, using the relationship from Kristensen (1973).

The neutron probe array consisted of 21 measurement locations (Figure A.1). Neutron probe access tubes were spaced 50 m apart along two transects, that crossed at the middle. The shape and size of the neutron probe array was chosen to have a large spatial measurement of root-zone soil moisture within the footprint of the cosmic-ray neutron probe. The radial pattern is similar to the cosmic-ray neutron probe, which is more heavily weighted towards the center. At each access tubes measurements were taken at 20 cm increments down to a depth of 160 cm. Neutrons counts were taken over 64 seconds and an average of the four 16 second intervals was recorded. The access tubes were installed at the beginning of August 2012 and readings were taken every two weeks during the warm months, till the end of 2013. In 2014, moisture was measured monthly.

A.3.2 Calibration

A field calibration method was used for the neutron probe. After access tube installation, the soil cores were divided into 20 cm increments and transported to the lab for volumetric water content determination by oven drying. On the same day, neutron counts were taken at each access tube using the neutron probe. A plot of volumetric water content (θ_v) and count ratio (CR) is shown in Figure A.3. The count ratio is the ratio of the neutron count to the standard daily neutron count. The best fit linear equation for the data is:

$$\theta_V = 0.159 \cdot CR - 0.054; \tag{A.10}$$

which has an R^2 = 0.79 and $RMSE$ = 0.018 cm^3/cm^3.

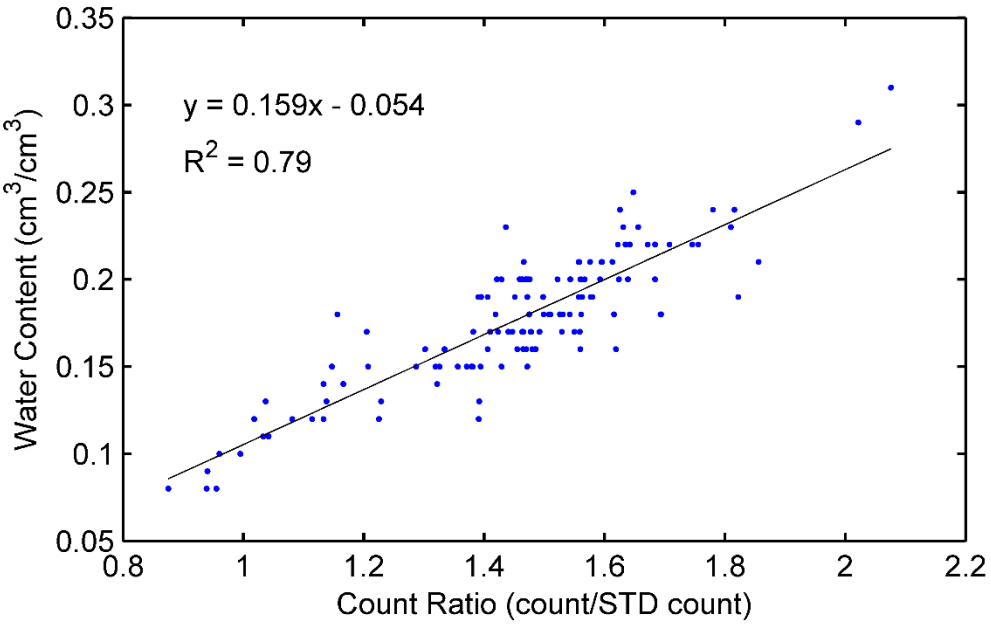

Figure A.4 Linear relationship between neutron counts and volumetric water content, determined from field calibration data.

APPENDIX B: SUPPLEMENTARY TABLES AND FIGURES

B.1 Chapter 3

Table B.1 Statistics of root-zone soil moisture array; volumetric water content (cm^3/cm^3).

	Jul. 31/12	Aug. 22/12	Aug. 30/12	Sep. 13/12	Sep. 26/12	Oct. 10/12	May 7/13	May 16/13
Minimum	0.138	0.118	0.113	0.102	0.093	0.091	0.125	0.125
Maximum	0.216	0.210	0.209	0.206	0.200	0.195	0.243	0.247
Range	0.078	0.092	0.096	0.104	0.107	0.104	0.118	0.122
Mean	0.178	0.166	0.165	0.158	0.154	0.148	0.199	0.197
25 Percentile	0.164	0.146	0.147	0.138	0.136	0.132	0.183	0.179
Median	0.180	0.162	0.164	0.156	0.152	0.146	0.194	0.192
75 Percentile	0.192	0.186	0.186	0.183	0.178	0.172	0.226	0.222
Standard Deviation	0.023	0.025	0.025	0.026	0.027	0.026	0.030	0.029
Skewness	-0.108	0.050	-0.061	-0.115	-0.172	-0.129	-0.620	-0.482
Kurtosis	2.220	2.206	2.360	2.498	2.581	2.504	2.928	3.002
Coefficient of Variation	0.128	0.148	0.150	0.164	0.174	0.177	0.150	0.149
Lilliefors Test	0	0	0	0	0	0	0	0
n	21	21	21	21	21	21	21	21

Lilliefors Test: 0: Normally Distributed 1:Not Normally Distributed

Table B.1 Continued.

	May 31/13	Jun. 19/13	Jul. 5/13	Jul. 16/13	Jul. 30/13	Aug. 14/13	Aug. 28/13	Sep. 17/13
Minimum	0.127	0.126	0.127	0.122	0.116	0.098	0.104	0.089
Maximum	0.231	0.221	0.214	0.204	0.193	0.185	0.179	0.171
Range	0.104	0.095	0.086	0.082	0.076	0.086	0.075	0.082
Mean	0.192	0.187	0.181	0.172	0.162	0.150	0.143	0.135
25 Percentile	0.177	0.170	0.166	0.155	0.144	0.132	0.124	0.111
Median	0.191	0.188	0.188	0.174	0.163	0.146	0.141	0.137
75 Percentile	0.216	0.208	0.196	0.187	0.184	0.175	0.166	0.156
Standard Deviation	0.027	0.025	0.024	0.024	0.024	0.024	0.024	0.026
Skewness	-0.594	-0.678	-0.564	-0.467	-0.339	-0.371	-0.164	-0.243
Kurtosis	2.902	2.997	2.594	2.289	2.068	2.248	1.705	1.803
Coefficient of Variation	0.141	0.134	0.132	0.138	0.151	0.163	0.169	0.193
Lilliefors Test	0	0	0	0	0	0	0	0
n	21	21	21	21	21	21	21	21

Lilliefors Test: 0: Normally Distributed 1: Not Normally Distributed

	Sep. 30/13	Oct. 18/13	May 27/14	Jul. 1/14	Jul. 29/14	Aug. 21/14	Sep. 17/14	Oct. 20/14
Minimum	0.101	0.103	0.146	0.146	0.141	0.116	0.121	0.112
Maximum	0.216	0.206	0.243	0.241	0.213	0.195	0.201	0.197
Range	0.114	0.103	0.097	0.094	0.072	0.079	0.079	0.085
Mean	0.154	0.155	0.200	0.207	0.175	0.156	0.159	0.155
25 Percentile	0.134	0.136	0.186	0.194	0.164	0.137	0.139	0.138
Median	0.157	0.159	0.204	0.210	0.176	0.153	0.156	0.152
75 Percentile	0.169	0.171	0.219	0.228	0.187	0.176	0.177	0.172
Standard Deviation	0.028	0.027	0.027	0.026	0.021	0.022	0.022	0.023
Skewness	0.124	-0.074	-0.558	-0.877	-0.115	0.142	0.249	0.237
Kurtosis	2.783	2.429	2.493	3.229	2.246	2.007	2.135	2.243
Coefficient of Variation	0.180	0.173	0.133	0.124	0.117	0.143	0.136	0.149
Lilliefors Test	0	0	0	0	0	0	0	0
n	21	21	21	21	21	21	21	21

Lilliefors Test: 0: Normally Distributed 1: Not Normally Distributed

Table B.2 Statistics for root-zone soil moisture array; changes in volumetric water content (cm^3/cm^3). Changes from the winter wetting and summer drying periods are denoted as W and S, respectively.

	ΔSM 12/13 W	ΔSM 13/14 W	ΔSM 2012 S	ΔSM 2013 S	ΔSM 2014 S
Minimum	0.008	0.006	-0.050	-0.120	-0.083
Maximum	0.116	0.085	-0.003	-0.015	0.005
Range	0.108	0.079	0.048	0.105	0.087
Mean	0.051	0.046	-0.029	-0.064	-0.046
25 Percentile	0.026	0.024	-0.035	-0.098	-0.066
Median	0.049	0.050	-0.029	-0.068	-0.052
75 Percentile	0.072	0.066	-0.022	-0.030	-0.024
Standard Deviation	0.030	0.027	0.011	0.035	0.025
Skewness	0.340	-0.053	0.273	-0.133	0.382
Kurtosis	2.318	1.792	2.938	1.586	1.957
Coefficient of Variation	0.583	0.582	-0.391	-0.543	-0.541
Lilliefors Test	0	0	0	0	0
n	21	21	21	21	21

Lilliefors Test: 0: Normally Distributed 1: Not Normally Distributed

Table B.3 Statistics of potential soil moisture controlling factors.

	Elevation (m)	Dry Bulk Density 0-80 cm (g/cm^3)	Max. SWE 2013 (mm)	Max. SWE 2014 (mm)
Minimum	576.55	0.79	25	19
Maximum	580.06	1.17	261	182
Range	3.51	0.38	236	163
Mean	579.20	0.98	100	68
25 Percentile	578.86	0.93	80	46
Median	579.47	0.97	89	62
75 Percentile	579.82	1.03	113	85
Standard Deviation	0.89	0.09	47	34
Skewness	-1.459	0.237	1.802	1.628
Kurtosis	4.837	3.410	7.614	6.812
Coefficient of Variation	0.002	0.093	0.472	0.505
Lilliefors Test	1	0	1	0
n	21	21	21	21

Lilliefors Test: 0: Normally Distributed 1: Not Normally Distributed

Table B.4 Statistics of surface soil moisture surveys. Soil moisture measured as volumetric water content (cm^3/cm^3).

	Jul. 24/13	Jul. 27/13	Aug. 14/13	May 1/14
Minimum	0.06	0.05	0.03	0.28
Maximum	0.42	0.32	0.26	0.61
Range	0.36	0.27	0.23	0.33
Mean	0.24	0.16	0.11	0.48
25 Percentile	0.19	0.13	0.09	0.45
Median	0.24	0.16	0.11	0.49
75 Percentile	0.28	0.19	0.13	0.51
Standard Deviation	0.07	0.05	0.04	0.04
Skewness	0.08	0.49	0.58	-0.33
Kurtosis	2.89	2.98	3.45	4.01
Coefficient Of Variation	0.28	0.29	0.34	0.09
Chi-square Test	0	1	1	0
n	624	624	623	584
Chi-square Test:	0: Normally Distributed		1: Not Normally Distributed	

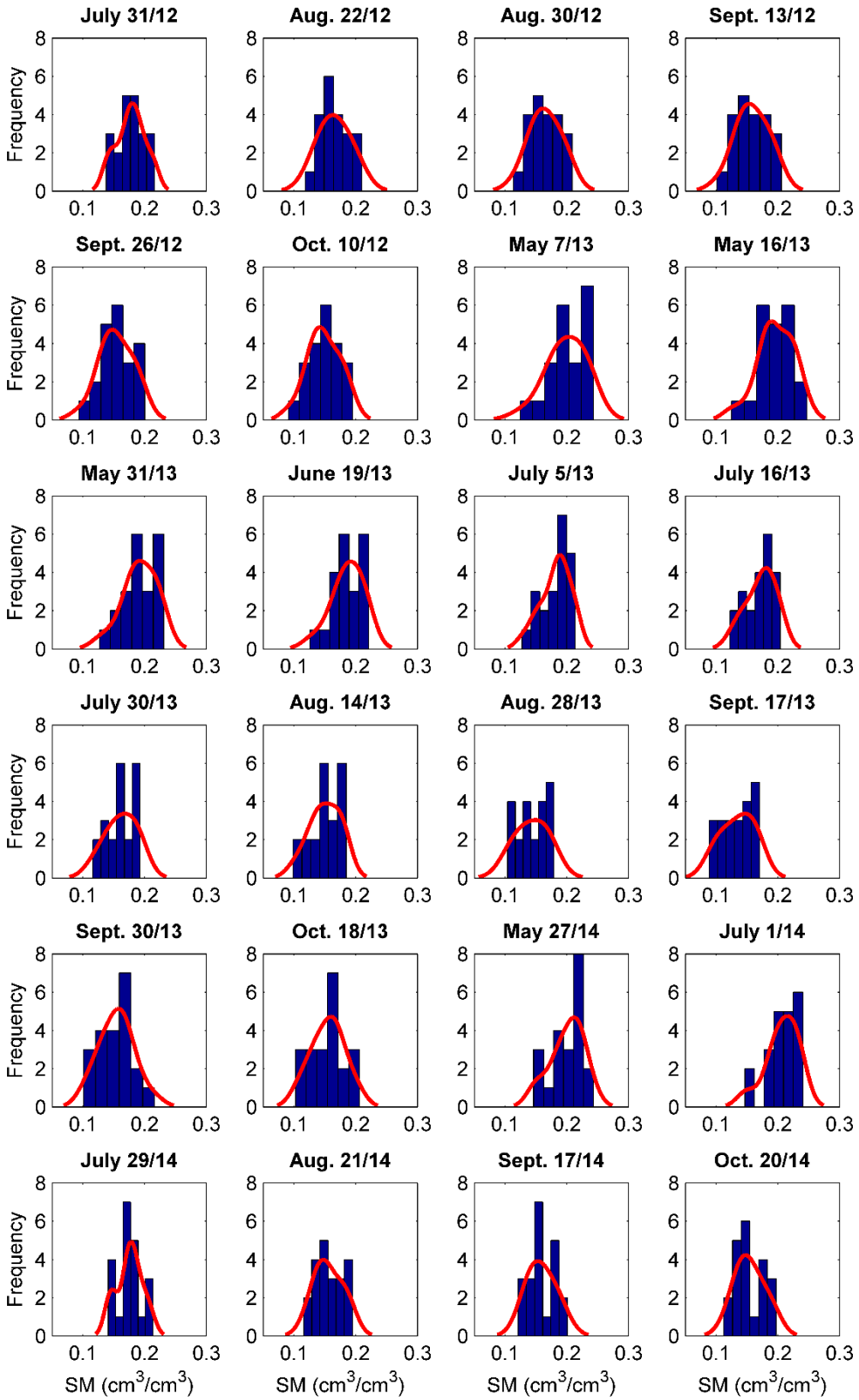

Figure B.1 Comparison of root-zone soil moisture distribution, histograms vs. kernel density estimate.

B.2 Chapter 4

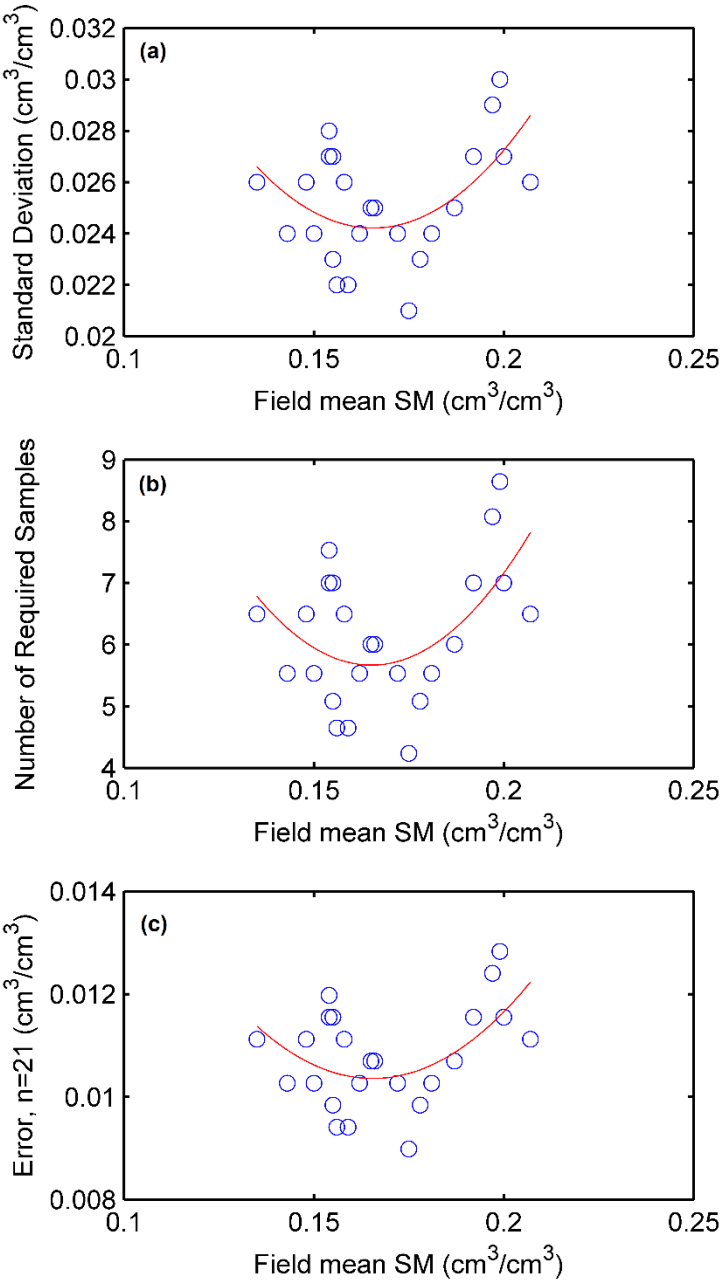

Figure B.2 Number of required samples to obtain accurate field average estimates (within ±0.02 cm^3/cm^3 at 95% confidence) from the neutron probe array (0-110cm) (b). The number of required samples was calculated using the statistical method found in Jacobs et al. (2004). (a) shows the mean and standard deviation of the neutron probe data. (c) shows the approximate error of using 21 point measurements at 95% confidence.

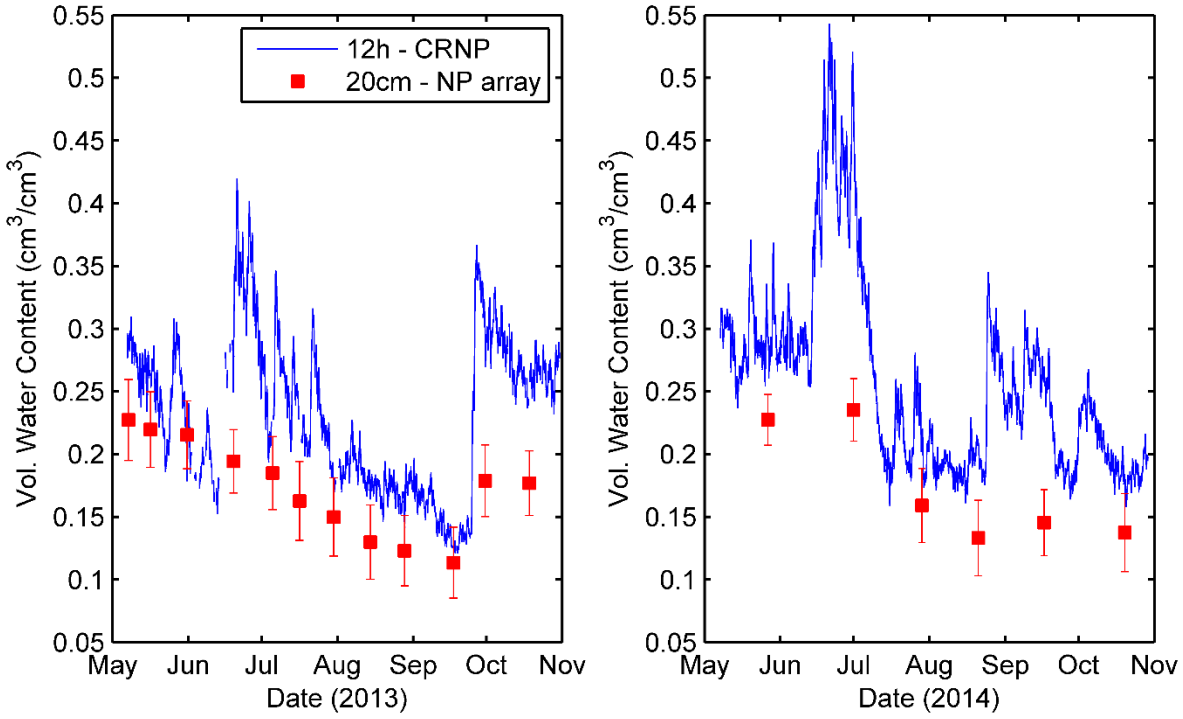

Figure B.3 Comparison of 12 hour running average soil moisture measurements from the cosmic-ray neutron probe with the 20 cm measurements from the neutron probe array (average ± 1 standard deviation). The 20 cm neutron probe measurements are less responsive, and do not match well with the cosmic-ray neutron probe. This is because the 20 cm neutron probe measurement represents average soil moisture for about 0–50 cm, while the depth of the cosmic-ray neutron probe is 0–20 cm.